

**PROGRAMME  
&  
BOOK OF ABSTRACTS**

**SIWAN7**

**7th Szeged International Workshop on  
Advances in Nanoscience**

October 12–15 • 2016 / Szeged • Hungary

**Hunguest Hotel Forrás\*\*\*\*  
Szent-Györgyi A. u. 16–24, H-6726 Szeged, Hungary**



**AKCongress**

Akadémiai Kiadó / AKCongress  
P.O. Box 245, H-1519 Budapest, Hungary  
[www.akcongress.com](http://www.akcongress.com)  
[siwan@akcongress.com](mailto:siwan@akcongress.com)

ISBN 978-963-05-9801-9

## **ORGANIZING COMMITTEE OF SIWAN7**

### **Conference Chair**

Zoltán KÓNYA

### **Conference Co-Chair**

Ákos KUKOVECZ

### **Local Organizing Committee (University of Szeged, Hungary)**

Pál SIPOS

István PÁLINKÓ

Csaba JANÁKY

Ágota TÓTH

### **Scientific Advisory Board**

László Péter BIRÓ (MTA MFA, Hungary)

Goran BOŠKOVIĆ (University of Novi Sad, Serbia)

Imre DÉKÁNY (University of Szeged, Hungary)

Klára HERNÁDI (University of Szeged, Hungary)

Katalin KAMARÁS (MTA SZFKI, Hungary)

Krisztián KORDÁS (University of Oulu, Finland)

Vladimir SRDIĆ (University of Novi Sad, Serbia)

Robert VAJTAI (Rice University, USA)

Paula VILARINHO (University of Aveiro, Portugal)

## TABLE OF CONTENTS

Foreword

Acknowledgements

Scientific Programme

Keynote Lectures

Invited Lectures

Oral Presentations

    Wednesday, 12 October, 2016

    Thursday, 13 October, 2016

    Friday, 14 October, 2016

    Saturday, 15 October, 2016

Poster Presentations

    T01 – Synthesis and properties of new nanostructured systems

    T02 – 2D nanostructures and van der Waals solids

    T03 – Nanomaterials in energy conversion and storage

    T04 – Pharmaceutical, health and biology-related aspects of nanomaterials

    T05 – Multidisciplinary nanoscience: new methods and application possibilities

Author Index

## FOREWORD

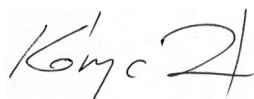
It is a great pleasure for us to offer you this Book of Abstracts for the *7th Szeged International Workshop on Advances in Nanoscience (SIWAN 2016)*. SIWAN was called to life in 2003 when we realized that the booming nanotechnology field was not represented adequately in the Hungarian conference scene. Our goal was to create a platform that introduces the newest results of internationally recognized experts to local students and colleagues and simultaneously displays relevant Hungarian achievements to the world. The positive feedback of the participants encouraged us to proceed and transform a single event into a workshop series. The previous SIWAN 2014 was honoured by colleagues from 40 countries.

Now at SIWAN 2016 we will enjoy 70+ talks and 40+ posters presented by a multicultural scientific community. We stayed true to the original SIWAN concept and accepted contributions from all fields of nanoscience and nanotechnology to promote multidisciplinary discussions. The focal points of the conference this year are two dimensional materials, electro- and photocatalysis, energy related applications of novel nanomaterials and spectroscopy.

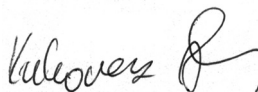
We are pleased to let you know that conference proceedings papers received by 31 January 2017 will be published after peer-review in the open access journal *Nanopages* (ISSN: 1788-0718) free of charge.

Our warmest thanks go to all plenary and invited speakers, authors and contributors of SIWAN 2016 for accepting our invitation, visiting Szeged and using SIWAN as a medium for communicating your research results! Let us encourage you to take advantage of the excellent conference facilities of Hotel Forrás, use every opportunity to make new acquaintances, cherish old ones and in general, to have a very good time at Szeged! We hope that you will enjoy the conference and look forward to meeting you again at a forthcoming SIWAN event.

Szeged, 12 September, 2016



Dr. Zoltán Kónya  
Conference Chair



Dr. Ákos Kukovecz  
Conference Co-Chair

## ACKNOWLEDGEMENTS

SIWAN is the joint effort of many individuals and organizations. First and foremost, we are indebted to our mentor and friend, the late Prof. Imre Kiricsi who initiated the SIWAN series in 2003. We thank the Hungarian nanoscience community, in particular Profs Katalin Kamarás, Imre Dékány and László P. Biró for their continuous support of SIWAN. Thanks are also due to our colleagues at the Department of Applied and Environmental Chemistry of the University of Szeged for their assistance in numerous practical issues and to the staff of Akadémiai Kiadó (Krisztina Tóth, Erna Sári and Balázs Réffy) for their faith and dedication to SIWAN.

SIWAN 2016 is the dedicated dissemination event of the projects in which our research groups are involved today. All of the following projects have provided support to the conference:

MTA-SZTE Reaction Kinetics and Surface  
Chemistry Research Group

MTA-SZTE “Lendület” Porous Nano-  
composites Research Group



NEMZETI KUTATÁSI, FEJLESZTÉSI  
ÉS INNOVÁCIÓS HIVATAL



NKFIH OTKA K 112531

NKFIH OTKA K 120115

GINOP-2.3.2-15-2016-00013 “Intelligent  
materials based on functional interfaces –  
from synthesis to applications”

# SIWAN7

7th Szeged International Workshop on  
Advances in Nanoscience

October 12–15 • 2016 / Szeged • Hungary

<b>WEDNESDAY, 12 OCTOBER, 2016</b>	
<b>12:00–14:00</b>	Registration
<b>14:00–14:20</b>	Opening Ceremony
Session Chair: T. Pichler (Austria)	
<b>14:20–15:20</b>	<b>K01 / R. Vajtai (USA): 2D materials beyond the edge for green energy applications</b>
<b>15:20–16:20</b>	<b>K02 / A. C. Ferrari (UK): The roadmap to applications of graphene, layered materials and hybrid systems</b>
<b>16:20–17:00</b>	<b>I01 / K. Kamarás (Hungary): Encapsulated molecules in boron nitride nanotubes</b>
<b>17:00–17:20</b>	Coffee Break
SESSION A Session Chair: L. P. Biró (Hungary)	
<b>17:20–17:40</b>	<b>001 / R. Sakamoto (Japan)</b> A photofunctional bottom-up bis(dipyrinato)zinc(II) complex nanosheet
<b>17:40–18:00</b>	<b>002 / T. Szabó (Hungary)</b> Size-dependent aggregation behavior of graphene oxide sheets in electrolyte solutions
<b>18:00–18:20</b>	<b>003 / P. Vancsó (Hungary)</b> STM investigation of point defects in various transition-metal dichalcogenide single layers
Session Chair: L. P. Biró (Hungary)	
<b>18:20–19:00</b>	<b>I02 / I. Halasz (USA): Distinguishing internal and external Brønsted acidity in molecular sieves by combining experimental and simulated FTIR spectra</b>
<b>19:00–21:00</b>	Welcome Reception

<b>THURSDAY, 13 OCTOBER, 2016</b>	
<b>Session Chair: R. Sakamoto (Japan)</b>	
<b>9:00–10:00</b>	<b>K03 / I. Willner (Israel): Switchable DNA-based nanostructures for sensing, machinery, drug delivery and switchable hydrogels</b>
<b>10:00–10:40</b>	<b>I03 / L. P. Biró (Hungary): Structural coloration of lycaenid butterflies: from sexual signaling to chemically selective sensing</b>
<b>10:40–11:00</b>	<b>Coffee Break</b>
<b>SESSION A</b>	
<b>Session Chair: I. Willner (Israel)</b>	
<b>11.00–11.20</b>	<b>007 / I. Szilágyi (Switzerland)</b> Stabilization of enzyme-layered double hydroxide nanocomposites in suspensions
<b>11:20–11:40</b>	<b>008 / M. Hubalek Kalbacova (Czech Republic)</b> <i>In vitro</i> study of silicon quantum dots in human cells
<b>11:40–12:00</b>	<b>009 / J. Demel (Czech Republic)</b> Nanoscaled porphyrinic metal-organic framework: towards applications in photodynamic therapy
<b>12:00–12:20</b>	<b>010 / H. Uchiyama (Japan)</b> Preparation of nanostructured SnO particles through crystal growth in the presence of biological polymers
<b>12:20–12:40</b>	<b>011 / Z. Dudás (Hungary)</b> Physicochemical characterization of organically modified silica gels obtained by sol-gel process
<b>12:40–13:00</b>	<b>012 / J. Hynek (Czech Republic)</b> Porphyrin-based conjugated microporous polymers as solid-state photosensitizers for singlet oxygen
<b>13:00–14:40</b>	<b>Lunch</b>
<b>SESSION B</b>	
<b>Session Chair: L. A. Chernozatonskii (Russia)</b>	
<b>013 / V. Demin (Russia)</b>	Piezoelectricity of graphene/BN in-plane heterostructures
<b>014 / P. B. Sorokin (Russia)</b>	Investigation of graphene-type layers in ultrathin films of the ionic compound
<b>015 / A. G. Kvashnin (Russia)</b>	Novel hybrid nanostructures based on graphitic zinc oxide/sulphide monolayers
<b>016 / P. Kuzhir (Belarus)</b>	Carbonaceous nano-films for microwave shielding applications
<b>017 / A. Plyushch (Belarus)</b>	Phosphate ceramics – carbon nanotube composites
<b>018 / G. I. Márk (Hungary)</b>	Bioinspired photonic structures active in a large wavelength scale

<b>THURSDAY, 13 OCTOBER, 2016</b>	
Session Chair: K. Kordas (Finland)	
14:40–15:20	<b>104 / A. V. Krashennnikov (Finland): Defects in two-dimensional inorganic materials</b>
15:20–16:00	<b>105 / P. Ayala (Austria): Understanding ultra-low doping in single-walled carbon nanotubes towards applications</b>
16:00–16:40	<b>106 / A. Rawal (India): Compression induced electrical response of entangled network of buckypaper</b>
16:40–17:00	Coffee Break
<b>SESSION A</b>	
Session Chair: P. M. Vilarinho (Portugal)	
17:00–17:20	<b>019 / O. Yu. Kurapova (Russia)</b> Thermal evolution of stabilized zirconia nanopowders obtained via cryochemical route
17:20–17:40	<b>020 / A. Kierys (Poland)</b> Porous polymers as a specific microenvironment of silica precursors transformation
17:40–18:00	<b>021 / R. Zairov (Russia)</b> High performance magneto-fluorescent nanoparticles assembled from terbium and gadolinium 1,3-diketones
18:00–18:20	<b>022 / C. Vasilescu (Romania)</b> Very high concentration aqueous magnetic nanofluids: synthesis, colloidal stability, magnetic and flow properties
18:20–18:40	<b>023 / S. B. Mishra (South Africa)</b> Empowering waste water treatment techniques using advanced materials at nanoscale
18:40–19:00	<b>024 / M. Saeed (Pakistan)</b> Nano sized zinc oxide: an efficient catalyst for degradation of rhodamine B dye in aqueous medium
19:00–21:00	<b>POSTER SESSION</b>
21:00–23:00	Conference Dinner (Optional)
<b>SESSION B</b>	
Session Chair: A. Rawal (India)	
17:00–17:20	<b>025 / Á. Gali (Hungary)</b> Time resolved emission study of nanoparticles with complex radiation mechanism
17:20–17:40	<b>026 / A. Sibal (India)</b> Theoretical modelling of 'smart' nanogenerators grown on nonwoven materials
17:40–18:00	<b>027 / L. Shi (Austria)</b> Synthesis and properties of long linear carbon chains
18:00–18:20	<b>028 / A. M. Dimiev (Russia)</b> Oxidative unzipping of carbon nanotubes. Controlling reaction parameters affords new types of graphene nanoribbon products
18:20–18:40	<b>029 / S. Javadian (Iran)</b> Pulsed current electrodeposition parameters to control the Sn particle size to enhance electrochemical performance as anode material in lithium ion batteries
18:40–19:00	<b>G. Brunetti (France)</b> New JEOL developments for scanning & transmission electron microscopes: IT300HR & F2



FRIDAY, 14 OCTOBER, 2016	
Session Chair: Cs. Janáky (Hungary)	
9:00–10:00	<b>K04 / K. Rajeshwar (USA): Leveraging solid state chemistry paradigms for solar fuels generation</b>
10:00–10:40	<b>107 / K. Takanabe (Saudi Arabia): Towards photocatalysis by design for efficient water splitting</b>
10:40–11:00	Coffee Break
Session Chair: K. Rajeshwar (USA)	
11:00–11:40	<b>108 / P. M. Vilarinho (Portugal): Nanoporous ferroelectrics for emerging applications</b>
SESSION A	
Session Chair: K. Rajeshwar (USA)	
11:40–12:00	<b>030 / L. Kavan (Czech Republic)</b> Nanostructured (photo)catodes for dye-sensitized solar cells
12:00–12:20	<b>031 / H. Shin (Korea)</b> Asymmetric nanostructure of metal/semiconductor: confined crystallization and their implications
12:20–12:40	<b>032 / Cs. Janáky (Hungary)</b> Hybrid nanoscale architectures of semiconductors and carbon nanomaterials tailored for photoelectrochemical applications
12:40–13:00	<b>033 / R. Kun (Germany)</b> Fabrication and electrochemical performance of flexible all-solid-state Li-ion microbatteries
13:00–13:20	<b>034 / S. Chernyak (Russia)</b> Co crystallinity and CNT evolution in CO and CO <sub>2</sub> hydrogenation over Co/CNT catalysts
13:20–13:40	<b>035 / K. Kortdas (Finland)</b> Diamond-like carbon and carbon nanotube hybrids for biochemical sensing
13:40–15:00	Lunch
15:00–18:00	Optional Programmes: Horseback Archery Show / Guided Walking Tour
SESSION B	
Session Chair: B. Pécz (Hungary)	
11:40–12:00	<b>036 / T. Pichler (Austria)</b> Tailored hybrid materials using nanochemistry inside carbon nanotubes
12:00–12:20	<b>037 / N. Strokova (Russia)</b> Adsorption properties of spark plasma sintered nitrogen-doped carbon nanomaterials
12:20–12:40	<b>038 / G. Németh (Hungary)</b> Near-field infrared nanoscopy on different types of carbon nanotube bundles
12:40–13:00	<b>039 / G. Vári (Hungary)</b> Interaction of gold with the hexagonal boron nitride nanomesh prepared on Rh(111)
13:00–13:20	<b>040 / I. Szentí (Hungary)</b> Promotion and inhibition effects of TiO <sub>2</sub> and MoO <sub>3</sub> species on the reactivity of atomically thin Rh films
13:20–13:40	<b>041 / H. M. Mamedov (Azerbaijan)</b> Electrical and photoelectrical properties of heterojunctions p-Si/Cd <sub>1-x</sub> Zn <sub>x</sub> O

<b>SATURDAY, 15 OCTOBER, 2016</b>	
Session Chair: <b>K. Kamarás (Hungary)</b>	
9:00–10:00	<b>K05 / P. M. Ajayan (USA): Materials science of 2D atomic layers</b>
10:00–10:40	<b>109 / B. Pécz (Hungary): Nanolayers in nitride high power devices grown on diamond and graphene</b>
10:40–11:00	<b>Coffee Break</b>
Session Chair: <b>L. Kavan (Czech Republic)</b>	
11:00–11:40	<b>110 / M. Haluska (Switzerland): Progress in integration of individual as grown single-walled carbon nanotubes into field-effect transistor based ultra-low power gas sensors</b>
11:40–12:00	<b>042 / M. Zúkalová (Czech Republic): Li and Na insertion into <math>\text{Li}_4\text{Tl}_5\text{O}_{12}</math> made by different synthetic protocol</b>
12:00–12:20	<b>043 / É. Kováts (Hungary): New family of Zn carboxylate MOFs with cubane linkers</b>
12:20–12:40	<b>111 / A. Gharib (Iran): ZnO nanoparticles catalyst in synthesis of xanthenes and 1,8-dioxo-octahydroxanthene</b>
12:40–13:00	<b>Closing Ceremony</b>

The organizer reserves the right to make changes in the Conference programme.

# Resolution & Discovery

## AIMS AND SCOPE

Resolution and Discovery is a new journal that provides a forum for the publication of original research in all kinds of microscopy in materials science and the life sciences, as well as developments in instrumentation and techniques.

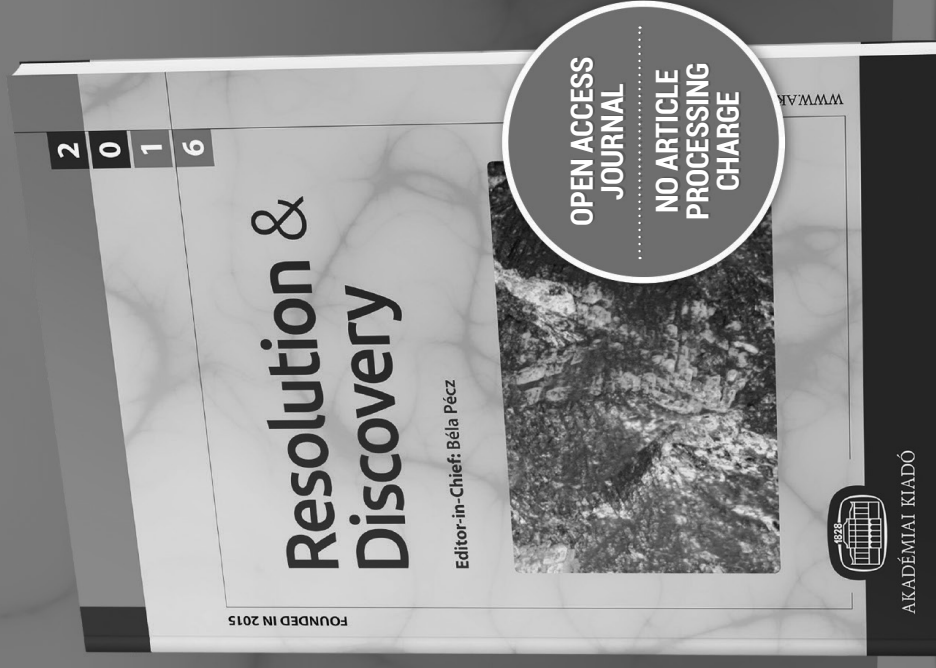
## BENEFITS OF SUBMITTING YOUR ARTICLE

- + **Rapid publication:** the journal is only published online according to an article-by-article model, meaning that articles are published immediately after the editorial process without needing to wait for a complete issue to be published.
- + **Free publication:** no article processing charges until the end of 2017.
- + **Rigorous peer review.**
- + **Highly skilled, professional, internationally renowned Editorial Board members.**

## THE SUBJECTS COVERED BY THE JOURNAL INCLUDE

structure and imaging of biomolecules • live cell imaging • neurobiology • materials for nanotechnology • metal alloys and intermetallics • ceramics • composites • minerals • microscopy in cultural heritage • advances in scanning probe microscopy • three-dimensional imaging and tomography • electron diffraction techniques • analytical microscopy

A NEW OPEN ACCESS  
MICROSCOPY JOURNAL



AKADÉMIAI KIADÓ

[www.akademiai.com](http://www.akademiai.com)

AKADÉMIAI KIADÓ

## KEYNOTE LECTURES

### K01

#### 2D MATERIALS BEYOND THE EDGE FOR GREEN ENERGY APPLICATIONS

*Robert Vajtai*

Department of Materials Science and NanoEngineering, 6100 Main Street, Houston, TX 77005, USA;  
e-mail: robert.vajtai@rice.edu

Green energy technologies, both generation (a.k.a. conversion) and storage, still faces challenges such as low efficiency, usage of rare and expensive precious metals, environmental issues at the production or disposal, etc. For answering these challenges new materials are needed in various steps of energy conversion. The recently popularized and widely researched 2-dimensional materials, graphene and materials beyond graphene are potent candidates for serving as a catalyst in multiple kinds of reactions. In this talk, I will summarize a few results of our work through showing three exemplary material systems for three important reactions; in each case, I will talk about the production, materials characterization and application aspects. Being hydrogen one of the most efficient energy carrier, an interesting example is hexagonal carbon nitride, this beautifully rugged materials is an efficient catalyst for hydrogen production under illumination of visible light. At the same time, a not as orderly distributed nitrogen dopant in graphene, where the nitrogen is predominantly found in pyridinic bonding environment, results in a highly active and stable catalyst for oxygen reduction. Furthermore, defect engineered monolayers of MoS<sub>2</sub>, one of the most studied 2D transition metal dichalcogenides, also can be applied for hydrogen evolution reaction.

What is common in all of these examples: even in these low dimensional materials, one needs to explore chemically active locations beyond their edges to achieve competitive performance.

### K02

#### THE ROADMAP TO APPLICATIONS OF GRAPHENE, LAYERED MATERIALS AND HYBRID SYSTEMS

*Andrea C. Ferrari*

Cambridge Graphene Centre, University of Cambridge, Cambridge CB3 0FA, UK;  
e-mail: acf26@hermes.cam.ac.uk

Disruptive technologies are usually characterised by universal, versatile applications, which change many aspects of our life simultaneously, penetrating every corner of our existence. In

order to become disruptive, a new technology needs to offer not incremental, but dramatic, orders of magnitude improvements. Moreover, the more universal the technology, the better chances it has for broad base success. The Graphene Flagship has brought together universities, research centres and companies from most European Countries. At the end of the ramp-up phase significant progress has been made in taking graphene, related layered materials and hybrid systems from a state of raw potential to a point where they can revolutionize multiple industries. I will overview the progress done thus far and the future roadmap.

### K03

#### SWITCHABLE DNA-BASED NANOSTRUCTURES FOR SENSING, MACHINERY, DRUG DELIVERY AND SWITCHABLE HYDROGELS

*Itamar Willner*

Institute of Chemistry, The Hebrew University of Jerusalem, Jerusalem 91904, Israel;  
e-mail: willnea@vms.huji.ac.il

The base sequence in nucleic acids encodes structural and functional information into the biopolymer. This encoded information is implemented to develop the area of DNA nanotechnology. Topics that will be addressed include:

The synthesis of DNA-semiconductor QDs (or Ag<sup>0</sup> nanoclusters) hybrid systems for optical sensing [1, 2].

1. The use of DNA as a functional material to construct DNA machines. Various supramolecular DNA machines, including tweezers [3], walkers [4], rotors and interlocked DNA structures (catenanes) will be described [5]. The use of the DNA machines to dictate structural patterns of nanoparticles and control plasmonic properties will be presented.
2. DNA-functionalized SiO<sub>2</sub> nanoparticles [6], metal organic frameworks (MOFs) [7] and microcapsules [8] will be introduced as stimuli-controlled carriers for controlled drug release.
3. The synthesis of stimuli-responsive DNA-based hydrogels will be introduced, and the application of these systems as shape-memory materials [9], sensors and signal-triggered mechanical devices will be introduced.

#### References

1. (a) R. Freeman, X. Liu and I. Willner, *J. Am. Chem. Soc.*, **133**, 11597–11604 (2011). (b) X. Liu, F. Wang, R. Aizen, O. Yehezkeli and I. Willner, *J. Am. Chem. Soc.*, **135**, 11832–11839 (2013).
2. X. Liu, F. Wang, A. Niazov-Elkan, W. Guo and I. Willner, *Nano Lett.*, **13**, 309–314 (2013).
3. J. Elbaz, Z.-G. Wang, R. Orbach and I. Willner, *Nano Lett.*, **9**, 4510–4514 (2009).
4. Z.-G. Wang, J. Elbaz and I. Willner, *Nano Lett.*, **11**, 304–309 (2011).
5. C.-H. Lu, A. Ceconello and I. Willner, *J. Am. Chem. Soc.*, in press.
6. (a) Z. Zhang, D. Balogh, F. Wang and I. Willner, *J. Am. Chem. Soc.*, **135**, 1934–1940 (2013). (b) C.-H. Lu and I. Willner, *Angew. Chem. Int. Ed.*, **54**, 12212–12235 (2015). (c) D. Balogh, M. A. Aleman-Garcia, H. B. Albada and I. Willner, *Angew. Chem. Int. Ed.*, **54**, 11652–11656 (2015).
7. J. S. Kahn, L. Freage, N. Enkin, M. A. Alema Garcia and I. Willner, *Adv. Mater.*, in press.
8. W.-C. Liao, C.-H. Lu, R. Hartmann, F. Wang, Y. S. Sohn, W. J. Parak and I. Willner, *ACS Nano*, **9**, 9078–9086 (2015).

9. (a) W. Guo, C.-H. Lu, R. Orbach, F. Wang, X.-J. Qi, A. Ceconello, D. Seliktar and I. Willner, *Adv. Mater.*, **27**, 73–78 (2015). (b) C.-H. Lu, W. Guo, Y. Hu, X.-J. Qi and I. Willner, *J. Am. Chem. Soc.*, **137**, 15723–15731 (2015).

## K04

### LEVERAGING SOLID STATE CHEMISTRY PARADIGMS FOR SOLAR FUELS GENERATION

*Krishnan Rajeshwar*

The University of Texas at Arlington, Arlington, TX, USA;  
e-mail: rajeshwar@uta.edu

Solid-state chemistry languished as an esoteric discipline till interest exploded on the so-called high-T<sub>c</sub> superconductor materials; oxides were discovered to have unique properties in this regard. Paralleling this was the gradual realization that solid-state chemistry principles underpinned many technologically-important areas such as batteries, supercapacitors, and even solar cells. The culmination of this trend was in the application of solid-state chemistry to the preparation and characterization of electrode materials in photoelectrochemical (PEC) cells.

This perspective talk will examine how solid-state chemistry principles have contributed both to the design and synthesis of photoelectrode materials for PEC applications related to water splitting, CO<sub>2</sub> reduction, and environmental remediation. The design of new-generation oxide semiconductors with the correct optoelectronic and bulk/interfacial chemistry characteristics needed to efficiently drive the above reactions will be addressed. The list of material pre-requisites for efficient solar fuels generation or photocatalytic degradation is daunting and it is hardly surprising that a “magic bullet” material has not emerged even after 4 decades of R&D effort. However, these same challenges have attracted researchers drawn from diverse communities including solid-state/device physics, photophysics/photochemistry, colloid chemistry, ultra-fast spectroscopy, classical inorganic chemistry, environmental chemistry and organometallics.

To keep the discussion coherent, only a very limited subset of topics will be addressed in this talk. The progression from binary to ternary, and even quaternary oxides will be examined from the perspective of “band-gap engineering” (a much-maligned word!) and tuning of the interfacial semiconductor surface/fluid energetics. Examples will be drawn from recent results, especially drawn from the successful collaboration with Professor Csaba Janaky’s group at the University of Szeged [1–5].

#### References

1. K. Rajeshwar, C. Janaky, W.-Y. Lin, D. A. Roberts and W. A. Wampler: Photocatalytically prepared metal nanocluster-oxide semiconductor-carbon nanocomposite electrodes for driving multielectron transfer. *J. Phys. Chem. Lett.* **4**, 3468–3478 (2013) (Perspective).
2. K. Rajeshwar, C. Janaky and A. Thomas: Photocatalytic activity of inorganic semiconductor surfaces: myths, hype, and reality. *J. Phys. Chem. Lett.* **6**, 139–147 (2015) (Viewpoint).
3. C. Janaky and K. Rajeshwar: The role of (photo)electrochemistry in the rational design of hybrid conducting polymer/semiconductor assemblies: from fundamental concepts to practical applications. *Prog. Poly. Sci.* **43**, 96–135 (2015).

4. K. Rajeshwar, C. Janaky and E. Kescenovy: Electrodeposition of inorganic oxide/nanocarbon composites: opportunities and challenges. *ChemElectroChem*. **3**, 181–192 (2016).
5. D. Hursan, A. Kormanyos, K. Rajeshwar and C. Janaky: Polyaniline films photoelectrochemically reduce CO<sub>2</sub> to alcohols. *Chem. Commun.* **52**, 8858–8861 (2016).

## K05

### MATERIALS SCIENCE OF 2D ATOMIC LAYERS

*Pulickel M. Ajayan*

Department of Materials Science and NanoEngineering, Rice University, Houston, Texas 77005, USA;  
e-mail: [ajayan@rice.edu](mailto:ajayan@rice.edu)

There has been tremendous interest in recent years to study two-dimensional atomic layers which form building blocks of many bulk layered materials. This was started by the spectacular discovery of graphene. This talk will focus on the materials science of the emerging field of 2D atomic layers and their hybrids. Several aspects that include synthesis, characterization and manipulation will be explored with the objective of achieving 2D functional structures. The concept of nanoscale engineering and the goal of creating new artificially stacked van der Waals solids will be discussed through a number of examples including graphene and other 2D layer compositions. The talk will explore the emerging landscape of 2D materials systems that include graphene, boron-nitrogen-carbon systems, and a large number of transition metal dichalcogenide compositions. Some of anticipated applications of these materials will also be discussed.

## INVITED LECTURES

### I01

#### ENCAPSULATED MOLECULES IN BORON NITRIDE NANOTUBES

*Katalin Kamarás*<sup>1</sup>, *Áron Pekker*<sup>1</sup>, *Anita Szám*<sup>1</sup>, *Hajnalka M. Tóháti*<sup>1</sup>, *Kate Walker*<sup>2</sup>,  
*Graham A. Rance*<sup>2</sup>, *Andrei N. Khlobystov*<sup>2</sup>

<sup>1</sup>Institute for Solid State Physics and Optics, Wigner Research Center for Physics, Hungarian Academy of Sciences, Budapest, Hungary; e-mail: kamaras.katalin@wigner.mta.hu

<sup>2</sup>University of Nottingham, Nottingham, United Kingdom

Boron nitride is an analogue of graphene where the  $\pi$ -electrons possess reduced mobility and the B-N bonds show pronounced ionic character. Despite these differences in electronic structure, this material can also form nanotubes and undergo encapsulation reactions with small molecules. Due to the much larger diameter, the multiwall character and the largely diminished van der Waals interaction between the guest molecules and the nanotube wall, these systems behave differently from carbon-based “peapods”. We will present a thorough characterization of  $C_{60}$ @BNNT and related compounds, based on microscopy and spectroscopy. From our results, we estimate the filling ratio of the nanotubes and the arrangement of the fullerene molecules in the cavities, and identify new products from chemical reactions inside the tubes.

### I02

#### DISTINGUISHING INTERNAL AND EXTERNAL BRØNSTED ACIDITY IN MOLECULAR SIEVES BY COMBINING EXPERIMENTAL AND SIMULATED FTIR SPECTRA

*Istvan Halasz*

PQ Corporation, Research and Development Center, 280 Cedar Grove Road, Conshohocken, PA 19428, USA; e-mail: Istvan.Halasz@pqcorp.com

Most catalytic processes, which affect about 90% of all chemical products, use heterogeneous catalysts. More than 50% of these catalysts contain nano or micro crystal-line, microporous ( $d < 2$  nm) aluminum silicates (zeolites) or their aluminum phosphate based alternatives. The Brønsted acidic hydroxyl groups (BA-OH) of these molecular sieves are catalytically active sites in numerous commercial processes. One can speculate that the strength and density of these BA-OH sites might differ on the crystallite surface from those of inside the pores. Also the micropore diffusion controlled accessibility of internal sites is presumably more difficult for the reactants than accessing the surface BA-OH sites. Yet, the distinction of these internal and external BA-OH sites is very difficult.



Here we report on an FTIR (Fourier Transform Infrared) method, which allows such distinctions. FTIR spectroscopy is a preferred technique for the quantitative and qualitative characterization of OH groups on metal oxides. Different laboratories interchangeably apply either diffuse reflectance (DRIFT) or transmission (TR) techniques, which are considered to give largely identical results, when the DRIFT spectra are modified by Kubelka-Munk or other functions to compensate for nonlinearity. Therefore, it was shocking to observe on a proton exchanged Chabazite (H-CHA) and also on a H-SAPO-34 sample quite different BA-OH FTIR spectra when measured by these two methods. These molecular sieves are important catalysts ingredients for example for a recently developed methanol-to-hydrocarbon (MTH) technology and the new, urea based NO<sub>x</sub> SCR (Selective Catalytic Reduction) treatment of diesel engine exhausts.

For an explanation, we tested the potential effect of several zeolite properties, like chemical composition, zeolite structure, pore diameter, crystallite size, and refractivity index, but none of these physical and chemical differences could generate such significant spectral deviations. Therefore, we conjectured that a potential cause of the extra band in the DRIFT spectra might be due to the increased significance of surface OH species while the TR spectra overwhelmingly reflect the vibrations of the bulk BA-OH groups.

We show in this presentation how we tested and proved the validity of the above hypothesis via comparative DRIFT and TR measurements on proton and alkaline exchanged samples and also by pyridine, PY adsorption. To learn more, we also carried out DFT simulations and found that i) the elevated DRIFT vibrations cannot come from deeper than 1–2 unit cell (15–20 Å); ii) a combination of models is needed to simulate realistic surfaces, but only the O1H site is stable on the surface; iii) the bulk Brønsted acidic sites can be associated with O1, O2 or O3 oxygen positions both in H-CHA and H-SAPO-34; iv) in contrast to the common belief the extra BA-OH band in the DRIFT spectra of H-SAPO-34 is associated with Al and not with P atoms.

## I03

### STRUCTURAL COLORATION OF LYCAENID BUTTERFLIES: FROM SEXUAL SIGNALING TO CHEMICALLY SELECTIVE SENSING

*L. P. Biró<sup>1</sup>, K. Kertész<sup>1</sup>, G. Piszter<sup>1</sup>, G. I. Márk<sup>1</sup>, Z. E. Horváth<sup>1</sup>, Zs. Bálint<sup>2</sup>*

<sup>1</sup>Nanostructures Department, Institute of Technical Physics and Materials Science, Centre for Energy Research, Hungarian Academy of Sciences, POB 49, H-1515 Budapest, Hungary; e-mail: biro@mfa.kfki.hu

<sup>2</sup>Department of Zoology, Hungarian Natural History Museum, Baross utca 13, H-1088 Budapest, Hungary

The photonic nanoarchitectures of biologic origin and in particular those occurring in the wing scales of several butterfly species, are more and more in the focus of attention both as sources of bioinspiration and as cheaply produced sensor material for chemically selective vapor sensors [1, 2]. These photonic nanoarchitectures are a nanocomposite of chitin and air, with structural elements typically of the 100 nm size. Beyond the normal biologic variability [3] generally found in any characteristic of living beings the structure and color of these nanoarchitectures is remarkably constant in time over a tested period of 100 years. This is the consequence of role

of sexual signaling color played by the blue coloration of the dorsal wings of the males. We investigated nine closely related lycaenid butterfly species living in the same type of habitat and we found that their coloration and the nanoarchitectures generating the color are species specific [4].

Due to the air filled nanovoids, these structures are well suited for the substance selective detection of the vapors of different volatiles. The capillary condensation of the volatile vapors in an air-vapor mixture into the nanovoids produces the shift of the refractive index contrast between the constituent elements of the photonic crystal type structure and by this the spectral shift of the reflectance maximum [5].

#### References

1. L. P. Biró and J. P. Vigneron: Photonic nanoarchitectures in butterflies and beetles: valuable sources for bioinspiration. *Laser & Photonics Reviews* 5, 27–51 (2011). doi: 10.1002/lpor.200900018
2. G. Piszter, K. Kertész, Z. Vértesy, Z. Bálint and L. P. Biró: Substance specific chemical sensing with pristine and modified photonic nanoarchitectures occurring in blue butterfly wing scales. *Optics Express* 22, 22649–22660 (2014). doi:10.1364/OE.22.022649
3. G. Piszter, K. Kertész, Z. Bálint and L. P. Biró: Variability of structural coloration in two butterfly species having different prezygotic mating strategy. *PLoS ONE*, under review (2016).
4. Z. Bálint, K. Kertész, G. Piszter, Z. Vértesy and L. P. Biró: The well-tuned blues: the role of structural colours as optical signals in the species recognition of a local butterfly fauna (Lepidoptera: Lycaenidae: Polyommatainae). *Journal of the Royal Society, Interface / the Royal Society* 9, 1745–1756 (2012). doi:10.1098/rsif.2011.0854
5. K. Kertész, G. Piszter, E. Jakab, Z. Bálint, Z. Vértesy and L. P. Biró: Color change of Blue butterfly wing scales in an air – vapor ambient. *Applied Surface Science* 281, 49–53 (2013). doi:10.1016/j.apsusc.2013.01.037

## I04

### DEFECTS IN TWO-DIMENSIONAL INORGANIC MATERIALS

Arkady V. Krasheninnikov<sup>1,2</sup>

<sup>1</sup>Helmholtz Zentrum Dresden-Rossendorf, Institute of Ion Beam Physics and Materials Research, Germany; e-mail: a.krasheninnikov@hzdr.de

<sup>2</sup>Department of Applied Physics, Aalto University, Finland

Following isolation of a single sheet of graphene, many other 2D systems such as hexagonal BN sheets and transition metal dichalcogenides (TMDs) were manufactured. Among them, TMDs have received particular attention, as these materials exhibit intriguing electronic and optical properties. Moreover, the properties can further be tuned by introduction of defects and impurities. In my talk, I will present the results [1–5] of our first-principles theoretical studies of defects (native and irradiation-induced) in inorganic 2D systems obtained in collaboration with several experimental transmission electron microscopy groups. I will further discuss defect- and impurity-mediated engineering of the electronic structure of 2D materials.

#### References

1. Y.-C. Lin et al.: *Nature Comm.* 6, 6736 (2015).

2. Y.-C. Lin et al.: *ACS Nano* **9**, 11249 (2015).
3. H.-P. Komsa and A. V. Krasheninnikov: *Phys. Rev. B* **91**, 125304 (2015).
4. O. Lehtinen et al.: *ACS Nano* **9**, 3274 (2015).
5. E. Sutter et al.: *Nano Letters* **16**, 21 (2016).

## I05

### UNDERSTANDING ULTRA-LOW DOPING IN SINGLE-WALLED CARBON NANOTUBES TOWARDS APPLICATIONS

*Paola Ayala*<sup>1,2</sup>

<sup>1</sup>Faculty of Physics, University of Vienna, Boltzmanngasse 5, A-1090 Vienna, Austria;  
e-mail: paola.ayala@univie.ac.at

<sup>2</sup>Yachay Tech, School of Physical Sciences & Nanotechnology, 100119-Urcuquí, Ecuador

The applicability of nanostructured materials owes great part of its success to the proper understanding of their physical properties and the interaction with the surrounding environment. Applications with single-walled carbon nanotubes have brought several breakthroughs in materials science. Among the related studies, several have reported functionalization pathways to control the physical behavior of those materials. One of those functionalization methods is substitutional doping but this method could embrace the presence of few or several foreign atoms. Especially for the low-doping case, understanding the behavior of nanomaterials is critical. I will present an overview and progress report of the use of photoemission spectroscopy, X-ray absorption spectroscopy and photoluminescence as key tools to understand the properties of low dimensional carbon systems with sp<sup>2</sup> hybridization. Keeping in mind that the properties of these materials can be nicely tuned via different functionalization methods like substitutional doping, lattice modifications, adsorption of species, among others, this overview will provide an approach to how these techniques can be utilized to understand and analyze changes in the site-selective valence and conduction bands of single-walled carbon nanotubes.

## I06

### COMPRESSION INDUCED ELECTRICAL RESPONSE OF ENTANGLED NETWORK OF BUCKYPAPER

*Amit Rawal*

Indian Institute of Technology Delhi, India; e-mail: amitrawal77@hotmail.com

Buckypaper (BP) is a planar film that consists of random network of multiwall carbon nanotubes (MWCNTs) held together by means of weak van der Waals interactions at tube-tube junctions. Although individual carbon nanotubes (CNTs) possess remarkable electrical properties but the realization of electrical response for BP is significantly lower but can be enhanced by application of modest compressive stresses. Herein, we report an analytical model for predicting

the electrical resistivity of BP under defined level of compression strain. The predictive piezoresistive model of BP has been developed by formulating a direct relationship with the structural parameters, physical and electrical properties of CNTs. The basis of the piezoresistive model relied upon the geometrical probability approach in combination with classical Hertzian contact mechanics and constriction resistance techniques. A comparison has been made between the theoretical and experimental results of electrical resistivity of BPs with varying densities. Through theoretical modeling, initial fiber volume fraction was found to be one of key parameters that can modulate the piezoresistive behavior of BP.

## I07

### TOWARDS PHOTOCATALYSIS BY DESIGN FOR EFFICIENT WATER SPLITTING

*Kazuhiro Takanabe*

King Abdullah University of Science and Technology (KAUST), KAUST Catalysis Center (KCC) and Physical Science and Engineering Division (PSE), 4700, Thuwal, 23955-6900, Saudi Arabia; e-mail: kazuhiro.takanabe@kaust.edu.sa

A simplified photocatalyst model was used to solve simulations of semiconductor-metal devices. Crucial properties were identified required to achieve a basic but effective design of a particulate system for water splitting. The electrocatalysts on the semiconductors surface are integral components providing anisotropic electric fields for charge separation in the semiconductor (and to enhance the kinetics of the redox reactions which were omitted from these simulations) [1–4]. In our simple model, the metal catalysts collect excited electrons to drive the hydrogen evolution reaction (ohmic junction); whereas the *n*-type semiconductor surface was considered as active for water oxidation under illumination and steady state water-splitting conditions (i.e. a Schottky type of contact was considered for the semiconductor-liquid junction interface). The established model enabled us to calculate the sensitivity of the quantum efficiency (QE) of the system to the various semiconductor properties; such as light absorption, carrier density, mobility and lifetime of the carriers, and to the dispersion of the metal particles, which create heterojunctions, considered as the driving force for charge separation [1, 2]. As a result, a pinch-off effect was prevalent underneath the hydrogen evolution site, suggesting an undesired energetic barrier for electron transport and transfer to the electrocatalyst. Using values reported in the literature [5–9], the simulation revealed that the QE was mostly governed by recombination of carriers in the bulk of the semiconductor particles.

#### References

1. K. Takanabe: *Top. Curr. Chem.* **371**, 73–103 (2016).
2. T. Hisatomi, K. Takanabe and K. Domen: *Catal. Lett.* **145**, 95–108 (2015).
3. K. Takanabe and K. Domen: *ChemCatChem* **4**, 1485–1497 (2012).
4. K. Takanabe and K. Domen: *Green* **1**, 313–322 (2011).
5. A. Ziani, E. Nurlaela, D. S. Dhawale, D. Alves Silva, E. Alarousu, O. F. Mohammed, K. Takanabe: *Phys. Chem. Chem. Phys.* **17**, 2670–2677 (2015).
6. E. Nurlaela, H. Wang, T. Shinagawa, S. Flanagan, S. Ould-Chikh, Z. Mics, P. Sautet, T. Le Bahers, E. Canovas, M. Bonn and K. Takanabe: *ACS Catal.* **6**, 4117–4126 (2016).

7. E. Nurlaela, M. Harb, S. Del Gobbo, M. Vashishta and K. Takanabe: *J. Solid State Chem.* **229**, 219–227 (2015).
8. M. Harb, P. Sautet, E. Nurlaela, P. Raybaud, L. Cavallo, K. Domen, J.-M. Basset and K. Takanabe: *Phys. Chem. Chem. Phys.* **16**, 20548–20560 (2014).
9. E. Nurlaela, S. Ould-Chikh, M. Harb, S. Del Gobbo, M. Aouine, E. Puzenat, P. Sautet, K. Domen, J.-M. Basset and K. Takanabe: *Chem. Mater.* **26**, 4812–4825 (2014).
10. E. Nurlaela, S. Ould-Chikh, I. Llorens, J.-L. Hazemann and K. Takanabe: *Chem. Mater.* **27**, 5685–5694 (2015).
11. A. T. Garcia-Esparza and K. Takanabe: *J. Mater. Chem. A* **4**, 2894–2908 (2016).

## I08

### NANOPOROUS FERROELECTRICS FOR EMERGING APPLICATIONS

*Paula M. Vilarinho*<sup>1</sup>, *Alichandra Castro*<sup>1</sup>, *Leontin Padurariu*<sup>2</sup>, *Liliana Mitoseriu*<sup>2</sup>,  
*Brian Rodriguez*<sup>3</sup>, *Paula Ferreira*<sup>1</sup>

<sup>1</sup>Department of Materials and Ceramic Engineering, University of Aveiro, Aveiro, Portugal;  
e-mail: paula.vilarinho@ua.pt

<sup>2</sup>Department of Physics, Alexandru Ioan Cuza University, Iasi, Romania

<sup>3</sup>School of Physics, University College Dublin, Dublin, Ireland

This talk is about ferroelectrics with nanometric porosity for emerging applications.

Traditional applications of porous materials involve ion exchange, adsorption (for separation) and catalysis. These relevant technical and industrial applications are based on the ability of porous materials to interact with atoms, ions and molecules not only at their surfaces but also throughout the bulk of the material [1]. In general porous materials are light, mechanically fragile and, in what concerns electrical transport (in a broad sense), porosity is generally viewed as deleterious. However, in non-traditional applications porosity may be considered as an added value and exploited as an asset of the material itself or even to host guest species that bring new functionalities. A good example is mesoporous silica as a low dielectric material (low- $k$ ) ( $k < 2$ ), responding for the current need of high-density microships with increasing feature size diminution [2].

In this talk other emerging applications for porous materials will be presented.

The role of nanoporosity in functional perovskite oxides as ferroelectrics and multiferroics is discussed and its beneficial effect for microelectronics presented. The pioneer work that our group has been carrying out in porous ferroelectrics will be presented. For ferroelectrics as BaTiO<sub>3</sub>, PbTiO<sub>3</sub>, BiFeO<sub>3</sub> aspects as the role of the porosity on the microstructure development and phase evolution and the relations between nanoporosity and the electrical properties at the nanoscale will be presented. It will be shown that the crystallization of the tetragonal phase is enhanced in nanoporous films and films with improved tetragonality exhibit enhanced piezoelectric coefficients, switchable polarization and low local coercivity. We also exploit the presence of nanoporosity on the ferroelectric switching behaviour and by using Monte Carlo simulation and Finite Element Model (FEM) we theoretically predict that pores with sizes and interdistances between them lower than the ferroelectric domain size behave as dispersion centers and originate electric field instabilities that promotes polarization switch-

ing, decreasing coercivity. These predictions are proven in  $\text{PbTiO}_3$  nanoporous thin films. This is a relevant result since nanoporosity contributing to decrease the coercive field of thin and ultrathin films may solve a main limitation of scaling ferroelectrics. We also exploit ways to functionalize nanopatterned thin films with magnetic nanoparticles and a proof of concept will be presented.

Similarly to low- $k$  dielectric mesoporous silicas, our work clearly demonstrates that porous ferroelectrics materials may find emerging application in non-traditional areas as microelectronics and related applications.

#### References

1. M. E. Davis. Ordered porous materials for emerging applications. *Nature* **417**, 813–821 (2002).
2. S. Baskaran, J. Liu, K. Domansky, N. Kohler, X. Li, C. Coyle, G. E. Fryxell, S. Thevuthasan and R. E. Williford. Low dielectric constant mesoporous silica films through molecularly templated synthesis. *Adv. Mater.* **12**, 291–294 (2000).

## I09

### NANOLAYERS IN NITRIDE HIGH POWER DEVICES GROWN ON DIAMOND AND GRAPHENE

*Béla Pécz*

Thin Film Physics, MTA EK MFA, Konkoly-Thege u. 29–33, 1121 Budapest, Hungary;  
e-mail: pecz@mfa.kfki.hu

Self-heating of high power devices is a major problem in GaN high electron mobility transistors (HEMT), in which the power reached the values of 10 W/mm (the length of the gate in mm). Therefore the heat dissipation became one of the major issues and substrates with high heat conductivity are needed. Apparently there are two kinds of materials with excellent thermal conductivity which can be used as a heat sink: diamond and graphene.

First a procedure is shown in which GaN layers (device structures) were grown on diamond substrates by molecular beam epitaxy and the deposition process was optimised using transmission electron microscopy (TEM). The grown GaN layers are free of inversion domains and are of high quality [1].

We explore the possibilities of nitride layer growth on graphene/SiC. The task is challenging thanks to the lack of chemical reactivity between the two materials. Therefore instead of direct growth on graphene we present how high quality nitrides can be grown on patterned graphene/SiC templates. The grown samples are analysed by transmission electron microscopy (TEM). The dislocation density is practically the same as in GaN grown on SiC. The thermal properties are investigated by thermo-reflectance over the different parts of the pattern, separately. The first preliminary results show, that the used graphene is a multilayer of 3–5 graphene sheets, but this is advantageous for the high heat conductivity [2].

Moreover we discuss how the graphene/SiC templates can be used in order to grow 2D materials.

## References

1. B. Pécz, L. Tóth, G. Tsiakatouras, A. Adikimenakis, A. Kovács, M. Duchamp, R. E. Dunin-Borkowski, R. Yakimova, P. L. Neumann, H. Behmenburg, B. Foltynski, C. Giesen, M. Heuken and A. Georgakilas: GaN heterostructures with diamond and graphene. *Semicond. Sci. Technol.* **30**, 114001 (6 pp) (2015).
2. A. Kovács, M. Duchamp, R. E. Dunin-Borkowski, R. Yakimova, P. L. Neumann, H. Behmenburg, B. Foltynski, C. Giesen, M. Heuken and B. Pécz: Graphoepitaxy of high-quality GaN layers on graphene/6H-SiC. *Advanced Materials Interfaces* **2**, 1400230 (6 pp) (2015).

## I10

**PROGRESS IN INTEGRATION OF INDIVIDUAL AS GROWN SINGLE-WALLED CARBON NANOTUBES INTO FIELD-EFFECT TRANSISTOR BASED ULTRA-LOW POWER GAS SENSORS**

*Miro Haluska, Wei Liu, Cosmin Roman, Christofer Hierold*

Micro and Nanosystems DMAVT ETH Zurich, Tannenstrasse 3, 8092 Zurich, Switzerland;  
e-mail: haluska@micro.mavt.ethz.ch

Exceptional properties of Single-Walled Carbon Nanotubes (SWCNTs) promote them to be the functional material of choice in a new generation of sensors with ultra-low detection limits, ultra-low power consumption and small size. Although outstanding performances of various types of demonstrator devices based on SWCNTs has been already shown, several challenges remain to be solved on the way to reach large scale fabrication needed by certain applications. A known bottleneck for SWCNT based sensors is the low quality of contacts between SWCNT and metal leads.

In this talk, we will review progress made in synthesis of SWCNTs with targeted properties because of its strong influence on performance and fabrication efficiency of devices based on individual SWCNTs. Further, we will focus on a fabrication of field-effect transistors with individual SWCNT channels (CNFETs) having electrical contacts with long lifetime and narrow distribution of device on-resistances. The presented approach is based on combination of a sacrificial layer protecting as-grown SWCNTs during CNFETs fabrication, plasma oxidation to remove photoresist residuals from contact areas and deposition of optimized thickness of the Cr adhesion layer prior to noble metal deposition for electrical contacts. The approach will be illustrated on fabrication of NO<sub>2</sub> gas sensors. The process flow starts with synthesis of SWCNTs using ferritins, biological nano-cages, as catalyst precursors because they allow independent control of size, composition and density of catalyst particles at the substrate surface [1, 2]. Nanotube synthesis is performed by CVD using CH<sub>4</sub>/H<sub>2</sub> at 850 °C [2]. As grown SWCNTs are covered by Al<sub>2</sub>O<sub>3</sub> sacrificial layer deposited by ALD to prohibit their direct exposition to resist [3] and to protect them from oxygen plasma impact during further processing. Al<sub>2</sub>O<sub>3</sub> layers thicker than 18 nm protect SWCNT sufficiently from the impact of 100 W oxygen plasma as we proved by CNFET electrical measurements and SWCNT Raman spectroscopy. The sacrificial alumina layer is then removed by H<sub>3</sub>PO<sub>4</sub> prior to contact metallization. We have shown [4] that utilization of this protective/sacrificial layer greatly improves the cleanliness of nanotube surfaces without detectable change of their original properties. The median on-resistance for

alumina passivated, Pd/Au-contacted CNFETs reached 190 kOhm which is 66% lower than the one of CNFETs prepared without using sacrificial layer and oxygen ashing. The inter-quartile dispersions of the CNFETs on-resistance and  $I_{sd}-V_g$  hysteresis width were narrowed from 2050 to 247 kOhm and 3.7 to 1.2 V, respectively. Additionally we will present the effect of the Cr adhesion layer thickness on the CNFET transfer characteristics of Cr/Au-contacted devices. We showed that 0.4 nm Cr deposit already has an impact on the charge carrier transport in Schottky-barrier-CNFETs. The ratio of the p- and n-branch on-resistances increased by 8 times when the Cr thickness increased from 0 to 8 nm. We observed long lifetime of devices (longer as 90 days) even for non-passivated CNFETs using Cr layer thinner than 2 nm in Cr/Au contacts [4]. Finally, limits of detection below 100 ppb of  $\text{NO}_2$  at room temperature utilizing individual suspended SWCNT as transistor channel will be shown [5] as well as investigations of the cross sensitivity to humidity. Sensor recovery by channel self-heating enabled by the suspended device architecture and consuming only about 3  $\mu\text{W}$  will also be presented.

#### References

1. K. Chikkadi et al.: *Microelectronic Eng.* **88**, 2478 (2011).
2. (a) L. Durrer et al.: *Sens. Actu. B* **132**, 485 (2008). (b) L. Durrer et al.: *Nanotechnol.* **20**, 355601 (2009).
3. W. Liu et al.: *Sensors and Actuators B* **198**, 479 (2014).
4. W. Liu et al.: *Nanotechnology* **27**, 015201 (2016).
5. K. Chikkadi et al.: *Appl. Phys. Lett.* **103**, 223109 (2013).

## I11

### ZnO NANOPARTICLES CATALYST IN SYNTHESIS OF XANTHENE AND 1,8-DIOXO-OCTAHYDROXANTHENE

Ali Gharib<sup>1,2</sup>

<sup>1</sup>Department of Chemistry, Islamic Azad University, Mashhad, Iran;

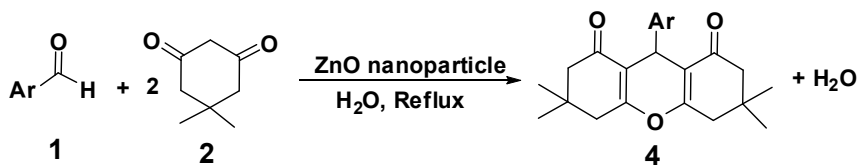
e-mail: organiccatalyst2008@gmail.com

<sup>2</sup>Agricultural Researches and Services Center, Mashhad, Iran

Xanthenes and benzoxanthenes are important class of compounds that are found in numerous biologically active molecules. This structural motif has also been investigated for a wide range of activities such as bactericidal [1], anti-inflammatory [2]. A simple and facile synthesis of 14-aryl-14H-dibenzo[a,j]xanthenes and 1,8-dioxo-octahydroxanthene derivatives has been successfully developed by treatment of  $\beta$ -naphthol or dimedone with aldehydes under mild conditions in the presence of ZnO nanoparticles catalyst. These catalytic condensation reactions represent green chemical processes and ZnO nanoparticles catalyst is cost-effective, easy to handle, and easily removed from the reaction mixtures and also, ZnO nanoparticles catalyst was found to be highly efficient, eco-friendly and recyclable heterogeneous catalyst for the multicomponent reaction of dimedone, aromatic aldehydes, and a nitrogen source (ammonium acetate or aromatic amines) under solvent-free conditions, giving rise to 1,8-dioxodecahydroacridines in high yields. We wish to report for the first time a facile and efficient synthetic strategy for the preparation of 1,8-dioxo-octahydroxanthenes by the reaction of dimedone with

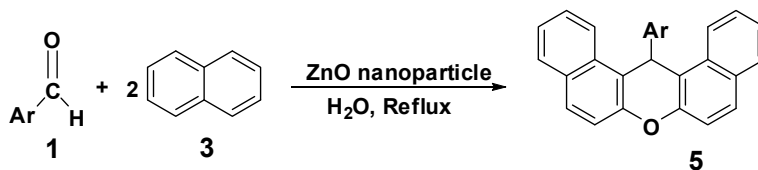


aromatic aldehydes at reflux and using ZnO nanoparticles as a heterogeneous catalyst under green solvent (water) conditions (Scheme 1).



**Scheme 1.** Synthesis of 1,8-dioxo-octahydroxanthene using ZnO nanoparticles catalyst

Herein report a new, convenient, mild, and efficient procedure for the synthesis of 14-aryl-14*H*-dibenzo[*a,j*]xanthene derivatives catalyzed by ZnO nanoparticles as an effective and novel nanocatalyst requiring only mild reaction conditions (Scheme 2).



**Scheme 2.** 14-aryl-14*H*-dibenzo[*a,j*]xanthene in the presence of ZnO nanoparticles catalyst under reflux conditions

#### References

1. T. Hideo: *Jpn Tokkyo Koho JP 56005480* (1981).
2. J. P. Poupelin, G. Saint-Ruf, O. Foussard-Blanpin, G. Narcisse, G. Uchida Ernouf and R. Lacroix: *Eur. J. Med. Chem.* **13**, 67 (1978).

## ORAL PRESENTATIONS

Wednesday, 12 October, 2016

**O01**

### **A PHOTOFUNCTIONAL BOTTOM-UP BIS(DIPYRRINATO)ZINC(II) COMPLEX NANOSHEET**

*Ryota Sakamoto*<sup>1,2</sup>

<sup>1</sup>Department of Chemistry, Graduate School of Science, The University of Tokyo, 7-3-1, Hongo, Bunkyo-ku, Tokyo 113-0033, Japan; e-mail: sakamoto@chem.s.u-tokyo.ac.jp

<sup>2</sup>JST-PRESTO, 4-1-8, Honcho, Kawaguchi, Saitama 332-0012, Japan

Two-dimensional polymeric nanosheets have recently gained much attention of scientists. Particularly, top-down nanosheets such as graphene, metal oxides, metal dichalcogenides, and metal hydroxides that originate from bulk layered mother materials are regarded as promising nanomaterials for applications in electronics, photonics and spintronics. Another type of nanosheets, namely molecule-based bottom-up nanosheets, is emerging. A significant advantage of the bottom-up synthesis is that structures can be customized at will through the selection of components (for example, metal ions and organic ligand molecules). Therefore, the bottom-up approach may broaden the diversity and utility of nanosheets. Although previous reports on bottom-up nanosheets have concentrated on the fabrication and analysis of various two-dimensional structures, no functionality has been demonstrated thus far. Here, the author shows the design and synthesis of a bottom-up nanosheet featuring a photoactive bis(dipyrrinato)zinc(II) complex motif. A liquid/liquid interfacial synthesis between a threeway dipyrrin ligand and zinc(II) ions results in a multi-layer nanosheet with large domain sizes. On the other hand, an air/liquid interfacial reaction produces a single-layer or few-layer nanosheet with domain sizes of  $>10\ \mu\text{m}$  on one side. These synthetic procedures are distinct from conventional one-phase reactions, which in this case result in disordered solids. The bis(dipyrrinato)zinc(II) metal complex nanosheet is easy to deposit on various substrates using the Langmuir–Schäfer process. The Langmuir–Schäfer process also affords quantitative layering of the single-layer nanosheet. The nanosheet deposited on a semiconductive transparent  $\text{SnO}_2$  electrode functions as a photoanode in a photoelectric conversion system, and is thus the first photofunctional bottom-up nanosheet.<sup>1</sup>

#### **Reference**

1. R. Sakamoto, K. Hoshiko, Q. Liu, T. Yagi, T. Nagayama, S. Kusaka, M. Tsuchiya, Y. Kitagawa, W.-Y. Wong and H. Nishihara: A photofunctional bottom-up bis(dipyrrinato)zinc(II) complex nanosheet. *Nat. Commun.* **6**, 6713, (2015).

## O02

## SIZE-DEPENDENT AGGREGATION BEHAVIOR OF GRAPHENE OXIDE SHEETS IN ELECTROLYTE SOLUTIONS

*Tamás Szabó*<sup>1</sup>, *Plinio Maroni*<sup>2</sup>, *István Szilágyi*<sup>2</sup>

<sup>1</sup>Department of Physical Chemistry and Materials Science, University of Szeged, Hungary;  
e-mail: sztamás@chem.u-szeged.hu

<sup>2</sup>Department of Inorganic and Analytical Chemistry, University of Geneva, Switzerland;  
e-mail: istvan.szilagyi@unige.ch

Aqueous-phase exfoliation (individual separation of elementary layers) of multilayered graphite oxide (MLGO) to single-layer graphene oxide (SLGO) is a promising strategy to prepare bulk amounts of graphene based materials. A crucial point to the reproducible fabrication of solution-processed graphene materials (thin films, nanocomposites, etc.) is the knowledge and possible control of the dispersion stability of MLGO and SLGO. While this issue has largely been overlooked until several years ago, Chowdhury et al. [1] presented first results on the aggregation of GO's, revealing that their aggregation and stability in the aquatic environment followed colloidal theory (DLVO and Schulze-Hardy rule), even though GO's shape is not spherical. Following, Wu et al. presented somewhat contradictory results pointing out a significant pH-dependence in the colloidal stability of GO samples prepared by the same (Hummers–Offeman) method [2].

Herein, we present new quantitative results of the charging and aggregation of graphene oxide dispersions. Particularly, we (i) clarify the effect of pH on the colloidal stability in light of the previously published contradictory results. Additionally, by obtaining MLGO samples by the Brodie method, we (ii) reveal the effect of this oxidation protocol, which also influences the exfoliation and dispersion properties by the marked difference in the surface chemistry of as-synthesized samples. Lastly, we (iii) explore the size dependence of the colloidal stability by demonstrating stability plots of GO fractionated into three size intervals by differential centrifugation of exfoliated suspensions. Our findings show that the size fractions with markedly different hydrodynamic radii (spanning from the micrometer to the nanometer size level) exhibit highly different coagulation kinetics in the presence of a simple monovalent salt. This result may find important use in the formulation of GO dispersions allowing for a simple way towards hindering their aggregation by the decrease of particle size.

## References

1. I. Chowdhury, M. C. Duch, N. D. Mansukhani, M. C. Hersam and D. Bouchard: Colloidal properties and stability of graphene oxide nanomaterials in the aquatic environment. *Environ. Sci. Technol.* **47**, 6288–6296 (2013).
2. L. Wu, L. Liu, B. Gao, R. Munoz-Carpena, M. Zhang, H. Chen, Z. Zhou and H. Wang: Aggregation kinetics of graphene oxides in aqueous solutions: experiments, mechanisms, and modeling. *Langmuir* **29**, 15174–15181 (2013).

**O03****STM INVESTIGATION OF POINT DEFECTS IN VARIOUS TRANSITION-METAL DICHALCOGENIDE SINGLE LAYERS**

Gábor Zsolt Magda<sup>1</sup>, János Pető<sup>1</sup>, Péter Vancsó<sup>1</sup>, Zakhar Popov<sup>2</sup>, Pavel B. Sorokin<sup>3</sup>, Chanyong Hwang<sup>4</sup>, László P. Biró<sup>5</sup>, Levente Tapasztó<sup>1</sup>

<sup>1</sup>Centre for Energy Research, Institute of Technical Physics and Materials Science, 2D Nanoelectronics “Lendület” Research Group, Budapest, Hungary

<sup>2</sup>National University of Science and Technology MISiS, Moscow, Russia

<sup>3</sup>Technological Institute of Superhard and Novel Carbon Materials, Moscow, Russia

<sup>4</sup>Korea Research Institute of Standards and Science, Center for Nanometrology, Daejeon, South Korea

<sup>5</sup>Centre for Energy Research, Institute of Technical Physics and Materials Science, Nanotechnology Department, Budapest, Hungary

In the last few years, more and more two dimensional (2D) materials have been isolated, most of them from the transition-metal dichalcogenide (TMDC) family. In order to use these materials in future electronic applications, experimental data on their realistic structure and properties are required. One of the limiting factors is expected to be the relatively high concentration of the native structural defects occurring in these materials, which substantially affect the electronic properties [1]. In this work we present detailed atomic resolution Scanning Tunneling Microscopy (STM) investigations of single layers of four members of the TMDC family: MoS<sub>2</sub>, MoSe<sub>2</sub>, WS<sub>2</sub>, WSe<sub>2</sub> and compare their native point defect concentration. The single layer TMDCs were prepared by a novel exfoliation technique [2]. The STM investigations show various types of point defects at high concentration for MoS<sub>2</sub>, WS<sub>2</sub> and lower concentration for MoSe<sub>2</sub>, WSe<sub>2</sub>. Using DFT density functional calculations the observed point defects were identified as vacancies and dopants, where the differences in the defect concentrations are related to the significantly different behavior of the sulfurs and selenides during the oxidation process.

Our results provide experimental and theoretical insight into atomic and electronic structure of point defects in single-layer TMDCs which is essential for understanding the operation of realistic devices.

**References**

1. J.-Y. Noh et al.: *Phys. Rev. B* **89**, 205417 (2014).
2. G. Zs. Magda et al.: *Sci. Rep.* **5**, 14714 (2015).

**O04****NANOHOLE STRUCTURES BASED ON BILAYERS OF 2D MATERIALS: FORMATION, THEIR ELECTRONIC PROPERTIES AND APPLICATIONS**

Leonid Chernozatonskii<sup>1</sup>, Stefano Bellucci<sup>2</sup>, Victor A. Demin<sup>1</sup>, Dmitry G. Kvashnin<sup>1</sup>, Philippe Lambin<sup>3</sup>, Pavel B. Sorokin<sup>1</sup>

<sup>1</sup>Emanuel Institute of Biochemical Physics of RAS, 119334 Moscow, Russia

<sup>2</sup>National Institute of Nuclear Physics, Via E. Fermi 40, 00044 Frascati, Italy

<sup>3</sup>Department of Physics, University of Namur, 61 Rue de Bruxelles, 5000 Namur, Belgium

Two-dimensional structures are attractive materials for application use, because they have many unique properties. For example, graphene and boron nitride – a plane of hexagonally arranged carbons – has such properties as high strength and thermal conductivity. The latest achievements in 2D material researches have shown perspective uses of sandwich structures in nano-devices. It is known that in single 2D layers electron or ionic beams form vacancy defects which lead to changing of their electronic and mechanic properties. During the cutting of bilayer graphene by electron beam the edges of neighboring layers are connected.

Here we present our last results of studying of nanohole structures based on bilayers of 2D materials (mainly bigraphene, G/BN) [1–5]. We consider possible formation of some specific structures by controlled cutting of bigraphene or graphene/boron nitride 2D bi-layers with holes in which the atoms on the edges interconnected sp<sup>2</sup>-hybridized C-C bonds (C-B and C-N) to form continuous transitions from one layer to the topological defects inside the holes. We studied stable atomic structures of these compounds moiré type (with different angles of rotation relative to a monolayer of graphene hexagonal boron nitride) with closed “circular” holes positioned in moiré superlattice AA and AB in packaging centers.

The method of density functional theory was applied for investigation the stability and electronic properties of bigraphene and G/BN nanomeshes. It was shown that they exhibit both metal (hole structures with symmetry of graphene) and semiconductor properties depending not only on the size of the holes and the distance between them, but also on the shape of the holes. Their electronic band structures differ from those of the individual single-layered nanomeshes with the same geometry and location of the holes.

Some applications of considered nanohole structures are proposed for nanoelectronic and nanooptics devices.

This work was supported by RSF № 14-12-01217 and 7th European Community Framework Programme (MC-IRSES proposal 318617 FAEMCAR project).

#### References

1. L. A. Chernozatonskii, V. A. Demin and A. A. Artyukh: *JETP Lett.* **99**, 309 (2014).
2. D. Kvashnin, P. Vancsó, L. Antipina, G. Márk, L. Biró, P. Sorokin and L. Chernozatonskii: *Nano Res.* **8**, 1250 (2015).
3. L. Chernozatonskii, V. Demin and P. Lambin: Bilayer graphene as platform of nanostructures with folded edge holes. *J. Phys. Chem. Chem. Phys.* in press (2016).
4. L. Chernozatonskii, V. Demin and S. Belucci: Bi-layered nanostructures with folded holes based on Moiré h-BN-graphene patterns: modeling of geometry and electronic properties. *Sci. Rep.* in press (2016).
5. L. Chernozatonskii, V. Demin and A. Artyukh: *JETP Lett.* **99**, (2016).

## O05

### THE STRUCTURE AND PROPERTIES OF GRAPHENE SUSPENDED ON NANOPARTICLES

*Zoltán Osváth*<sup>1,3</sup>, *György Molnár*<sup>1</sup>, *Krisztián Kertész*<sup>1,3</sup>, *András Deák*<sup>1</sup>, *Norbert Nagy*<sup>1</sup>, *Chanyong Hwang*<sup>2,3</sup>, *László P. Biró*<sup>1,3</sup>

<sup>1</sup>Institute of Technical Physics and Materials Science, MFA, Centre for Energy Research, HAS, P.O. Box 49, 1525 Budapest, Hungary; e-mail: zoltan.osvath@energia.mta.hu

<sup>2</sup>Center for Nano-metrology, Korea Research Institute of Standards and Science, Daejeon 305-340, South Korea

<sup>3</sup>Korea-Hungary Joint Laboratory for Nanosciences (KHJLN), P.O. Box 49, 1525 Budapest, Hungary

Corrugated graphene can be a good candidate for sensor applications due to its enhanced chemical activity [1]. The possibility of using nanoparticles to impart extrinsic rippling to graphene has not been fully explored yet. Here we study the structure and elastic properties of graphene grown by chemical vapour deposition (CVD) and transferred onto a continuous layer of SiO<sub>2</sub> nanoparticles with diameters of around 25 nm, prepared on a Si substrate by the Langmuir–Blodgett technique. We show that the corrugation of the transferred graphene, and thus the membrane strain, can be modified by annealing at moderate temperatures. The graphene parts bridging the nanoparticles are suspended and can be reversibly lifted by the attractive forces between an atomic force microscope tip and graphene [2]. This allows the dynamic control of the local morphology of graphene nanomembranes.

Furthermore, we prepared a graphene-gold hybrid nanomaterial by transferring CVD grown graphene onto closely spaced gold nanoparticles produced on a silica wafer. Such material provides a unique platform to study metal–graphene interactions at the nanoscale and constitutes an advanced substrate for surface-enhanced Raman scattering (SERS). The morphology and physical properties of nanoparticle-supported graphene are investigated by atomic force microscopy, optical reflectance spectroscopy, scanning tunneling microscopy and spectroscopy (STM/STS), and confocal Raman spectroscopy [3]. This study shows that the graphene Raman peaks are enhanced by a factor which depends on the excitation wavelength, in accordance with the surface plasmon resonance of the gold nanoparticles, and also on the graphene–nanoparticle distance which is tuned by annealing at moderate temperatures. STM and STS measurements show that the electrostatic doping of graphene is modulated by the quasi-periodicity of the underlying gold nanoparticles.

#### References

1. D. W. Boukhvalov and M. I. Katsnelson: Enhancement of chemical activity in corrugated graphene. *J. Phys. Chem. C* **113**, 14176–14178 (2009).
2. Z. Osváth, E. Gergely-Fülöp, N. Nagy, A. Deák, P. Nemes-Incze, X. Jin, C. Hwang and L. P. Biró: Controlling the nanoscale rippling of graphene with SiO<sub>2</sub> nanoparticles. *Nanoscale* **6**, 6030–6036 (2014).
3. Z. Osváth, A. Deák, K. Kertész, Gy. Molnár, G. Vértesy, D. Zámbo, C. Hwang and L. P. Biró: The structure and properties of graphene on gold nanoparticles. *Nanoscale* **7**, 5503–5509 (2015).

## O06

### INVESTIGATION OF GRAPHENE-GOLD HYBRID NANOSTRUCTURES BY SCANNING TUNNELLING MICROSCOPY AND SPECTROSCOPY

*András Pálinkás*<sup>1,3</sup>, *Péter Süle*<sup>1</sup>, *György Molnár*<sup>1</sup>, *Chanyong Hwang*<sup>2,3</sup>, *László P. Biró*<sup>1,3</sup>, *Zoltán Osváth*<sup>1,3</sup>

<sup>1</sup>Institute of Technical Physics and Materials Science, MFA, Centre for Energy Research, HAS, 1121 Budapest, Hungary

<sup>2</sup>Center for Nano-metrology, Korea Research Institute of Standards and Science, Daejeon 305-340, South Korea

<sup>3</sup>Korea-Hungary Joint Laboratory for Nanosciences (KHJLN), 1121 Budapest, Hungary

Two-dimensional graphene shows promise for many technological applications. Combining graphene with other materials can multiply its benefits by engineering the desired properties. Graphene-metal nanoparticle hybrid materials potentially display not only the unique properties of metal nanoparticles and those of graphene, but also additional novel properties due to the interaction between graphene and nanoparticles [1]. In this work we prepared such new type of hybrid nanomaterials by transferring graphene onto polycrystalline gold nanoislands. We investigated the samples by STM and STS [2]. After multiple annealing procedures we found that graphene induces surface re-crystallisation of the supporting gold nanoparticles. We showed that gold nanoislands, in turn, can be used to tailor the local electronic properties of graphene. Graphene on crystalline gold nanoislands exhibits moiré superlattices, which generate secondary Dirac points in the local density of states. Room temperature charge localization and anomalously large wavelength moiré patterns are observed. Such large wavelength moiré cannot be formed simply by the rotation misorientation of the moiré superlattice. We show using DFT-adaptive molecular dynamics simulations that in such cases the graphene and the interfacial metallic layer is strained, leading to altered lattice constants in both graphene and the interfacial gold layer. These findings can open a route towards the realization of engineered graphene/metal surfaces and interfaces with various moiré superlattices and tailored local electronic properties.

#### References

1. K. T. Nguyen and Y. Zhao: Integrated graphene/nanoparticle hybrids for biological and electronic applications. *Nanoscale* **6**, 6245–6266 (2014).
2. A. Pálinkás, P. Süle, M. Szendrő, G. Molnár, C. Hwang, L. P. Biró and Z. Osváth: Moiré superlattices in strained graphene-gold hybrid nanostructures. *Carbon* (2016). doi: 10.1016/j.carbon.2016.06.081

## ORAL PRESENTATIONS

Thursday, 13 October, 2016

O07

### STABILIZATION OF ENZYME-LAYERED DOUBLE HYDROXIDE NANOCOMPOSITES IN SUSPENSIONS

Marko Pavlovic, Paul Rouster, István Szilágyi

Department of Inorganic and Analytical Chemistry, University of Geneva, CH-1205 Geneva, Switzerland; e-mail: istvan.szilagyi@unige.ch

Enzyme delivery in biomedical processes is challenging due to the complex environment in the biofluids. Immobilizing enzymes on nanoparticles may lead to successful targeted transport and can also protect the biocatalysts. However, colloidal stability has to be well-controlled since the aggregation of the carrier particles gives rise to inefficient delivery [1]. The present study focuses on the immobilization of superoxide dismutase (SOD) on layered double hydroxide (LDH) nanoparticles and on the formulation of the resulted nanocomposites. SOD adsorption (LDH-SOD) was confirmed by IR spectroscopy and by determining the adsorbed amount with spectrophotometry. Very similar enzymatic activities were observed for both bare and immobilized enzymes. Colloidal stability of the obtained material was studied in time-resolved dynamic light scattering experiments at different ionic strengths. The aggregation rates were expressed in terms of stability ratios, which are close to one in case of unstable samples, while higher values refer to more stable suspensions. As shown in *Figure 1*, LDH-SOD platelets possessed only limited stability indicated by a low critical coagulation concentration (CCC) value. Heparin (a highly charged

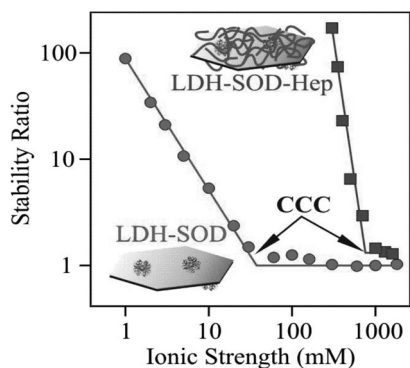


**Fig. 1.** Stability ratios of LDH-SOD and LDH-SOD-Hep particles as a function of the ionic strength determined in aqueous suspensions

natural anticoagulant) coating resulted in charge inversion, i.e., negatively charged particles (LDH-SOD-Hep), which were substantially more resistant to aggregation than the LDH-SOD. For LDH-SOD-Hep, highly stable suspensions were obtained until very high ionic strengths, even in the range where the traditional theories predict rapid particle aggregation. We assume that both steric and electrostatic repulsions are responsible for this enormous stabilizing effect. The obtained LDH-SOD-Hep nanocomposites showed good SOD-like activity. Due to the improved colloidal stability, the developed enzymatic system is a promising antioxidant candidate for biomedical or other manufacturing processes wherever the aim is to decompose reactive oxygen species in suspensions.

#### Reference

1. M. Pavlovic, L. Li, F. Dits, Z. Gu, M. Adok-Sipiczki and I. Szilágyi: Aggregation of layered double hydroxide in the presence of heparin: towards highly stable delivery systems. *RSC Adv* **6**, 16159–16167 (2016).



**O08****IN VITRO STUDY OF SILICON QUANTUM DOTS IN HUMAN CELLS**

*Lucie Ostrovská<sup>1</sup>, Hiroshi Sugimoto<sup>2</sup>, Anna Fucikova<sup>3</sup>, Tereza Belinova<sup>4</sup>, Takashi Kanno<sup>2</sup>, Minoru Fujii<sup>2</sup>, Jan Valenta<sup>3</sup>, Marie Hubalek Kalbacova<sup>1,5</sup>*

<sup>1</sup>Biomedical Centre, Faculty of Medicine in Pilsen, Charles University in Prague, Pilsen, Czech Republic

<sup>2</sup>Department of Electrical and Electronic Engineering, Graduate School of Engineering, Kobe, Japan

<sup>3</sup>Faculty of Mathematics and Physics, Charles University in Prague, Prague, Czech Republic

<sup>4</sup>Department of the Cell Biology, Faculty of Science, Charles University in Prague, Prague, Czech Republic

<sup>5</sup>Institute of Inherited Metabolic Disorders, 1st Faculty of Medicine, Charles University in Prague, Prague, Czech Republic; e-mail: marie.kalbacova@lf1.cuni.cz

Silicon (Si) is by far the most important semiconductor material enabling high-performance microelectronic and photovoltaic devices. Application spectrum of silicon further expands in the field of optoelectronics and photonics and at the same time, significant potential of silicon quantum dots (SiQD) has been revealed for their possible application in biology and medicine. SiQD can fulfil their potential in biomedicine because of their biocompatibility, low toxicity and natural biodegradability unlike the current semiconductor quantum dots. In this study, SiQDs co-doped with boron and phosphorus were used for *in vitro* evaluation of the cytotoxicity for human osteoblastic cell line (SAOS-2). Experiments were performed with 2 types of SiQD labeled according to their annealing temperatures 1100 (~4 nm) and 1050 (~3 nm) which both display long lasting dispersion in methanol or aqueous solutions and photoluminescence insensitive to the changes of the environment and to surface modification.

Results revealed a significant difference between tested SiQD in their behavior in cell culture environment depending on their increasing concentrations (25–125 µg/ml). Mainly, the crucial influence of the proteins from fetal bovine serum (component of cultivation medium) on SiQD is described. Cytotoxicity and capability of SiQD to enter the cells over time was subsequently affected by these conditions. Description of the optical parameters and evaluation of zeta potential of SiQD were carried out for a more complex understanding of observed *in vitro* findings.

**O09****NANOSCALED PORPHYRINIC METAL-ORGANIC FRAMEWORK: TOWARDS APPLICATIONS IN PHOTODYNAMIC THERAPY**

*Jan Demel<sup>1</sup>, Daniel Bůžek<sup>1</sup>, Jaroslav Zelenka<sup>2</sup>, Tomáš Ruml<sup>2</sup>, Kaplan Kirakci<sup>1</sup>, Kamil Lang<sup>1</sup>*

<sup>1</sup>Institute of Inorganic Chemistry of the Czech Academy of Sciences, v.v.i., Husinec-Řež 1001, 250 68 Řež, Czech Republic; e-mail: demel@iic.cas.cz

<sup>2</sup>University of Chemistry and Technology, Technická 5, 166 28 Prague, Czech Republic

Metal-organic frameworks (MOFs) are porous coordination polymers. MOFs consist of coordinated metal atoms forming secondary building units (SBU) which are connected by organic linkers. In recent years, MOFs are extensively studied for gas storage and separation, drug delivery, catalysis and sensing applications.

Porphyrin containing MOFs are attracting attention due to their rigid geometry, variable structure. Recently, we showed that porphyrin-containing MOFs effectively produce singlet oxygen,  $O_2(^1\Delta_g)$ , a reactive form of oxygen [1]. Singlet oxygen has cytotoxic effects and its ability to inactivate tumour cells is a basis for the applications in photodynamic therapy (PDT). In our work, we prepared nanoparticles of MOF-545/PCN-222, composed of 5,10,15,20-tetrakis(4-carboxyphenyl)porphyrin units and  $Zr_6O_4(OH)_4$  secondary building units, and investigated their toxic/phototoxic effects.

Three different sizes of MOF-545/PCN-222 nanoparticles, ranging from 30 to 300 nm, were prepared. The XRD patterns and textural parameters documented that pure MOF-545/PCN-222 phases were obtained in all cases. The shape and size distributions were determined by SEM and TEM measurements (*Figure 1*). UV-vis absorption and fluorescence measurements indicated that incorporated porphyrin units in the MOF framework keep suitable photophysical properties and productivity of  $O_2(^1D_g)$ . Dark toxicity as well as phototoxicity upon light irradiation was studied on the human cervix carcinoma HeLa cell line. The performed tests showed negligible dark toxicity of the MOF nanoparticles, whereas phototoxicity led to deactivation over 90% of tumour cells.

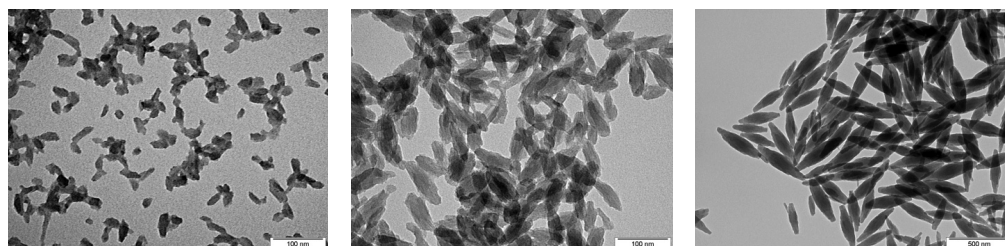


Fig. 1. TEM images of MOF nanoparticles

#### Reference

1. J. Demel, P. Kubát, F. Millange, J. Marrot, I. Císařová and K. Lang: Lanthanide-porphyrin hybrids: from layered structures to metal-organic frameworks with photophysical properties. *Inorg. Chem.* 52, 2779–2786 (2013).

## O10

### PREPARATION OF NANOSTRUCTURED SnO PARTICLES THROUGH CRYSTAL GROWTH IN THE PRESENCE OF BIOLOGICAL POLYMERS

*Hiroaki Uchiyama, Shunsuke Nakanishi, Hiromitsu Kozuka*

Department of Chemistry and Materials Engineering, Kansai University, 3-3-35 Yamate-cho, Suita, 564-8680, Japan; e-mail: h\_uchi@kansai-u.ac.jp

Biomineralization has attracted much attention as a good model for aqueous solution processes for preparing nanostructured inorganic materials. Carbonate-based biominerals such as naces and eggshells are found to consist of oriented and bridged calcite nanounits of 10–50 nm and to contain biological polymers in the bridged structures [1]. Biological polymers are adsorbed

on the surface of carbonate crystals, leading to the formation of hierarchical nanostructures. These suggest that biomimetic aqueous solution routes with biological polymers would allow us to achieve the fabrication of the nanostructured inorganic materials. In this work, we addressed the preparation of nanostructured SnO particles via an aqueous solution route assisted by biological polymers. Crystalline SnO particles were prepared by aging  $\text{Sn}_6\text{O}_4(\text{OH})_4$  at 60 °C in aqueous solutions containing gelatin. We investigated the effect of gelatin on the nanostructure of SnO crystals [2, 3].

1.25 g of  $\text{SnF}_2$  were added into a 40  $\text{cm}^3$  NaOH aqueous solutions of pH 13.5 under stirring at room temperature ( $[\text{SnF}_2] = 0.2 \text{ M}$ ), where  $\text{Sn}_6\text{O}_4(\text{OH})_4$  precipitates were immediately produced. The  $\text{Sn}_6\text{O}_4(\text{OH})_4$  precipitates were removed from the solutions by centrifugation. HCl aqueous solutions of pH 2.0 were prepared separately, and then 0–0.12 g of gelatin were dissolved in 40  $\text{cm}^3$  of the HCl solutions under stirring at 80 °C ( $[\text{gelatin}] (C_{\text{ge}}) = 0\text{--}3.0 \text{ g L}^{-1}$ ). The gelatin solutions were cooled to room temperature and then mixed with the  $\text{Sn}_6\text{O}_4(\text{OH})_4$  precipitates. The suspensions thus obtained were aged at 60 °C for 1–20 days, resulting in the formation of SnO crystals.

The XRD patterns attributed to SnO were observed irrespective of  $C_{\text{ge}}$ . The SnO particles prepared at  $C_{\text{ge}} = 0 \text{ g L}^{-1}$  were found to be random aggregates of platy units of 100–200  $\mu\text{m}$  in width and below 1  $\mu\text{m}$  in thickness. The morphology of the SnO products changed from random aggregates to spheres with increasing  $C_{\text{ge}}$ . Spherical particles with a smooth surface were produced at  $C_{\text{ge}} = 3.0 \text{ g L}^{-1}$ , which consisted of densely branched platy units below 100 nm in thickness (Figure 1). The addition of gelatin could lead to the diffusion-controlled growth of SnO crystals, resulting in the branching of crystals. As a result, the spheres consisting of radial-ly-branched platy units were obtained with increasing  $C_{\text{ge}}$ .

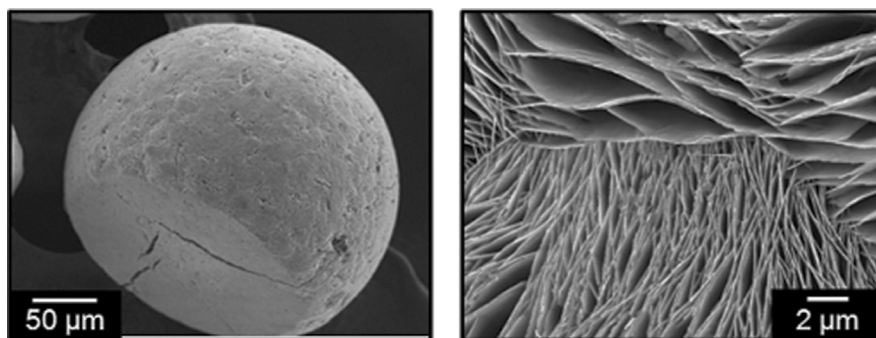


Fig. 1. FE-SEM images of the SnO particles prepared at  $C_{\text{ge}} = 3.0 \text{ g L}^{-1}$

#### References

1. Y. Oaki and H. Imai: *Angew. Chem., Int. Ed.* **44**, 6571 (2005).
2. H. Uchiyama, S. Nakanishi and H. Kozuka: *J. Solid State Chem.* **217**, 87 (2014).
3. H. Uchiyama, S. Nakanishia and H. Kozuka: *CrystEngComm* **17**, 628 (2015).

**O11****PHYSICOCHEMICAL CHARACTERIZATION OF ORGANICALLY MODIFIED SILICA GELS OBTAINED BY SOL-GEL PROCESS***Zoltán Dudás, Adél Len, László Almásy*

MTA Wigner Research Center for Physics, Konkoly Thege Miklós Street 29–33, 1121 Budapest, Hungary;  
e-mail: [dudas.zoltan@wigner.mta.hu](mailto:dudas.zoltan@wigner.mta.hu)

Nowadays development of biocompatible materials with tuneable properties remains challenging regarding the desired physicochemical properties and the easiness of modification of these properties in function of the guest molecules properties.

Silica gels proved to be versatile materials with a high biocompatibility. The full potential of these materials can only be achieved when properties are tailored for the desired application. In order to obtain silica gels with tunable hydrophobicity and porosity, organically modified precursors can be used.

The aim of the present work is to compare the structural modifications caused by the utilization of different type and quantity of alkyl or aryl substituted silica precursors in the sol-gel process. The different ORMOSIL structures were obtained by using a combination of 0–80 molar percent of mono-alkylated/-arylated precursors in combination with tetraethoxysilane.

The surface modified silica xerogels were characterized according to their: local structures (FT-IR, <sup>29</sup>Si-NMR and XRD spectroscopies), textural (nitrogen adsorption and small angle neutron scattering), morphologic (TEM and SEM) properties and by their thermal stability (thermal analysis).

**O12****PORPHYRIN-BASED CONJUGATED MICROPOROUS POLYMERS AS SOLID-STATE PHOTSENSITIZERS OF SINGLET OXYGEN***Ian Hynek<sup>1</sup>, Jiří Rathouský<sup>2</sup>, Jan Demel<sup>3</sup>, Kamil Lang<sup>3</sup>*

<sup>1</sup>Faculty of Science, Charles University, Hlavova 8, 128 43, Prague, Czech Republic;  
e-mail: [hynek@iic.cas.cz](mailto:hynek@iic.cas.cz)

<sup>2</sup>J. Heyrovský Institute of Physical Chemistry of the CAS, Prague, Czech Republic

<sup>3</sup>Institute of Inorganic Chemistry of the CAS, Řež, Czech Republic

Conjugated microporous polymers (CMPs) are polymeric materials with large surface areas and microporous nature [1]. CMPs built of porphyrin units can be used as solid sensitizers of reactive singlet oxygen, O<sub>2</sub>(<sup>1</sup>Δ<sub>g</sub>), under visible light irradiation for the preparation of bactericidal materials. Presented CMPs, prepared using the Suzuki coupling polycondensation reactions, were rationally designed in order to maximize their photosensitizing properties by tuning the porphyrins environment. Combination of tetrasubstituted porphyrin and para-disubstituted benzene as a linker led to CMPs with planar arrangement of porphyrin units (2D CMPs), whereas the utilization of trans-disubstituted porphyrins with substituted tetraphenyl methane led to materials with a diamond-like structure (3D CMPs). The prepared materials were char-

acterized by MAS-NMR, FTIR, and thermal and elemental analyses. The surface areas and pore characteristics were investigated by nitrogen sorption measurement at 77K.

To elucidate the structure – properties relationship we investigated the photophysical and photochemical properties of the CMPs and compared them with the properties of two known porphyrin-based 2D CMPs and metal-organic frameworks (MOFs). The efficiency of the  $O_2(^1\Delta_g)$  generation was determined using an *in-situ* reaction with 9,10-diphenylanthracene. 3D CMPs displayed a markedly higher  $O_2(^1\Delta_g)$  productivity in comparison with 2D CMPs and MOFs. CMPs were stable in organic solvents and underwent no measurable photobleaching. The  $O_2(^1\Delta_g)$  production activity of the CMPs correlated with neither the surface area nor with the pore volume. Enlarging the distance between neighboring porphyrin cores leads to materials producing  $O_2(^1\Delta_g)$  in higher yields. Thus, short-range environment of the porphyrin units plays crucial role on the photophysical properties of the CMPs. Compared with the MOFs, the CMPs offer the control over the porphyrin environment and superior stability by replacing the susceptible coordination bonds with the robust covalent bonds; therefore, the CMPs are more suitable and more efficient photosensitizers [2].

#### References

1. J.-X. Jiang et al.: *Angew. Chem. Int. Ed.* **46**, 8574–8578 (2007).
2. J. Hynek, J. Rathouský, J. Demel and K. Lang: *RSC Advances* **6**, 44279–44287 (2016).

## O13

### PIEZOELECTRICITY OF GRAPHENE/BN IN-PLANE HETEROSTRUCTURES

*Victor Demin, Leonid Chernozatonskii*

Emanuel Institute of Biochemical Physics of Russian Academy of Sciences, 119334, 4 Kosygin st., Moscow, Russia; e-mail: victordemin88@gmail.com

Two dimensional materials (graphene, hexagonal boron nitride monolayers) are attractive for future applications in nanoelectronics. Graphene has unique mechanical and electronic properties, such high Young modulus and mobility of charge carriers. Hexagonal boron nitride has semiconductive and piezoelectric properties.

It is well known Graphene/h-BN composites such in-plane heterostructures [1]. Heterostructures can be synthesized in different views: graphene with h-BN domains or sandwiched structure graphene/h-BNC/h-BN strip. Antiferromagnetism, minimum thermal conductance and robust half-metallic behavior were predicted theoretically for such in-plane heterostructures [1].

Here we present DFT investigation of piezoelectric properties of in-plane h-BN/graphene heterostructures. We consider 2D material, which consists of alternating h-BN and graphene covalent bonded ribbons with different widths. Electric field influence leads to mechanical deformation (compression/extension) of BN parts and, therefore, to mechanical deformation of graphene parts and their electronic properties [2]. We consider influence of graphene and h-BN part widths changing on piezoelectric and electronic properties of these heterostructures.

**References**

1. Q. Li, M. Liu, Y. Zhang and Z. Liu: Hexagonal boron nitride-graphene heterostructures: synthesis and interfacial properties. *Small* **12**, 32–50 (2016).
2. M. Topsakal and S. Ciraci: Elastic and plastic deformation of graphene, silicene, and boron nitride honeycomb nanoribbons under uniaxial tension: a first-principles density-functional theory study. *Phys. Rev. B* **81**, 024107 (2010).

**O14****INVESTIGATION OF GRAPHENE-TYPE LAYERS IN ULTRATHIN FILMS OF THE IONIC COMPOUND**

*Pavel B. Sorokin*<sup>1-3</sup>, *Alexander G. Kvashnin*<sup>4</sup>, *Egor Y. Pashkin*<sup>3</sup>, *David Tománek*<sup>5</sup>

<sup>1</sup>Emanuel Institute of Biochemical Physics, Moscow, Russian Federation

<sup>2</sup>National University of Science and Technology MISiS, Moscow, 119049, Russian Federation

<sup>3</sup>Technological Institute for Superhard and Novel Carbon Materials, Troitsk, Moscow, Russian Federation

<sup>4</sup>Skolkovo Institute of Science and Technology (Skoltech), Skolkovo Innovation Center 143026,

3 Nobel Street, Moscow, Russian Federation

<sup>5</sup>Physics and Astronomy Department, Michigan State University, East Lansing, Michigan, USA

Structural changes at surfaces including atomic relaxation and reconstruction are a manifestation of their effort to minimize the total free energy. Atomic rearrangements are typically moderate at surfaces of semi-infinite systems and in thick slabs in order to minimize the energy penalty associated with structural mismatch at the interface between the reconstructed surface and the unreconstructed bulk. In ultra-thin slabs, surface contribution dominates the total energy, as only a small fraction of atoms experience bulk-like atomic environment. There, large-scale reconstruction involving not only the topmost layers, but the entire structure may become energetically favorable. A good example of such a large-scale reconstruction is the observed surface graphitization of diamond nanoparticles, driven by a tendency to reduce the surface energy. This graphitization scenario, if energetically viable in a large range of compounds, may turn into a valuable approach to synthesize ultrathin layered structures for nanoelectronics applications in the post-graphene era.

Our results based on ab initio density functional calculations indicate a general graphitization tendency in ultrathin slabs of the ionic compound including rocksalt and cesium chloride-type structures [1]. Whereas the bulk of many compounds show an energy preference for cubic rather than layered atomic arrangements, the surface energy of layered systems is commonly lower than that of their cubic counterparts. Using established general equation based only on the elements basic parameters, we determine the critical slab thickness for a range of systems, below which a spontaneous conversion from a cubic to a layered graphitic structure occurs, driven by surface energy reduction in surface-dominated structures.

Such graphitization process in ionic materials was investigated in details for thin slabs of simplest and most accurately studied cubic sodium chloride [2]. We found that in the nanoscale region rock salt B1-NaCl thin slabs are unstable and spontaneous split to graphitic phase which was confirmed by the calculations of the energy barriers for the transitions.

It was also found that bulk counterpart of the graphitic NaCl is previously theoretically predicted wurtzite phase of NaCl. It was found that the phase is stable but the negative value of phase transition hindering of synthesis of this phase. This phase located in the negative pressure region of the NaCl phase diagram due to the higher energy and lower density compared to B1 phase. We calculated NaCl (P,T) phase diagram where three phases (two cubic phases (B1, B2) and wurtzite phase called) were indicated. The stability and physical properties of a new NaCl phase were investigated in details.

This work was supported by the Russian Science Foundation project 14-12-01217.

#### References

1. P. B. Sorokin, A. G. Kvashnin, Z. Zhu and D. Tománek: *Nano Letters* **14**, 7126 (2014).
2. A. G. Kvashnin, P. B. Sorokin and D. Tománek: *J. Phys. Chem. Lett.* **5**, 4014 (2014).

## O15

### NOVEL HYBRID NANOSTRUCTURES BASED ON GRAPHITIC ZINC OXIDE/ SULPHIDE MONOLAYERS

*Alexander G. Kvashnin*<sup>1,2</sup>, *Leonid A. Chernozatonskii*<sup>1</sup>

<sup>1</sup>Emanuel Institute of Biochemical Physics, 4 Kosigina Street, Moscow, Russia;  
e-mail: agkvashnin@gmail.com

<sup>2</sup>Skolkovo Institute of Science and Technology (Skoltech), 3 Nobel Street, Moscow, Russia

A great interest of the scientists nowadays directed to investigations of new composite materials and heterostructures with new physical properties. Such interest is often paid to the van der Waals heterostructures [1]. The possibility to build two-dimensional material with new properties just by placing one material on another opens a new wave of synthesis of two-dimensional materials of different compounds.

In recent works made by Claeysens et al. [2] a new hexagonal phase of ZnO was observed. This effect was theoretical analyzed by Freeman et al. [3] and reported that polar materials with favorable zinc blende structures (with dominant covalent-ionic bonding) tend to split into layered structures for the case of two-dimensionality. This prediction was confirmed in a number of experimental works [2, 4–6] where the graphitic-like thin ZnO, AlN and SiC films were fabricated by different experimental techniques.

We carried out the investigation of electronic properties of van der Waals vertical heterostructure based on monolayers of MoS<sub>2</sub>, ZnO and ZnS. Considered structure reveals small indirect band gap. More complicated structure based on MoS<sub>2</sub> and ZnO monolayers placed between two graphene layers was considered. Electronic structure calculations show high doping ratio of graphene layers and energy band structure with zero band gap and high DOS peaks in sunlight wave region which allows conclusion about the good possibility of using such structures in photovoltaic applications.

This work is supported by the Russian Scientific Foundation (14-12-01217).

**References**

1. A. K. Geim and I. V. Grigorieva: Van der Waals heterostructures. *Nature* **499**, 419–425 (2013).
2. F. Claeysens et al.: Growth of ZnO thin films – experiment and theory. *J. Mater. Chem.* **15**, 139–148 (2005).
3. C. L. Freeman, F. Claeysens, N. L. Allan and J. H. Harding: Graphitic nanofilms as precursors to wurtzite films: theory. *Phys. Rev. Lett.* **96**, 66102 (2006).
4. C. Tusche, H. L. Meyerheim and J. Kirschner: Observation of depolarized ZnO(0001) monolayers: formation of unreconstructed planar sheets. *Phys. Rev. Lett.* **99**, 26102 (2007).
5. S. S. Lin: Light-emitting two-dimensional ultrathin silicon carbide. *J. Phys. Chem. C* **116**, 3951–3955 (2012).
6. P. Tsipas et al.: Evidence for graphite-like hexagonal AlN nanosheets epitaxially grown on single crystal Ag(111). *Appl. Phys. Lett.* **103**, 251605 (2013).

**O16****CARBONACEOUS NANO-FILMS FOR MICROWAVE SHIELDING APPLICATIONS**

*Polina Kuzhir*<sup>1</sup>, *Alesia Paddubskaya*<sup>1</sup>, *Nadezhda Valynets*<sup>1</sup>, *Konstantin Batrakov*<sup>1</sup>,  
*Sergey Maksimenko*<sup>1</sup>, *Tommi Kaplas*<sup>2</sup>, *Yuri Svirko*<sup>2</sup>

<sup>1</sup>Research Institute for Nuclear Problems, Belarusian State University, Minsk, Belarus;  
e-mail: polina.kuzhir@gmail.com

<sup>2</sup>Institute of Photonics, University of Eastern Finland, Joensuu, Finland

As the microwave spectrum becomes more crowded and electromagnetic compatibility problem becomes more stressful, one needs new functional materials with high electromagnetic (EM) interference shielding efficiency (EMI SE) for EM coatings and shields. Recently we demonstrated [1–3] that in the microwave frequency range (26–37 GHz), pyrolytic carbon (PyC) films, multilayered graphene (multiGr) and graphene/polymer sandwiches with thickness as small as few thousandth of graphite skin depth can absorb up to 50% of the incident power, being free standing in free space.

We report a comparative study of EMI SE of sandwich structures based on of PyC, multiGr and PyC reinforced graphene (GrPyC) separated by thin polymer slabs (100–700 nm).

The optimal – in terms of thickness of carbonaceous films and/or number of layers in heterostructures – configurations are proposed. The designed functional materials allow us to maximize the shielding efficiency due to absorption of electromagnetic signal at the minimum thickness. The important advantage of all studied materials (PyC, multiGr, GrPyC) is that in contrast to graphene they can be either easily deposited onto the dielectric substrate via CVD [4] technique or robust enough to survive during the transfer process from a Cu substrate without a template polymer layer [5], which is typically used in graphene transfer process. That is why PyC, multiGr and GrPyC offer important alternative to graphene opening an avenue towards development of a scalable protocol of cost-efficient production of ultra-light electromagnetic shields that can be transferred to commercial applications.

**References**

1. K. Batrakov et al.: Enhanced microwave shielding effectiveness of ultrathin pyrolytic carbon films. *Applied Physics Letters* **103**, 073117 (2013).



2. P. Kuzhir et al.: Multilayered graphene in Ka-band: nanoscale coating for aerospace applications. *J. Nanosci and Nanotechn* **13**, 5864–5867 (2013).
3. K. Batrakov et al.: Flexible transparent graphene/polymer multilayers for efficient electromagnetic field absorption. *Scientific Reports* **4**, 7191 (2014).
4. T. Kaplas and Y. Svirko: Direct deposition of semitransparent conducting pyrolytic carbon films. *Journal of Nanophotonics* **6**, 061703 (2012).
5. T. Kaplas and P. Kuzhir: Pyrocarbon reinforced graphene: synthesis and physical properties. *Nanoscale Research Letters* **11**, 54 (2016).

## O17

### PHOSPHATE CERAMICS – CARBON NANOTUBES COMPOSITES

*Artyom Plyushch*<sup>1</sup>, *Jan Macutkevič*<sup>2</sup>, *Polina Kuzhir*<sup>1</sup>, *Aliaksei Sokal*<sup>3</sup>, *Konstantin Lapko*<sup>3</sup>, *Jūras Banys*<sup>2</sup>

<sup>1</sup>Research Institute for Nuclear Problems of the Belarusian State University, 11 Bobruiskaya Str., Minsk 220030, Belarus; e-mail: artyom.plyushch@gmail.com

<sup>2</sup>Faculty of Physics, Vilnius University, Sauletekio 9, Vilnius LT-10222, Lithuania

<sup>3</sup>Research Institute for Physical Chemical Problems of the Belarusian State University, 4 Leningradskaya Str., Minsk 220030, Belarus

Many modern industrial applications ranging from electromagnetic (EM) shielding to nuclear energetic require new functional materials with advanced and controlled physical properties, including hardness, mechanical strength, high thermal stability, electrical conductivity, etc. The progress on this is mainly achieved by the design of novel composite materials providing synergy and correlation of material properties. Advanced materials based on inorganic hosts demonstrate a prominent thermal stability [1]. Some of them remain stable even at temperatures as high as 3000 °C, demonstrating excellent heat insulating properties without emitting gas in the vacuum environment. Among the variety of inorganic hosts phosphates are the most manufacturable and processable ceramics.

The aim of this communication is to present the novel multifunctional composite material based on the thermostable alumina – phosphate ceramics with small (up to 2 wt.%) inclusions of multi-walled carbon nanotubes (MWCNT). We report the dielectric, EM interference shielding, mechanical and thermal properties of the composites. The influence of MWCNT aspect ratio, alumina mean grain size, MWCNT chemical modification and utilising different binders on dielectric properties in wide frequency (20 Hz – 37 GHz) and temperature (25–500 K) ranges have been studied.

It was demonstrated that addition of 2 wt.% of MWCNT improves ceramics conductivity up to 9 orders of magnitude, significantly affect shielding properties, and influence the mechanical properties in a positive way. Thermal destruction of embedded into ceramics nanotubes occurs at higher temperatures in comparison with the case of bulk MWCNTs powder.

#### Reference

1. C. L. Xu, B. Q. Wei, R. Z. Ma, J. Liang, X. K. Ma and D. H. Wu: *Carbon* **37**, 855–858 (1999).

**O18****BIOINSPIRED PHOTONIC STRUCTURES ACTIVE IN A LARGE WAVELENGTH SCALE**

*G. I. Márk<sup>1</sup>, K. Kertész<sup>1</sup>, G. Piszter<sup>1</sup>, I. Biró<sup>2</sup>, P. Kuzhir<sup>3</sup>, Ph. Lambin<sup>4</sup>, L. P. Biró<sup>1</sup>*

<sup>1</sup>Institute of Technical Physics and Materials Science, (MFA), Centre for Energy Research, Hungarian Academy of Sciences, Budapest, Hungary; <http://www.nanotechnology.hu/>

<sup>2</sup>“3D Kívánság”, Bíró u. 44/A/2, 2030 Érd, Hungary; <http://3dkivansag.blog.hu/>

<sup>3</sup>Research Institute for Nuclear Problems, Belarusian State University, Bobruiskaya Str. 11, 220030 Minsk, Belarus

<sup>4</sup>Department of Physics of Matter and Radiation, University of Namur, Namur, Belgium

Long range order in photonic crystal structures causes diffraction phenomena, e.g. a wavelength- and scattering angle selection. Large angle- and large wavelength range scattering, by contrast, seems to always involve [1] some form of long-range disorder. A structure can deviate from a perfect long-range order in many different ways, and different type of “randomnesses” yield different photonic properties, which means that by changing the disorder one can create photonic structures with predefined properties. Using disordered butterfly scale- and beetle elytron [2] optical nanostructures as blueprints we constructed bioinspired 3D printed microwave device structures active in a wide angle- and wavelength range. Utilizing a combination of dielectric and conducting ingredients (plastic and nanocarbon composite) [3] it is possible to fabricate devices with predefined BRDF (Bidirectional Reflection Distribution Function) and BTDF (Bidirectional Transmittance Distribution Function). 3D printing of bioinspired microstructures offers a flexible and cheap technology to produce complex structures with tuneable electromagnetic characteristics, which provides a new route for microwave devices.

**References**

1. G. I. Mark et al.: *Phys. Rev. E* **80**, 051903 (2009).
2. L. P. Biró et al.: *J. R. Soc. Interface* **7**, 887 (2010).
3. A. Paddubskaya et al.: *J. Appl. Phys.* **119**, 135102 (2016).

**O19****THERMAL EVOLUTION OF STABILIZED ZIRCONIA NANOPOWDERS OBTAINED VIA CRYOCHEMICAL ROUTE**

*Olga Yu. Kurapova, Vladimir G. Konakov, Alexander V. Ivanov*

Institute of Chemistry, St. Petersburg State University, Universitetskii pr. 26, Petrodvorets, St. Petersburg, 198504, Russia; e-mail: [olga.yu.kurapova@gmail.com](mailto:olga.yu.kurapova@gmail.com)

The development of the novel approach for nanosized low-agglomerated zirconia powders manufacturing gains much attention both for theoretical investigation and from practical point of view for the fabrication of various advanced nanomaterials with enhanced properties as nanostructured oxygen-conducting ceramics, metal-matrix, organic polymer-matrix based composites, etc. Thus, the present work is devoted to the development of a new approach for

nanosized stabilized zirconia precursors manufacturing of low agglomeration degree. For the study,  $x\text{CaO}-(100-x)\text{ZrO}_2$ ,  $x = 5, 9, 12, 15$  mol.%, was used as a model system. The synthesis of precursors was performed by reversed co-precipitation from aqueous solution under certain optimized conditions. The resulted filtered and washed gel was freeze-dried with and without cryoprotectants addition. The other part of gel was rapidly frozen into liquid nitrogen ( $-178\text{ }^\circ\text{C}$ ) and then was left for drying under the ambient conditions. For the first time the systematic information about the effect of cryochemical treatment on the thermal evolution of the final precursor powder size, phase formation and its microstructure up to  $1300\text{ }^\circ\text{C}$  was obtained via STA, XRD, BET, SEM, X-ray tomography and PSD-analysis. At  $\leq 800\text{ }^\circ\text{C}$  simultaneous dehydration, crystallization and recrystallization lead to prolonged deagglomeration and evolution of sponge-type 3D porous structure to the globular comprised of small crystallites ( $\sim 20\text{ nm}$ ). In case of freeze-drying for all the compositions examined the formation of metastable cubic solid solution takes place prior to main exothermic effect on DSC curve; in the range from  $800$  to  $1000\text{ }^\circ\text{C}$  deagglomeration is extended due to recrystallization and prolonged water loses;  $1000\text{--}1300\text{ }^\circ\text{C}$  baking of agglomerates is observed following slow crystallite growth. The use of these powders makes possible to fabricate nanoceramics free of organic binders suitable as membranes for oxygen sensors. This work was supported by the special President's scholarship for young scientists (research project CP-1967.2016.1).

## O20

### POROUS POLYMERS AS A SPECIFIC MICROENVIRONMENT OF SILICA PRECURSORS TRANSFORMATION

*Agnieszka Kierys*<sup>1</sup>, *Andrzej Sienkiewicz*<sup>1</sup>, *Radosław Zaleski*<sup>2</sup>

<sup>1</sup>Department of Adsorption, Faculty of Chemistry, M. Curie-Skłodowska University, M. Curie-Skłodowska Sq.3, 20-031 Lublin, Poland; e-mails: [agnieszka.kierys@umcs.lublin.pl](mailto:agnieszka.kierys@umcs.lublin.pl), [andrzej.sienkiewicz@umcs.lublin.pl](mailto:andrzej.sienkiewicz@umcs.lublin.pl)

<sup>2</sup>Department of Nuclear Methods, Institute of Physics, Maria Curie-Skłodowska University, Pl. M. Curie-Skłodowskiej 1, 20-031 Lublin, Poland; e-mail: [radek@zaleski.umcs.pl](mailto:radek@zaleski.umcs.pl)

Porous materials are an essential part of numerous technological processes including: laboratory, large-scale (catalysis, separation, energy storage, tissue engineering, environmental remediation, etc.), and daily life usage. Among this large group of materials, porous polymer resins are valued due to the easiness of their manufacturing, great stability and convenient functionalization processes [1]. There are various methods whereby such porous resins are produced; however, those produced by suspension polymerization in the presence of appropriate porogen, exist primarily in the form of spherical beads. Removal of the porogen agent, after polymerization, creates voids of different size which are interconnected and available for various molecules. This pore network is set within a continuous polymer phase of a specific chemical character. Thus, the highly developed internal pore structure of individual polymer beads may be regarded as a reaction system, ensuring the specific microenvironment for different chemical reactions. Indeed, the polymer resins are commonly used in polymer-supported processes, especially in the context of combinatorial chemistry [2]. On the other hand, polymer resins can be regarded as carriers and/or polymer frameworks in the synthesis of multicomponent composites.

The present paper describes the recent progress in understanding *in situ* transformation of silica precursors (selected from alkoxysilanes and organofunctional alkoxysilanes) within the porous polymer support in the presence of a catalyst in the vapour phase, with a particular focus on the relationship between the nature of precursors, synthesis method and properties of final products. The Amberlite XAD7HP (insoluble polymeric material) has been employed to ensure a microenvironment for reactions in the sol-gel process. Polymer beads, acting like tiny sponges, have been saturated with silica precursors, or their mixtures, and subsequently exposed to a vapour consisting of water and a catalyst. In this way, hydrolysis and condensation reactions have been initiated, causing precipitation of solid silica species of the desired composition. It may be assumed that the final structure and properties of composites will be affected not only by the nature of the precursors and their transformation but also by the size of voids and chemical nature of the support. Therefore, various factors influencing the precursors transformation and the formation of silica gel network in the spatially limited system of polymer pores are discussed.

#### References

1. D. C. Wu, F. Xu, B. Sun, R. W. Fu, H. K. He and K. Matyjaszewski: Design and preparation of porous polymers. *Chem. Rev.* **112**, 3959–4015 (2012).
2. P. Hodge: Polymer-supported organic reactions: what takes place in the beads? *Chem. Soc. Rev.* **26**, 417–424 (1997).

## O21

### HIGH PERFORMANCE MAGNETO-FLUORESCENT NANOPARTICLES ASSEMBLED FROM TERBIUM AND GADOLINIUM 1,3-DIKETONES

*Rustem Zairov*<sup>1,2</sup>, *Nataliya Shamsutdinova*<sup>1,2</sup>, *Asiya Mustafina*<sup>1,2</sup>

<sup>1</sup>A. E. Arbuzov Institute of Organic and Physical Chemistry, Kazan Scientific Center of Russian Academy of Sciences, Arbuzov str., 8, 420088, Kazan, Russia; e-mail: rustem02@yandex.ru

<sup>2</sup>Kazan Federal University, Kremlyovskaya str. 18, 420008, Kazan, Russia

Noninvasive diagnostics provides *in situ* insight to the structural and functional features of the investigated systems and organs at their original place in the living organism. The use of magnetic and optical techniques is emerging for these purposes. Improved sensing in tissues, which in turn can differentiate normal tissue from diseased one, can be achieved by using magnetic contrast agents (CA) and optical emissive probes. f-Block elements (rare Earths) are outstanding candidates for this, since their chelates combine unique magnetic and luminescent characteristics.

The precipitation of lanthanide complexes from water miscible organic solvents to polyelectrolyte-containing water solutions under effective stirring is an example of easy and effective synthetic pathway to embed large amount of lanthanide functional complexes to the nanoparticle. The synthesis of europium-doped luminescent polyelectrolyte colloids was first described four years ago [1] and later was applied to various terbium [2], and gadolinium [3] complexes.

Polyelectrolyte-coated nanoparticles consisting of terbium and gadolinium complexes with calix[4]arene tetra-diketone ligand were first synthesized. An antenna effect of the ligand on

Tb(III) green luminescence and presence of water molecules in the coordination sphere of Gd(III) bring strong luminescent and magnetic performance to core-shell nanoparticles. The size and the structure of the colloids were studied using transmission electron microscopy (TEM) and dynamic light scattering (DLS). The correlation between photophysical and magnetic properties of the nanoparticles and their core composition is highlighted. The core composition was optimized for the longitudinal relaxivity being greater than that of the commercial magnetic resonance imaging (MRI) contrast agents together with high level of Tb(III)-centered luminescence. The easy synthesis of the bifunctional species provides the tuning of both magnetic and luminescent output of nanoparticles via simple variation of lanthanide chelates concentrations in the initial synthetic solution. The exposure by the nanoparticles results in negligible effect on cell viability of periphery human blood lymphocytes, decreased platelet aggregation and bright coloring of pheochromocytoma 12 (PC 12) tumor cells, indicating the nanoparticles as promising candidates for dual magneto-fluorescent bioimaging.

#### References

1. A. Mustafina et al.: *Coll. Surf. B: Biointerfaces* **88**, 490–496 (2011).
2. N. Shamsutdinova et al.: *New Journal of Chemistry* **38**, 4130–4140 (2014).
3. N. Shamsutdinova et al.: *Chemistry Select* **1**, 1377–1383 (2016).

## O22

### VERY HIGH CONCENTRATION AQUEOUS MAGNETIC NANOFUIDS: SYNTHESIS, COLLOIDAL STABILITY, MAGNETIC AND FLOW PROPERTIES

*Corina Vasilescu*<sup>1,4</sup>, *Vlad Socoliuc*<sup>1</sup>, *Daniela Susan-Resiga*<sup>1</sup>, *Oana Marinică*<sup>2</sup>, *Vasil M. Garamus*<sup>3</sup>, *Geza Bandur*<sup>4</sup>, *Francisc Peter*<sup>4</sup>, *Rodica Turcu*<sup>5</sup>, *Etelka Tombácz*<sup>6</sup>, *Ladislau Vékás*<sup>1</sup>

<sup>1</sup>Lab. Magnetic Fluids, Center for Fundamental and Advanced Technical Research, Romanian Academy, Timisoara Branch, 24 Mihai Viteazul Str., 300223 Timisoara, Romania;

e-mails: corina\_m\_vasilescu@yahoo.com; vekas@acad-tim.tm.edu.ro; vekas.ladislau@gmail.com

<sup>2</sup>Research Center for Engineering of Systems with Complex Fluids, University Politehnica of Timisoara, 1 Mihai Viteazul Str., 300222 Timisoara, Romania

<sup>3</sup>Helmholtz-Zentrum Geesthacht, Zentrum für Material- und Küstenforschung GmbH, Max-Planck-Str., 21502 Geesthacht, Germany

<sup>4</sup>Department of Applied Chemistry and Engineering of Organic and Natural Compounds, University Politehnica of Timisoara, 6 Carol Telbisz Str., Timisoara, Romania

<sup>5</sup>National Institute for Research and Development of Isotopic and Molecular Technologies, 67-103 Donat Str., 400293 Cluj-Napoca, Romania

<sup>6</sup>Physical Chemistry and Material Science, University of Szeged, Aradi Vértanúk tere 1, Szeged, Hungary

Aqueous ferrofluids are a special class of magnetic nanofluids employed both in engineering and biomedical applications. Concentrated samples were synthesized by chemical co-precipitation and electro-steric stabilization of magnetite nanoparticles of approx. 7 nm mean size with oleic acid double layer, applying a modified version of the procedure described in [1]. The solid, hydrodynamic and magnetic size distributions were studied by Transmission Electron Microscopy (TEM), X-ray diffraction (XRD), DLS and magnetogrulometry. Different characterization techniques, such as Thermogravimetry (TGA), Fourier Transformed Infrared

Spectroscopy (FTIR), X-ray photoelectron spectroscopy (XPS), zeta potential (NanoZS), static light scattering (SLS), Dynamic Light Scattering (DLS), Small Angle X-ray Scattering (SAXS) and magnetorheometry were used to evaluate particle surface properties, surfactant adsorption, colloidal stability at different pH and particle volume fraction values, cluster formation and flow properties. The saturation magnetization of aqueous ferrofluids with steric stabilization investigated by Vibrating Sample Magnetometry (VSM) attained 600 G (magnetite solid volume fraction approx. 15%), among the highest values reported up to now.

#### Acknowledgements

This work was supported by the MagNanoMicroSeal research project (nr.157/2012-PNII-UE-FISCDI) and by the Research Program LLM-CCTFA 2016-2019 of the Romanian Academy. We acknowledge the DESY-EMBL Hamburg and German Engineering Material Science Centre (GEMS) Geesthacht for providing beam time at the BioSAXS facility. Financial support from the Romanian National Authority for Scientific Research and Innovation - ANCSI, Core Programme, Project PN16-30 02 02 is gratefully acknowledged.

#### Reference

1. D. Bica, L. Vékás, M. V. Avdeev, O. Marinica, V. Socoliuc, M. Balasoiu and V. M. Garamus: Sterically stabilized water based magnetic fluids: synthesis, structure and properties. *J. Magn. Magn. Mater.* **311**, 17–21(2007).

## O23

### EMPOWERING WASTE WATER TREATMENT TECHNIQUES USING ADVANCED MATERIALS AT NANOSCALE

*S. B. Mishra, A. K. Mishra*

Nanotechnology and Water Sustainability Unit, College of Science, Engineering and Technology, University of South Africa, Florida Campus, Johannesburg, South Africa; e-mail: bhards@unisa.ac.za

Clean water is always essential which often calls for a cheap and efficient water purification system. Nanomaterials are being used to develop more cost-effective and high-performance water treatment systems. Nanotechnology allows scientists to develop materials at nanoscale that can be developed with tailor made properties such as faster, lighter, stronger, and more efficient and stimuli responsive. These materials have been investigated for their efficiencies to remove organic, inorganic and biological pollutants providing better options for waste water technologies such as filtration, photo catalysis, and membrane techniques. These nanomaterials have shown an unprecedented adsorption capacity, demineralization and reverse osmosis to deal with toxic contaminants in water. The focus of the talk will be the recent advancement and development of the nanoscale sovereignty for the waste water remediation.

**O24****NANO SIZED ZINC OXIDE: AN EFFICIENT CATALYST FOR DEGRADATION OF RHODAMINE B DYE IN AQUEOUS MEDIUM***Muhammad Saeed, Hafiz Abdur Raof*

Department of Chemistry, Government College University, Faisalabad, Pakistan;  
 e-mail: msaeed@gcuf.edu.pk

This work explores the preparation and characterization of zinc oxide nano particles (ZnO NPs) and investigation of their catalytic activity for the degradation of rhodamine B dye in aqueous medium. ZnO NPs were prepared by reaction of zinc acetate dihydrate and sodium hydroxide in distilled water. The prepared ZnO NPs were characterized by XRD, FTIR, SEM TGA and surface area analysis. ZnO NPs were employed as catalyst for oxidative degradation of rhodamine B dye with molecular oxygen in aqueous medium. The effects of various parameters like time, temperature, initial concentration of dye, speed of agitation and catalyst dose on degradation experiments were investigated. Oxidative degradation reaction followed Eley–Rideal mechanism. According to Eley–Rideal mechanism the gaseous reactant, oxygen adsorbs at the surface of catalyst while rhodamine B dye reacts in fluid phase. Adsorbed oxygen transform to reactive radicals through the formation of electron-hole pair between conduction and valence band of zinc oxide catalyst. These active radicals mineralized the dye into water and carbon dioxide.

**References**

1. M. Saeed and M. Ilyas: Oxidative removal of phenol from water catalyzed by lab prepared nickel hydroxide. *Applied Catalysis B Environmental* **129**, 247–254 (2013).
2. M. Saeed, M. Ilyas and M. Siddique: Oxidative degradation of oxalic acid in aqueous medium using manganese oxide as catalyst at ambient temperature and pressure. *Arabian Journal for Science & Engineering* **38**, 1739–1748 (2013).
3. M. Ilyas, A. Ahmad and M. Saeed: Removal of Cr (VI) from aqueous solutions using peanut shell as adsorbent. *Journal of the Chemical Society of Pakistan* **35**, 760–768 (2013).
4. M. Ilyas, M. Siddique and M. Saeed: Liquid-phase aerobic oxidation of benzyl alcohol catalyzed by mecha-nochemically synthesized manganese oxide. *Chinese Science Bulletin* **58**, 2354–2359 (2013).

**O25****TIME RESOLVED EMISSION STUDY OF NANOPARTICLES WITH COMPLEX RADIATION MECHANISM***Dávid Beke<sup>1</sup>, Tibor Z. Jánosi<sup>2,3</sup>, János Erostyák<sup>2,3</sup>, Katalin Kamarás<sup>1</sup>, Ádám Galí<sup>1,4</sup>*

<sup>1</sup>Institute for Solid State Physics and Optics, Wigner Research Centre for Physics, Hungarian Academy of Sciences, P.O. Box 49, H-1525 Budapest, Hungary

<sup>2</sup>University of Pécs, Institute of Physics, Ifjúság útja 6, H-7624 Pécs, Hungary

<sup>3</sup>University of Pécs, Szentágothai Research Centre, Spectroscopy Research Group, Ifjúság útja 20, H-7624 Pécs, Hungary

<sup>4</sup>Department of Atomic Physics, Budapest University of Technology and Economics, Budafoki út 8, H-1111 Budapest, Hungary

Understanding the fluorescence of complex systems such as small nanocrystals with various surface terminations in solution is still a scientific challenge. We developed a method based on time resolved emission spectroscopy (TRES) to find and identify spectrally overlapping emission species by studying surface engineered silicon carbide (SiC) colloids [1]. While most of the time resolved techniques study systems by measuring the emission at a proper wavelength, time-resolved area-normalized emission spectroscopy (TRANES) is made by recording the decay curves in the whole emission range allowing us to study optical properties in more detail. Reconstructing decay associated spectra from TRANES was mostly limited for organic dyes because of the non-exponential decay curves of quantum dots and complex systems. We found that decay associated spectra are reconstructible even for such complex systems and resolving emission centres with emission wavelength differences less than 20 nm is even possible. The aqueous solutions of SiC nanocrystals are exceedingly promising candidates to realize bioinert nonperturbative fluorescent nanoparticles for *in vivo* bioimaging [2], and thus the identification of their luminescent centres is of immediate interest [3]. Two emission centres of this complex system were identified: surface groups involving carbon–oxygen bonds and a defect consisting of silicon–oxygen bonds. Our suggested interpretation of TRES proved its potential by helping reconcile previous experimental results on the surface and pH-dependent emission of SiC nanocrystals and it could be a versatile tool for understanding the complex recombination mechanisms of other luminescent nanomaterials.

#### References

1. D. Beke, T. Z. Jánosi, B. Somogyi, D. Á. Major, Z. Szekrényes, J. Erostyák, K. Kamarás and A. Gali: Identification of luminescence centers in molecular-sized silicon carbide nanocrystals. *J. Phys. Chem C* **120**, 685–691 (2016).
2. B. Somogyi and A. Gali: Computational design of in vivo biomarkers. *J. Phys.: Condensed Matter* **26**, 143202 (2014).
3. D. Beke, Z. Szekrényes, Z. Czigány, K. Kamarás and A. Gali: Dominant luminescence is not due to quantum confinement in molecular-sized silicon carbide nanocrystals. *Nanoscale* **7**, 10982–10988 (2015).

## O26

### THEORETICAL MODELLING OF ‘SMART’ NANOGENERATORS GROWN ON NONWOVEN MATERIALS

*Apurv Sibal, Vijay Kumar, Amit Rawal*

Department of Textile Technology, Indian Institute of Technology Delhi, India

During the last decade, one dimensional nanomaterial, i.e. Zinc Oxide (ZnO) has been successfully explored for various applications of self-powered systems. In this research work, an analytical model for predicting the piezoelectric characteristics of fibrous assemblies consisting of Zinc oxide (ZnO) nanorods assembled in the form of nonwoven structures has been developed. A combination of stochastic and stereological approaches has been followed to compute the voltage output observed between the nanorods grown on the surface of nonwoven fibres. Compression induced potential generation in piezoelectric nanorods based nonwovens is governed



by fibre orientation, nanorods dimensions and their density. Nonwovens with preferentially oriented fibres show more voltage output than randomly oriented fibres.

## O27

### SYNTHESIS AND PROPERTIES OF LONG LINEAR CARBON CHAINS

*Lei Shi*<sup>1</sup>, *Philip Rohringer*<sup>1</sup>, *Kazu Suenaga*<sup>2</sup>, *Yoshiko Niimi*<sup>2</sup>, *Jani Kotakoski*<sup>1</sup>, *Jannik C. Meyer*<sup>1</sup>, *Herwig Peterlik*<sup>1</sup>, *Marius Wanko*<sup>3</sup>, *Seymur Cahangirov*<sup>3</sup>, *Angel Rubio*<sup>3,4</sup>, *Zachary Lapin*<sup>5</sup>, *Lukas Novotny*<sup>5</sup>, *Paola Ayala*<sup>1,6</sup>, *Thomas Pichler*<sup>1</sup>

<sup>1</sup>University of Vienna, Faculty of Physics, Strudlhofgasse 4, A-1090 Vienna, Austria

<sup>2</sup>AIST, Nanotube Research Center, Tsukuba 305-8562, Japan

<sup>3</sup>Nano-Bio Spectroscopy Group and European Theoretical Spectroscopy Facility (ETSF), Universidad del País Vasco, CFM CSIC-UPV/EHU-MPC & DIPC, 20018 San Sebastian, Spain

<sup>4</sup>Max Planck Institute for the Structure and Dynamics of Matter, Hamburg, Germany

<sup>5</sup>ETH Zürich, Professur für Photonik, Hönggerberggring 64, HPP M21, 8093 Zürich, Switzerland

<sup>6</sup>Yachay Tech University, School of Physical Sciences and Nanotechnology, 100119-Urcuqui, Ecuador

The extreme instability and strong chemical activity of carbyne, the infinite  $sp^1$  hybridized carbon chain, are responsible for its low possibility to survive at ambient conditions. We successfully synthesized extremely long linear carbon chains (LLCCs) inside thin double walled carbon nanotubes as nanoreactors and protectors [1]. Their existence, structure, lengths and yield have been proved by Raman, HRTEM, STEM and XRD. The results show that the single-triple bonded LLCCs including thousands of carbon atoms have at least six new Raman peaks, some of which are even stronger than the G-band. The optimum growth conditions, for example, diameter of the host tubes, annealing temperatures and time were carefully studied. The interaction and charge transfer between the LLCCs and their host nanotubes were explored using resonance Raman, low-temperature Raman and DFT calculations [2]. Furthermore, the band gap of the LLCCs was examined by resonance Raman spectroscopy. The results suggest that the band gap of LLCCs in the range of 1.8–2.3 eV is inversely proportional to their lengths, which is also perfectly consistent with our DFT calculations [3].

#### References

1. L. Shi et al.: *Nature Materials* **15**, 634–639 (2016).
2. M. Wanko et al.: arXiv:1604.00483.
3. L. Shi et al.: Band gap of long linear carbon chains. In preparation.

## O28

### OXIDATIVE UNZIPPING OF CARBON NANOTUBES. CONTROLLING REACTION PARAMETERS AFFORDS NEW TYPES OF GRAPHENE NANORIBBON PRODUCTS

*Ayrat M. Dimiev*<sup>1</sup>, *Arthur A. Khannanov*<sup>1</sup>, *James M. Tour*<sup>2</sup>

<sup>1</sup>Laboratory of Advanced Carbon Nanomaterials, Kazan Federal University, Kremlyovskaya Street 8, Kazan, Russian Federation; e-mail: AMDimiev@kpfu.ru

<sup>2</sup>Department of Chemistry, Department of Material Science and NanoEngineering, and NanoCarbon Center, Rice University, MS-222, 6100 Main Street, Houston, TX 77005, USA; e-mail: tour@rice.edu

Graphene nanoribbons (GNRs), a narrow stripes of graphene, have several advantages over their 2D counterpart due to their pseudo-1D character. Properties of GNRs vary significantly on the size, edge configuration, and number of layers, which in turn, depend on the manufacturing method. One of the manufacturing methods is based on longitudinal opening or unzipping of multi-walled carbon nanotubes (MWCNTs). The major advantage of this approach over the other methods is the potential of mass production in a kilogram scale at a moderate cost. Unzipping of MWCNTs is afforded by their exposure to two different reactant systems: a) potassium metal vapor or Na/K alloy in organic solvents [1], and b)  $\text{KMnO}_4$  in concentrated sulfuric acid [2]. The K-unzipping yields intact GNRs, while, the oxidative  $\text{KMnO}_4$ -unzipping yields highly damaged graphene oxide nanoribbons (GONRs); the subsequent reduction of as-produced GONRs does not fully restore the graphenic structure. While K-unzipping is intercalation driven, the mechanism of oxidative unzipping is not yet fully understood.

Here we demonstrate intercalation assisted oxidative splitting of MWCNTs by treatment with the three-component system, comprising: ammonium persulfate ( $(\text{NH}_4)_2\text{S}_2\text{O}_8$ ), sulfuric acid, and oleum. The use of this system coupled with properly chosen time of exposure to oxidizing agent, results in formation of intact (or insignificantly oxidized) GNRs that require no subsequent reduction. The method can approach 100% yield, be highly reproducible, safe, low cost, and suitable for scaled mass production.

Further, we take advantage from our understanding of the mechanism of graphene oxide formation [3] to control the process of oxidative unzipping of MWCNTs in the  $\text{KMnO}_4/\text{H}_2\text{SO}_4$  media. Even with  $\text{KMnO}_4$  as an oxidizing agent, we obtain not GONRs, but GNR/GONR hybrids with minimally damaged graphenic structure. All the GNR products are fully characterized by SEM, Raman microscopy, TGA, XRD and XPS. Our findings suggest that the oxidative unzipping of MWCNTs has intercalation driven mechanism.

#### References

1. D. V. Kosynkin et al.: Longitudinal unzipping of carbon nanotubes to form graphene nanoribbons. *Nature* **458**, 872–876 (2009).
2. B. Genorio et al.: In-situ intercalation replacement and selective functionalization of graphene nanoribbon stacks. *ACS Nano* **6**, 4231–4240 (2012).
3. A. M. Dimiev et al.: Mechanism of graphene oxide formation. *ACS Nano*, **8**, 3060–3068 (2013).

## O29

### PULSED CURRENT ELECTRODEPOSITION PARAMETERS TO CONTROL THE Sn PARTICLE SIZE TO ENHANCE ELECTROCHEMICAL PERFORMANCE AS ANODE MATERIAL IN LITHIUM ION BATTERIES

*Soheila Javadian, Jamal Kakemam, Abbas Sadeghi*

Department of Physical Chemistry, Faculty of Science, Tarbiat Modares University, Tehran, Iran; e-mails: javadian\_s@modares.ac.ir, javadians@yahoo.com

The Sn nano-particles were synthesized through pulsed current electrodeposition in an acidic electrochemical bath containing polyvinylpyrrolidone (PVP) in order to control the electrodeposition rate of Sn reduction on copper collector electrode. The anode prepared at electrochemical bath containing PVP concentration of about  $10 \text{ gr}\cdot\text{l}^{-1}$  showed highest discharge capacity and cycleability as two main criteria in lithium ion batteries. Also, the pulsed current characteristics such as frequency and current density were investigated and 10 Hz and  $20 \text{ mA}\cdot\text{cm}^{-2}$  respectively, are obtained as the optimum parameters. The synthesis of Sn nanoparticles in such media was successfully developed. The sizes and morphologies of NPs were characterized by X-ray diffraction and scanning electron microscopy. Our findings indicated that the nano-sized spherical particles with a diameter ranging from 80 to 100 nm could be formed at optimum co. Discharge capacity of synthesized Sn nano particles was obtained about  $1350 \text{ mA}\cdot\text{h}\cdot\text{g}^{-1}$  indicating a 32% increase compared to the synthesized Sn particles with constant current electrodeposition method. Additionally, discharge capacity of around  $550 \text{ mA}\cdot\text{h}\cdot\text{g}^{-1}$  is obtained in 50th cycle which shows an appropriate cycleability compared to the Sn film electrode prepared by a constant current electrodeposition. The discharge capacities obtained indicated a considerable improvement compared to similar works. The particles size of coated Sn on collector electrode is resulted from interplay between the rate of nucleation and growing rate of particles. PVP affects the kinetic of electrodeposition through surface capping and complexing of  $\text{Sn}^{2+}$  species.

## NEW JEOL DEVELOPMENTS FOR SCANNING & TRANSMISSION ELECTRON MICROSCOPES: IT300HR & F2

*G. Brunetti*

JEOL (EUROPE) SAS, Croissy-sur-Seine, France

After 50 years of SEM, It's time to .... Change the Rule of the game. This sentence summarizes the development idea of IT300HR. This new SEM developed by JEOL brings many changes in the SEM domain. IT300HR is equipped with a high brightness electron gun with long life time, one click one picture, new automatic algorithm, any sample size can fit the "Premium Chamber". You will get high resolution image & ultrafast chemical analysis for any kind of sample (from conductive to non-conductive sample, biology to nano-materials). The IT300HR will solve your problems in minutes. This SEM with  $\mu\text{metal}$  protected column can fit any room.

The F2 (a) is a new concept of 20–200 kV TEM equipped with a Cold FEG. This new generation of multi-purpose electron microscope is designed specifically to meet today's diversified needs. Many features have been developed for this new microscope: Improved Cold FEG, Advanced EELS, Dual SDD EDS, Advanced Scan System, Smart Design, SpecPorter, Environmentally Friendly. Thanks to the high brightness and small probe size of the Cold FEG, the F2 is able to reach an unprecedented guaranteed resolution for STEM (0.14 nm), EDS (1.7 sr) and EELS (0.3 eV); creating a new class of high-end non-corrected TEM.

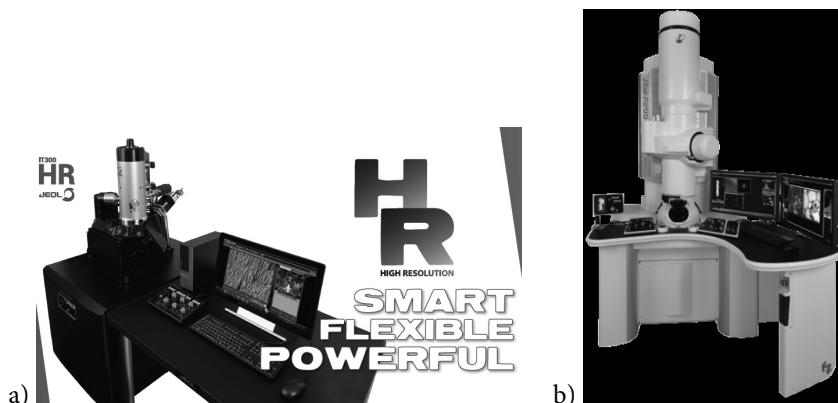


Fig. 1. (a) IT300HR, (b) JEOL F2

F2 has “Dual SDD system”, which is composed of two silicon drift detectors (SDD) having large sensor area, resulting in total solid angle of 1.7 sr. The combination of dual SDD system, the improved Cold FEG and the advanced scan system, allows us to perform various techniques such as highly sensitive microanalysis and 3D-EDS, atomic resolution EDS map (c), high speed mapping, light element mapping (from Be to U), the study of beam damageable samples, etc.

High-resolution analytical systems, such as transmission electron microscope (TEM) and scanning transmission electron microscope (STEM), are attracting increasing attention. Higher resolution and higher efficiency are required for modern systems, along with upgraded and intuitive ease of operation. As the Schottky was not able to meet all these needs, the Cold FEG F2 has been developed as a next-generation electron microscope.

## ORAL PRESENTATIONS

Friday, 14 October, 2016

### O30

#### NANOSTRUCTURED (PHOTO)CATHODES FOR DYE-SENSITIZED SOLAR CELLS

*Ladislav Kavan*<sup>1</sup>, *Zuzana Vlckova-Zivcova*<sup>1</sup>, *Hana Krysova*<sup>1</sup>, *Petr Cigler*<sup>2</sup>, *Paul Liska*<sup>3</sup>,  
*Shaik M. Zakeeruddin*<sup>3</sup>, *Michael Grätzel*<sup>3</sup>

<sup>1</sup>J. Heyrovský Institute of Physical Chemistry, v.v.i., Academy of Sciences of the Czech Republic, Dolejškova 3, CZ-18223 Prague 8, Czech Republic

<sup>2</sup>Institute of Organic Chemistry and Biochemistry, v.v.i. Academy of Sciences of the Czech Republic, Flemingovo nám. 2, 166 10 Prague 6, Czech Republic

<sup>3</sup>Laboratory of Photonics and Interfaces, Institute of Chemical Sciences and Engineering, Swiss Federal Institute of Technology, CH-1015 Lausanne, Switzerland

The cathode of dye-sensitized solar cell (DSC) is usually a platinized F-doped SnO<sub>2</sub> (FTO) which, however, contributes by about >20–60% to the cost of the DSC-module. The search for cheaper cathode materials points at nanocarbons and graphene-based materials, particularly for Co-mediated DSCs [1, 2]. Another alternative, is the woven fabric consisting of transparent PEN fibers in warp and platinized (or graphene-coated) metal wires in weft [3, 4]. This electrode exhibits similar or better performance than the corresponding FTO-supported alternatives in serial ohmic resistance, charge-transfer resistance for mediator reduction and optical transparency in the visible and particularly in the near-IR spectral region. In the field of p-DSCs (with sensitized photocathode) the generic semiconductor material is p-NiO. An alternative p-semiconductor is B-doped nanodiamond which offers excellent chemical and electrochemically stability, optical transparency and favorable electrical properties [5]. The electrochemical inertness of BDD is beneficial in view of the corrosive nature of certain electrolyte solutions used in DSCs. Spectral sensitization of nanodiamond was carried out by anchoring of several dyes and stable cathodic photocurrents were found under visible light illumination in aqueous electrolyte solution with dimethylviologen serving as electron mediator [6, 7].

#### Acknowledgements

This work was supported by the Czech National Foundation, contract No. 13-07724S and by the European Union Programme (No. 604391 Graphene Flagship).

#### References

1. L. Kavan, J.-H. Yum and M. Grätzel: *Electrochim. Acta* **128**, 349 (2014).
2. L. Kavan: *Top. Curr. Chem.* **348**, 53 (2014).
3. L. Kavan, P. Liska, S. M. Zakeeruddin et al.: *ACS Appl. Mater. Interfaces* **6**, 22343 (2014).
4. L. Kavan, P. Liska, S. M. Zakeeruddin et al.: *Electrochim. Acta* **195**, 34 (2016).
5. L. Kavan, Z. Vlckova-Zivcova, V. Petrak et al.: *Electrochim. Acta* **179**, 626 (2015).
6. H. Krysova, Z. Vlckova-Zivcova, J. Barton et al.: *Phys. Chem. Chem. Phys.* **17**, 1165 (2015).
7. H. Krysova, L. Kavan, Z. Vlckova-Zivcova et al.: *RSC Adv.* **5**, 81069 (2015).

**O31****ASYMMETRIC NANOSTRUCTURE OF METAL/SEMICONDUCTOR:  
CONFINED CRYSTALLIZATION AND THEIR IMPLICATIONS***Hyunjung Shin*

Department of Energy Science, Sungkyunkwan University, Suwon, Korea; e-mail: hshin@skku.edu

Electron–hole charge separation is the most core process in the photovoltaic applications such as solar cells, photocatalysts, and photoelectrochemical cells. Electrons in valence band of semiconducting materials are excited by photons with higher energy than bandgap and, consequently, electron–hole separation is occurred. In this process, charge separation and injection is the major factor to determine the efficiency of photoactive devices. Especially, metal/semiconductor heterojunction nanostructures are the most attractive structure as promising structures for the enhancement of charge separations. Therefore, understanding of charge transfer and separation is required to design for the efficient photoactive devices. TiO<sub>2</sub> nanotubes (NTs) have been fabricated by template-assisted atomic layer deposition (ALD) method [1]. High crystalline and mono-dispersed TiO<sub>2</sub> NT arrays were obtained by conformal coating of anodic aluminum oxides (AAO) and subsequent annealing. By simply changing the wall thickness of NT's, the optimum boosting condition of confined crystallization has been attained [2]. Few micron-meter long anatase single grains in the NTs resembling the physical properties of the original bulk materials were obtained. Photoluminescence (PL) and Raman spectroscopy were performed for the understanding of TiO<sub>2</sub> NT arrays' charge transport properties. We observed fingerprints of the self-trap excitons from our well organized and crystallized anatase NTs using by low temperature – PL and Raman study [3]. Inner space of the TiO<sub>2</sub> NT provides another opportunity for the confined crystal growth. Asymmetric single crystalline Au nanowires with very high aspect ratio under the illumination were obtained only inside of TiO<sub>2</sub> NTs. Kelvin probe force microscopy can provide the information about surface potential with a high lateral resolution [4]. We investigated charge separation behavior in Au nanoparticles attached TiO<sub>2</sub> nanotubes by direct imaging of light induced surface potential differences. Surface potential change according to the presence of Au NPs and different substrates such as metal substrates and highly doped Si substrate with oxide layer were also investigated.

**References**

1. H. Shin et. al.: *Adv. Mater.* **16**, 1197 (2004); *Chem. Mater.* **20**, 756 (2008); *J. Mater. Chem.* **18**, 1362 (2008); *MRS Bull.* **36**, 887 (2011); *J. Mater. Chem. C* **1**, 621 (2013).
2. H. Shin et. al.: *J. Mater. Chem. A* **1**, 14080 (2013).
3. H. Shin et. al.: *J. Phys. Chem. C* **118**, 9726 (2014).
4. H. Shin et al.: *Nano Lett.* **14**, 4413 (2014); *Nanoscale* **3**, 2560 (2011); *Nano Lett.* **11**, 1428 (2011); *Appl. Phys. Lett.* **94**, 032907, (2009).

## O32

## HYBRID NANOSCALE ARCHITECTURES OF SEMICONDUCTORS AND CARBON NANOMATERIALS TAILORED FOR PHOTOELECTROCHEMICAL APPLICATIONS

*Csaba Janáky*<sup>1,2</sup>, *Dorottya Hursán*<sup>1,2</sup>, *Attila Kormányos*<sup>1,2</sup>, *Egon Kecsenovity*<sup>1,2</sup>, *Balázs Endrődi*<sup>1,2</sup>

<sup>1</sup>Department of Physical Chemistry and Materials Science, University of Szeged, Aradi tér 1, 6720 Szeged, Hungary; e-mail: janaky@chem.u-szeged.hu

<sup>2</sup>MTA-SZTE “Lendület” Photoelectrochemistry Research Group, Rerrich tér 1, 6720 Szeged, Hungary

Carbon nanomaterials, especially carbon nanotubes and graphene (either alone, or as building blocks of organized 3-D superstructures), are attracting significant attention as large surface area electrode support materials. Their composites with both inorganic and organic semiconductors represent an interesting class of new functional materials. In the first part of my talk I will focus on the use of electrosynthetic methods for preparing semiconductors on nanocarbon-modified electrode surfaces [1, 2]. I will show how electrodeposition can be used to tune composition, crystal structure, and morphology of the nanocomposites for targeted applications.

In the second part, selected examples will be given for how these electrosynthesized hybrid assemblies can be deployed in various photoelectrochemical application schemes, most importantly CO<sub>2</sub> conversion. Given that CO<sub>2</sub> is a greenhouse gas, using sunlight to convert CO<sub>2</sub> to transportation fuel (such as methanol or methane) represents a value-added approach to the simultaneous generation of alternative fuels and environmental remediation of carbon emissions from the continued use of conventional fuels. I will present the controlled synthesis and photoelectrochemical behavior of CNT/Cu<sub>2</sub>O [3] and CNT/polyaniline composites [4] for the CO<sub>2</sub> reduction application. In the case of the second system, we demonstrated that polyaniline, as the very first example of an organic semiconductor, is a promising photocathode material for the conversion of CO<sub>2</sub> to alcohol fuels.

Carefully designed, multiple-step electrodeposition protocols were developed that ensured homogeneous coating of the CNTs with the respective semiconductors. The enhanced charge transport property for the hybrids resulted in a drastic increase in the photocurrents measured for the CO<sub>2</sub> reduction, compared to the bare semiconductor counterparts. In addition to this superior performance, long term photoelectrolysis measurements proved that the hybrids were more stable than the oxide alone. Structure property relationships will be shown, which may act as guidelines for the rational design of nanocomposite photoelectrodes.

## References

1. C. Janáky and K. Rajeshwar: *Prog Pol Sci* **43**, 396–435 (2015).
2. C. Janáky, E. Kecsenovity and K. Rajeshwar: *ChemElectroChem* **3**, 181–192 (2016).
3. E. Kecsenovity, B. Endrődi, Z. Pápa, K. Hernádi, K. Rajeshwar and C. Janáky: *J Mater Chem A* **4**, 3199–3147 (2016).
4. D. Hursán, A. Kormányos, K. Rajeshwar and C. Janáky: *Chem Comm*, in press. doi: 10.1039/C6CC04050K

**O33****FABRICATION AND ELECTROCHEMICAL PERFORMANCE OF FLEXIBLE ALL-SOLID-STATE LI-ION MICROBATTERIES***Robert Kun<sup>1,2</sup>, Jens Glenneberg<sup>1</sup>, Ingo Bardenhagen<sup>2</sup>, Frederieke Langer<sup>1</sup>*

<sup>1</sup>Department of Production Engineering, Innovative Sensor and Functional Materials Research Group, University of Bremen, Badgasteiner Str. 1, 28359 Bremen, Germany; e-mail: robert.kun@uni-bremen.de

<sup>2</sup>Fraunhofer Institute for Manufacturing Technology and Advanced Materials – IFAM, Wienerstr. 12, 28359 Bremen, Germany

Miniaturized and fully integrated energy storage devices draw currently much technological and research attention. Successful implementation of self-powered, maintenance free autonomous micro-devices (microsensors, medical implants, self-powered MEMS), and applications such as Internet-of-Things (IoT), flexible electronics and wearables need high performance energy storage devices. Lithium ion technology because of its highest energy density among other battery chemistries seems to be the ideal solution if limited areal space or volume is available. However, using state-of-the-art lithium ion technology intention for miniaturization and structural-, as well as on-chip integration of the energy storage device will fail. Furthermore, conventional lithium ion battery technology must cope with inherent safety issues, such as electrolyte leakage, explosion hazard, toxicity. Direct integration of energy storage components into microscale electronic devices will be enabled using all-solid-state lithium ion microbatteries. Since all-solid-state lithium ion batteries contain no liquid components, therefore application of easier sealing technology, significant reduction of electrochemically inactive components of the cell is possible. Further advantages are the more flexible integration of the storage device and increased intrinsic cell safety. Planar, thin-film, all-solid-state lithium ion microbatteries can be easily processed by physical vapor deposition (PVD) techniques. In the present contribution realization of thin film all-solid-state lithium battery on both rigid (glass) and flexible (polymer) substrate at ambient processing temperatures is presented. The PVD deposited microbattery consists of amorphous molybdenum(IV) oxide cathode and lithium phosphorous oxy-nitride (LiPON) glass-type solid-state electrolyte. Thermally evaporated metallic lithium serves as anode layer. Electrochemical performance of the as-processed battery cells was evaluated through electrochemical impedance spectroscopy (EIS) and galvanostatic cycling. Regardless of applied substrate Li/LiPON/MoO<sub>3</sub> cells exhibited excellent cycling stability. Cycling the cells at moderate 10C rate 15% capacity fade was determined after 550 full cycles. Rate performance tests of the batteries showed that charging and discharging the cells even at very high currents (145C) 30% of the initial reversible discharge capacity will be retained. The results demonstrate that we were able to transfer the Li/LiPON/MoO<sub>3</sub> system from a rigid glass substrate onto a flexible polyimide one without sacrificing any performance of the microbattery cell.



## O34

Co CRYSTALLINITY AND CNT EVOLUTION IN CO AND CO<sub>2</sub> HYDROGENATION OVER Co/CNT CATALYSTS

*Sergei Chernyak, Eugeniya Suslova, Anthon Ivanov, Konstantin Maslakov, Alexander Egorov, Serguei Savilov, Valery Lunin*

Department of Chemistry, Lomonosov Moscow State University, 1–3 Leninskiye Gory, Moscow, 119991, Russia; e-mail: chernyak.msu@gmail.com

The role of Co crystallinity in the catalytic performance of Co catalysts is still debated by scientists studying the process of hydrogenation of carbon oxides and other reactions involving Co as an active site. In this work we studied the effect of Co crystallinity in CO and CO<sub>2</sub> hydrogenation over Co/CNT catalysts by means of TEM combined with electron diffraction. Surface state of CNTs during the catalyst preparation and catalytic process was also investigated by TEM, nitrogen adsorption, XPS and Raman spectroscopy. Pure CNTs were oxidized via refluxing in nitric acid at different temperatures to generate surface with different oxygen content. Obtained samples were impregnated by Co nitrate and tested in CO and CO<sub>2</sub> hydrogenation.

TEM and electron diffraction showed that high oxidation degree of CNTs and low Co loading resulted in the formation of Co particles with the average diameter of ~2 nm and extremely poor crystallinity (*Figure 1a*). These particles were “smeared” over CNT surface (*Figure 1b*). Catalyst supported on less oxidized CNTs contained crystal particles with the average diameter of ~3 nm (*Figure 1c, d*).

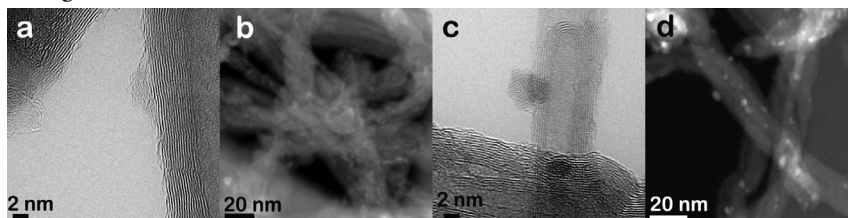


**Fig. 1.** TEM images of the catalysts supported on CNTs oxidized at higher (a, b) and lower  $T$

Co with poor crystallinity was inactive in CO<sub>2</sub> hydrogenation and almost inactive in CO hydrogenation in opposite to catalyst supported on less oxidized CNTs<sup>1</sup>. Thermal activation of amorphous catalyst led to its crystallization and this catalyst showed noticeable catalytic activity. It was found that amorphous Co particles promote CO disproportionation and formation of carbon shells around active sites.

Reduction and activation of catalysts lead to the etching of their surface which resulted in the increase of specific surface area and Raman defectiveness of CNTs. XPS data proved that only about a quarter of initial oxygen remained on CNT surface after calcination, reduction and 70 h of CO hydrogenation.

The reported study was funded by RFBR according to the research project No. 16-29-06439 ofim and Russian Academy of Sciences Program of Basic Research (#1)

#### Reference

1. S. Chernyak et al.: Effect of Co crystallinity on Co/CNT catalytic activity in CO/CO<sub>2</sub> hydrogenation and CO disproportionation. *Appl. Surf. Sci.* **372**, 100–107 (2016).

**O35****DIAMOND-LIKE CARBON AND CARBON NANOTUBE HYBRIDS FOR BIOCHEMICAL SENSING***Krisztian Kordas*<sup>1</sup>, *Olli Pitkänen*<sup>1</sup>, *Sainio Sami*<sup>2</sup>, *Tommi Laurila*<sup>2</sup><sup>1</sup>Microelectronics Research Unit, University of Oulu, Finland<sup>2</sup>Department of Electrical Engineering and Automation, School of Electrical Engineering, Aalto University, Finland

Sensing of amines is ubiquitous in food industry and medical applications to detect decomposition products of proteins as well as to measure biogenic compounds responsible e.g. for the operation of our nervous system. In the present talk, we demonstrate novel hybrid structures of diamond-like carbon and carbon nanotubes as electrochemical sensing electrodes, with wide and stable water window, almost reversible electron transfer kinetics and highly sensitive characteristics towards dopamine down to a concentration of 1  $\mu$ M. The sensor is realized using entirely scalable methods compatible with standard Si fabrication thus suggesting further applications having industrial relevance [1–3].

**References**

1. S. Sainio, T. Palomaki, N. Tujunen, V. Protopopova, J. Koehne, K. Kordas, J. Koskinen, M. Meyyappan and T. Laurila: Integrated carbon nanostructures for detection of neurotransmitters. *Molecular Neurobiology* **52**, 859–866 (2015).
2. T. Laurila, S. Sainio, H. Jiang, T. Palomaki, O. Pitkanen, K. Kordas and J. Koskinen: Multi-walled carbon nanotubes (MWCNTs) grown directly on tetrahedral amorphous carbon (ta-C): an interfacial study. *Diamond and Related Materials* **56**, 54–59 (2015).
3. S. Sainio, T. Palomaki, S. Rhode, M. Kauppila, O. Pitkanen, T. Selkala, G. Toth, M. Moram, K. Kordas, J. Koskinen and T. Laurila: Carbon nanotube (CNT) forest grown on diamond-like carbon (DLC) thin films significantly improves electrochemical sensitivity and selectivity towards dopamine. *Sensors and Actuators B* **211**, 177–186 (2015).

**O36****TAILORED HYBRID MATERIALS USING NANOCHEMISTRY INSIDE CARBON NANOTUBES***Thomas Pichler*, *Paola Ayala*, *Hidetsugu Shiozawa*, *Lei Shi*, *Phillip Rohringer*

Faculty of Physics, University of Vienna, Boltzmannngasse 5 1090 Vienna, Austria;

e-mail: thomas.pichler@univie.ac.at

In this contribution I will present recent progress in the synthesis of novel materials based on filled carbon nanotubes followed by nanochemical reactions. This covers the bulk growth metallocenes inside single walled carbon nanotubes and the bulk growth of metal chains [1] and of carbyne inside double walled carbon nanotubes [2]. I will show recent progress on unravelling the influence of charge transfer, local strain and hybridization on their electronic transport properties As selective examples I will present a gas sensing model based on external function-

alization and shows how the interaction with reactive gases like nitric oxides can be tailored by advanced filling reactions with metallocenes and metalacetylacetonates towards room temperature selectivity and sensitivity. As a last example I will review how stabilized carbyne chains with more than 6000 carbon atoms length exhibit novel electronic and optical properties such as a huge resonance Raman signal and act as functional elements enhancing the photoluminescence of inner tubes [3].

Work supported by FWF and the EU.

#### References

1. H. Shiozawa et al.: *Scientific Reports* 5, 15033 (2015). doi: 10.1038/srep15033
2. L. Shi et al.: *Nature Materials* (2016). doi: 10.1038/NMAT4617
3. P. Rohringer, P. Ayala and T. Pichler: *Advanced Functional Materials* (2016). doi: 10.1002/adfm.201505502

## O37

### ADSORPTION PROPERTIES OF SPARK PLASMA SINTERED NITROGEN-DOPED CARBON NANOMATERIALS

*Natalia Strokova, Serguei Savilov, Valery Lunin, Serguei Aldoshin*

Chemistry Department, M.V. Lomonosov Moscow State University, Leninskie gory, 1–3, Moscow, 119991, Russia; e-mail: natalia.strokova@gmail.com

There are plenty of merits for supercapacitors electrode materials from different nanostructured carbon forms. Most important are high specific surface area, long lifetime under cycling and tunable pore distribution. Introduction of nitrogen atoms to the structure of graphene layers of carbon nanotubes or 3D graphenes can provide the rise of characteristics of electrochemical devices due to pseudocapacitance. Although specific surface interactions between electrode material and electrolyte may also affect on electrochemical properties [1]. Present work deals with porous powders of N-doped carbon nanomaterials [carbon nanotubes (CNT) and carbon nanoshells (CNS)], which were compacted using spark plasma sintering technique. Adsorption properties of nitrogen-doped carbon nanostructured powders as well as pellets from them in respect to ethanol, acetonitrile, heptane, benzene, water and 1-methylimidazole were studied by liquid vapours uptake, performed using DVS Advantage instrument (SMS, UK). Experimental heats of sorption for all the solvents used were calculated after measurements at 20, 30 and 40 °C. Elemental composition and chemical state of nitrogen atoms at CNTs and CNS surface were identified by XPS method.

According to Raman spectroscopy compacted carbon materials demonstrated less defect structure, comparing with initial ones. Shape of adsorption-desorption isotherms shows the presence of micro- and mesopores in all of the materials under discussion; sintered samples also revealed reduction of total pores volume. The uptake of all solvents on powder samples was greater than on compacted ones because of sealing of pores. Experimental heats of sorption of studied pellets do not differ dramatically from original powders [2]. Experimental heats of sorption of acetonitrile and 1-methylimidazole on N-doped materials are found to be higher than

on non-doped carbon nanomaterials pellets that can be attributed to the chemical interaction of the surface N atoms with polar adsorbate.

#### Acknowledgements

Authors gratefully thank Russian Science Foundation (project 14-43-00072) and Russian Foundation for Basic Research (project 16-33-00916) for financial support.

#### References

1. X. Wu, J. Zhou et al.: Insight into high areal capacitances of low apparent surface area carbons derived from nitrogen-rich polymers. *Carbon* **94**, 560–567 (2015).
2. S. V. Savilov, N. E. Strokova et al.: Nanoscale carbon materials from hydrocarbons pyrolysis: structure, chemical behavior, utilisation for non-aqueous supercapacitors. *Mater. Res. Bull.* **69**, 13–19 (2015).

## O38

### NEAR-FIELD INFRARED NANOSCOPY ON DIFFERENT TYPES OF CARBON NANOTUBE BUNDLES

*Gergely Németh, Dániel Datz, Hajnalka M. Tóháti, Áron Pekker, Katalin Kamarás*

Institute for Solid State Physics and Optics, Wigner Research Centre for Physics, Hungarian Academy of Sciences, Budapest, Hungary

Scattering-type scanning near-field optical microscopy (s-SNOM) yields information on the optical characteristics from the scattered light enhanced by a strong, localized electromagnetic field between a metal-coated tip and the sample. The spatial resolution of the infrared s-SNOM method is 20–50 nm. We demonstrate that this technique at infrared frequencies can be effectively used to distinguish between carbon nanotube bundles based on their electrical properties. In this frequency range, the difference in the free-carrier concentration between metallic and semiconducting tubes is expected to influence the properties of the scattered light. The remarkable difference in the optical phase images proves that this is indeed the case: the metallic and semiconducting bundles are unambiguously identifiable in the sample, even in case of 5 nm diameter bundles. The measurements agree qualitatively with our calculations based on the extended finite dipole model using the known optical functions of the constituting nanotubes [1].

#### Reference

1. H. M. Tóháti, A. Pekker, B. Á. Pataki, Zs. Szekrényes and K. Kamarás: *Eur. Phys. J. B* **87**, 126-1-6 (2014).

## O39

## INTERACTION OF GOLD WITH THE HEXAGONAL BORON NITRIDE NANOMESH PREPARED ON Rh(111)

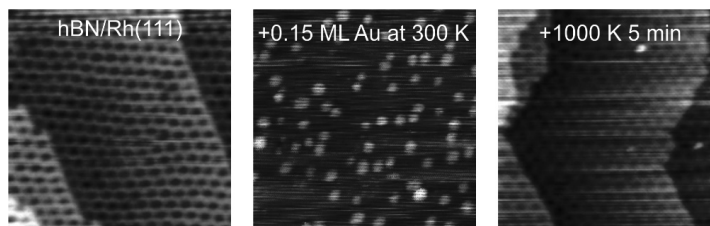
*Gábor Vári*<sup>1</sup>, *Richárd Gubó*<sup>1</sup>, *János Kiss*<sup>2</sup>, *Arnold Farkas*<sup>3</sup>, *László Óvári*<sup>2</sup>, *András Berkó*<sup>2</sup>, *Zoltán Kónya*<sup>1,2</sup>

<sup>1</sup>Department of Applied and Environmental Chemistry, University of Szeged, Szeged, Hungary

<sup>2</sup>MTA-SZTE Reaction Kinetics and Surface Chemistry Research Group, Szeged, Hungary

<sup>3</sup>Department of Physical Chemistry and Materials Science, University of Szeged, Szeged, Hungary;  
e-mail: ovari@chem.u-szeged.hu

Two dimensional hexagonal boron nitride (hBN) monolayers (MLs) are promising insulator components for nanoelectronics. When prepared on certain low index transition metal surfaces, like Rh(111), a periodic corrugation of the single hBN layer takes place, and a so-called nanomesh is formed consisting of “wires” and “pores” [1, 2]. This feature allows its application as a nanotemplate with a hexagonal periodicity of 3.2 nm [3], with implications also for plasmonics. Here we report on the growth of Au on the hBN/Rh(111) surface and subsequent thermal effects, studied by scanning tunneling microscopy (STM), X-ray photoelectron spectroscopy (XPS), and low energy ion scattering spectroscopy (LEIS). The latter technique reveals the elementary composition of the outermost atomic layer. When a small amount of gold (~0.15 ML) is evaporated at 300 K, 1–2 atomic layer high nanoparticles form, both on the wires and in the pores. At higher coverages the growth mode is three dimensional. Although typically on other inert surfaces small gold particles are characterized by a Au 4f<sub>7/2</sub> binding energy higher than the bulk value due to final state effects [4], in this case the gold peak was observed at a rather low position (83.7 eV), indicating significant electronic interaction either with hBN or with the rhodium substrate through the hBN monolayer. Indeed, previous density functional theory (DFT) calculations indicated an electron transfer from boron nitride to gold [5, 6]. The intercalation of gold is the dominant process upon stepwise thermal annealing to 1050 K, but agglomeration and evaporation also occurs to a limited extent. Interestingly, gold and rhodium, which are bulk-immiscible, form a surface alloy after the intercalation, but the presence of ~0.15–0.5 ML of Au below the hBN layer does not significantly influence the nanomesh structure (see figure; image size: 50 nm × 50 nm). At higher gold doses the flattening of the nanomesh was observed.



## References

1. M. Corso et al.: *Science* **303**, 217 (2004).
2. R. Laskowski et al.: *J. Phys.: Condens. Matter* **20**, 064207 (2008).
3. I. Brihuega et al.: *Surf. Sci.* **602**, L95 (2008).
4. J. Kiss et al.: *e-J. Surf. Sci. Nanotech.* **12**, 252 (2014).
5. H.-P. Koch et al.: *Phys. Rev. B* **86**, 155404 (2012).
6. M. Patterson et al.: *Phys. Rev. B* **89**, 205423 (2014).

**O40****PROMOTION AND INHIBITION EFFECTS OF TiO<sub>x</sub> AND MoO<sub>x</sub> SPECIES ON THE REACTIVITY OF ATOMICALLY THIN Rh FILMS***Imre Sze<sup>1,2</sup>*, *László Deák<sup>1</sup>*, *Zoltán Kónya<sup>1,2</sup>*<sup>1</sup>MTA-SZTE Reaction Kinetics and Surface Chemistry Research Group, Szeged, Hungary;  
e-mail: sze<sup>1</sup>@chem.u-szeged.hu<sup>2</sup>Department of Applied and Environmental Chemistry, University of Szeged, Rerrich Béla tér 1,  
6720 Szeged, Hungary

Metal oxides are mostly involved in heterogeneous catalysis inherently since they are used widely to support the finely dispersed, catalytically active metal particles. Moreover, from the so-called reducible oxide supports particles like TiO<sub>x</sub> and MoO<sub>x</sub> are able to migrate on the surface of metal nanoclusters and can act as promotors. They were found to enhance considerably the catalytic activity of Rh particles in the CO hydrogenation reaction performed at high pressure [1, 2], which motivated our UHV model study.

The structure of TiO<sub>x</sub> and MoO<sub>x</sub> overlayers and their effect on the bonding of CO test molecule to different Rh surfaces supported by TiO<sub>2</sub>(110) single crystal was investigated by Thermal desorption Spectroscopy (TPD), Auger Electron Spectroscopy (AES), and work function (WF) measurements. The TiO<sub>x</sub> encapsulation layers produced by heating the 0.1–20.0 monolayer (ML) thick Rh deposits suppressed the molecular CO desorption ( $T_p = 580$  K) and generated a recombinative CO state ( $T_p = 770$  K). The MoO<sub>x</sub> overlayers formed by the oxidation of Mo deposits showed similar characteristics, inhibiting the CO adsorption, but inducing a recombinative state with  $T_p = 700$  K. The lower peak temperature of associative CO desorption suggests the presence of less strongly bonded C and O atoms than on the TiO<sub>x</sub>-covered rhodium, allowing an enhanced reaction rate for these intermediates in the catalytic reactions of dissociatively adsorbed CO. In harmony with the findings of high pressure studies, the extent of CO dissociation was maximal at 0.2–0.3 ML TiO<sub>x</sub> and MoO<sub>x</sub> coverages, where the number of active centers at the rhodium-oxide interfaces was maximized. A 1 ML thick overlayer of both oxides suppressed completely the CO uptake, indicating that the oxide/rhodium mass ratio must be low enough to ensure a promotional effect. Other critical issue is that the development of recombinative CO states needs a threshold Rh coverage, attributable to particle size effect and geometric factors governing the CO adsorption.

The impact of a TiO<sub>x</sub> film being underneath an Rh deposit on the surface chemistry was also studied. The Rh-TiO<sub>x</sub>-Rh structure formed at 230 K by the deposition of Rh on a continuous TiO<sub>x</sub> film supported by Rh multilayer showed high chemical reactivity. Noticeably, the stability of MOM structure was greatly affected by the adsorbed CO. This structure was destroyed at 265 K in the absence, but was preserved up to 550 K in the presence of the adlayer, suggesting that in general the stability of atomically thin, reactive MOM structures may be significantly influenced by adsorbates.

**References**

1. A. Boffa, C. Lin, A. T. Bell and G. A. Somorjai: *J. Catal.* **149**, 149 (1994).
2. E. E. Lowenthal, L. F. Allard, M. Te and H. C. Foley: *J. Mol. Catal. A-Chem.* **100**, 129 (1995).

## O41

ELECTRICAL AND PHOTOELECTRICAL PROPERTIES OF HETEROJUNCTIONS  
p-Si/Cd<sub>1-x</sub>Zn<sub>x</sub>O

*H. M. Mamedov, M. B. Muradov, V. J. Mamedova, Kh. M. Ahmadova*

Department of Physical Electronics, Faculty of Physics, Baku State University, 370148, Z.Khalilov str., 23, Baku, Azerbaijan; e-mail: mhhuseyng@gmail.com

In this paper we demonstrate Cd<sub>1-x</sub>Zn<sub>x</sub>O based heterojunction using p-type Si as substrate. The purpose of the given work is the investigation of electric and photoelectrical properties of heterojunctions n-Cd<sub>0.4</sub>Zn<sub>0.6</sub>O/p-Si deposited by electrochemical way, depending on the deposition and heat treatment regimes.

The electrochemical deposition has been performed with a three electrode configuration: graphite as anode, Ag/AgCl<sub>3</sub> electrode as reference electrode and glass/p-Si thin films (200 nm) as cathode. The glass/p-Si substrates were cleaned with ethanol, acetone and deionized water and then dried in flowing N<sub>2</sub>. At electrodeposition we used the high purity zinc and cadmium salts. The electrodeposition was carried out potentiostatically at -0.9, -1.2 V, -1.28 V and -1.35 V vs. Ag/AgCl for 1–2 hour. According to the top-view SEM images, the surface of electrodeposited Cd<sub>0.4</sub>Zn<sub>0.6</sub>O films more rough and non-homogenous deposited at -0.9 V. The morphology of films changes from non-homogenous surface to nano-granular structures with increasing the deposition potential up to -1.2 ÷ -1.28 V and then ( $\geq -1.3$  V) to micro-granular arrays. It indicated that the applied potentials exhibited more influence on the morphology and structures of top layer of Cd<sub>0.4</sub>Zn<sub>0.6</sub>O films. It is found that the mechanism of current passage through the heterojunctions essentially changes with increasing deposition potential from -0.9 V to -1.28 V: recombination currents sharply decrease, which shows the reduction of defects and decreasing of the series resistance of films. Films with nano-structured surface, which deposited at -1.2 ÷ -1.28 V, shows good rectification ( $k = 30\text{--}40$ ). The ideality factor of heterojunctions deduced from semi-logarithm I–V plot was decreased up to  $n = 1.8$ . This high value of ideality factor suggests the domination of recombination process in these devices which occurs in the junction region. We also studied the effect of films surface morphology on the photoelectric properties of these heterojunctions. There occurs a reconstruction of the photosensitivity spectrum with increasing deposition potential up to -1.2 V. As the deposition potential increased from -0.9 V to -1.28 V, photosensitivity at  $\lambda_m = 0.36 \mu\text{m}$ . The near infrared photosensitivity fall-off for all heterojunctions indicated Si absorber band gaps of 1.1 eV. Under AM1.5 conditions the maximal values of open-circuit voltage, short-circuit current, fill factor and efficiency of our best cell, were  $V_{oc} = 202$  mV,  $J_{sc} = 1.3$  mA/cm<sup>2</sup>, FF = 0.4 and  $\eta = 1.7\%$ , respectively. The value of short-circuit-photocurrent varies nonmonotonically with HT duration. Initially,  $J_{sc}$  increases with duration, reaches a maximum value and at >11 min, decreases drastically. After the HT at 500–560 °C for 11 min in argon atmosphere photoelectric parameters of junctions were  $V_{oc} = 240$  mV,  $J_{sc} = 2.5$  mA/cm<sup>2</sup>, FF = 0.46 and  $\eta = 2.6\%$ , respectively.

Thus, electrical and photoelectrical parameters of Cd<sub>0.4</sub>Zn<sub>0.6</sub>O/p-Si heterojunctions can be controlled by deposition potential and the HT condition.

## ORAL PRESENTATIONS

Saturday, 15 October, 2016

### O42

#### Li AND Na INSERTION INTO $\text{Li}_4\text{Ti}_5\text{O}_{12}$ MADE BY DIFFERENT SYNTHETIC PROTOCOL

*M. Zúkalová, B. Pitná Lasková, L. Kavan*

J. Heyrovský Institute of Physical Chemistry, v.v.i., AS CR, Dolejšková 3, CZ-18223 Prague 8, Czech Republic

Li-Ti ternary oxides are attractive candidates for anodes in rechargeable Li-ion batteries, due to their low cost, non-toxicity, cycling stability at high charging rate and reasonable capacity. In parallel with an employment of Li-ion batteries as prominent power sources for many portable devices and their perspectives in large-scale applications more and more research teams realize limited sources of lithium and transition metals. In search for possible alternative a substitution of Li with Na seems to be a feasible solution. Na resources as NaCl in seawater are practically unlimited. However, due to larger radius of Na ion (Na: 1.02 Å, Li: 0.76 Å) there is only limited number of possible Na-ion host materials in contrary to relatively broad variety of materials inserting Li. Recently, lithium titanate spinel ( $\text{Li}_4\text{Ti}_5\text{O}_{12}$ , LTO), used as the negative electrode material in Li-ion batteries, has also been examined for the Na-ion battery.  $\text{Li}_4\text{Ti}_5\text{O}_{12}$  is known as a “high potential” negative electrode material with a formal potential of 1.55 V vs. Li/Li<sup>+</sup>, whereby one can avoid the dendrite problem. This character should also prevent the Na-dendrite deposition. Na insertion in  $\text{Li}_4\text{Ti}_5\text{O}_{12}$  is accompanied with development of extra phase with an about 4–5% larger unit cell volume which co-exists with  $\text{Li}_4\text{Ti}_5\text{O}_{12}$  in a single particle and is identified as a Na-substituted LTO phase [1, 2].

In our work we studied Li and Na insertion into LTO spinel of different particle size and synthetic history, either commercial or laboratory made. The highest capacity and charging rate both for Li and Na insertion exhibited nanocrystalline LTO prepared by sol-gel process pioneered in our laboratory. During testing of Li insertion/extraction by galvanostatic chronopotentiometry at 1 C this material exhibited excellent stability over tens of cycles with almost 100% of theoretical capacity (175 mAh/g). In contrary, commercial materials exhibited a capacity drop of about 30% after 50 cycles. In case of Na insertion, the charge capacity of nanocrystalline LTO prepared by sol-gel process was 158 mAh/g in the first cycle, however considerable capacity drop of about 40% was observed during cycling. This is obviously the consequence of irreversible structural changes induced by Na accommodation in the  $\text{Li}_4\text{Ti}_5\text{O}_{12}$  lattice. The best cycling stability for Na insertion exhibited commercial LTO from Altair. After 50 cycles at 1 C the charge capacity of this material (with 20% Super P additive) decreased from initial 105 mAh/g to 85 mAh/g, i. e. of about 20%.



**Acknowledgements**

This work was supported by the Grant Agency of the Czech Republic (contracts No. 13-07724S and 15-06511S).

**References**

1. M. Kitta, K. Kuratani, M. Tabuchi, N. Takeichi, T. Akita, T. Kiyobayashi and M. Kohyama: *Electrochimica Acta* **148**, 175–179 (2014).
2. L. Kavan, J. Prochazka, T. M. Spitler, M. Kalbac, M. T. Zukalova, T. Drezen and M. Gratzel: *Journal of the Electrochemical Society* **150**, A1000–A1007 (2003).

**O43****NEW FAMILY OF Zn CARBOXYLATE MOFs WITH CUBANE LINKERS**

*Éva Kováts*<sup>1</sup>, *Dávid Földes*<sup>1,2</sup>, *Gábor Bortel*<sup>1</sup>, *Emma Jakab*<sup>3</sup>, *Sándor Pekker*<sup>1,2</sup>

<sup>1</sup>Institute for Solid State Physics and Optics, Wigner Research Centre for Physics, P.O. Box 49, H-1525 Budapest, Hungary; e-mail: eva.kovats@wigner.mta.hu

<sup>2</sup>Óbuda University, Doberdó út 6, H-1034 Budapest, Hungary

<sup>3</sup>Institute of Materials and Environmental Chemistry, Research Centre for Natural Sciences, Magyar tudósok körútja 2, H-1117 Budapest, Hungary

Metal-organic frameworks (MOFs) are a rapidly developing family of crystalline solids [1]. The high symmetry, rigid extended solid state structures usually contain voids with remarkable size capable of incorporation of small molecules, enabling several potential applications like gas storage, selective absorption or catalysis. MOFs are highly modular systems, their frameworks built up from metal ions or clusters connected to rigid organic linker molecules by strong bonds of covalent and ionic character. The large variety of these two basic structural units facilitates efficient crystal engineering: new series of MOFs with desired structural properties can be easily designed.

The most famous MOF family is based on zinc-containing clusters and terephthalic acid linkers. A well-known member is the cubic MOF-5 [2], its structure consists of basic zinc carboxylate units and terephthalic acid linkers. It has exceptional gas absorption properties based on its high volume 3D pore system. In order to change the basic structural and absorption properties of these frameworks we used rigid aliphatic organic molecules with similar size as that of the terephthalic acid as linkers. We successfully built in cubane-1,4-dicarboxylic acid as organic linker and synthesised several new MOF structures. The crystal structures were determined by single crystal X-ray diffraction. By changing the synthesis conditions we obtain several polymorphic structures. Besides high symmetry cubic 3D networks with large voids, 2D MOFs consisting of layers and lower symmetry interpenetrated structures were also designed. Here we will analyse the frameworks based on the main structural features. The relation between the effect of the Zn coordination and the structure and stability of the crystals is revealed. By changing the organic linker we can establish their effect on the crystal symmetry. Incorporated solvents can also modify the structure by coordination to the metal centre. Based on these experiments we can fine tune the shape and size of the voids in the prepared crystal structures.

Besides the crystal structures and the basic structural properties, thermal stability based on TG-MS measurements will also be discussed.

**References**

1. T. R. Cook, Y.-R. Zheng and P. J. Stang: Metal–organic frameworks and self-assembled supramolecular coordination complexes: comparing and contrasting the design, synthesis, and functionality of metal–organic materials. *Chem. Rev.* **113**, 734–777 (2013).
2. H. Li, M. Eddaoudi, M. O’Keeffe and O. M. Jaghi: Design and synthesis of an exceptionally stable and highly porous metal-organic framework. *Nature* **402**, 276–279 (1999).

## POSTER PRESENTATIONS

T01 – Synthesis and properties  
of new nanostructured systems

### T01\_01

#### IONENE-STABILIZED SILVER AND GOLD NANOPARTICLES: SYNTHESIS AND APPLICATION FOR DETERMINATION OF PYROPHOSPHATE AT HIGH CONCENTRATION LEVEL

*Ekaterina A. Terenteva, Vladimir V. Apyari, Stanislava G. Dmitrienko, Yury A. Zolotov*

Analytical Chemistry Division, Department of Chemistry, Lomonosov Moscow State University, Leninskie gory, 1/3, Moscow 119991, Russia; e-mail: ekaterinaaleks92@mail.ru

Pyrophosphates are actively used as food additives to increase the mass of muscle tissue and the yield of a final product. Also pyrophosphates improve organoleptic characteristics and product consistency, stabilize the color, and slow down the oxidative processes. When excessive use of this additive, it can cause indigestion, as well as disorders related to an imbalance of phosphorus and calcium in the body. One of the prospect ways to develop simple and fast spectrophotometric or naked-eye colorimetric procedures can be based on the optical properties of silver and gold nanoparticles (AgNPs and AuNPs).

In this work, we studied the possibility of using AgNPs and AuNPs stabilized with 6,6-ionene for spectrophotometric determination of pyrophosphate based on their aggregation.

Silver and gold nanoparticles stabilized with 6,6-ionene were first obtained by the borohydride method. Conditions of the syntheses were selected. The average diameter of AgNPs and AuNPs is 23 and 16 nm, respectively. It has been shown that they have ability to easily aggregate in the presence of pyrophosphate. Dihydrophosphate, nitrate, chlorate, perchlorate, bromide, fluoride, chloride and hydrocarbonate do not affect the NP aggregative state remarkably. We assume that this effect is associated with different charge and size of the anions, and hence, the different ability to form bonds with NPs. Aggregation is accompanied by decreasing the surface plasmon resonance band of AgNPs at 400 nm and AuNPs at 520 nm, and appearing the absorption bands of aggregates at 500 and 675 nm, respectively. This can be used for spectrophotometric determination of pyrophosphate.

The degree of aggregation was characterized by the absorbance ratio at 500 and 400 nm ( $A_{500}/A_{400}$ ) and at 675 and 520 nm ( $A_{675}/A_{520}$ ), respectively. Dependence of this ratio on the concentration of pyrophosphate can be used for plotting a calibration curve. The influence of various factors such as reaction time, pH, and the concentration of pyrophosphate and nanoparticles on their aggregation was studied. The limit of detection is  $12 \mu\text{g mL}^{-1}$ , and the analytical range is  $15\text{--}50 \mu\text{g mL}^{-1}$  in case of AgNPs; the limit of detection is  $45 \mu\text{g mL}^{-1}$ , and the analytical range is  $50\text{--}70 \mu\text{g mL}^{-1}$  in case of AuNPs. Thus, the method developed is prospective for determination of high concentration levels of pyrophosphate. It was used to analysis a baking powder and a

copper plating solution. The results agree well with the declared data and results obtained by an independent method, indicating good accuracy of the proposed procedure.

#### Acknowledgments

This work was financially supported by the Russian Science Foundation (grant N 14-23-00012).

### T01\_02

#### EFFECT OF ACID TREATMENT ON THE MORPHOLOGY AND SURFACE PROPERTIES OF NITROGEN-DOPED CARBON NANOTUBES

*Ekaterina Arkhipova*<sup>1,2</sup>, *Anton Ivanov*<sup>1</sup>, *Serguei Savilov*<sup>1</sup>, *Konstantin Maslakov*<sup>1</sup>, *Valery Lunin*<sup>1</sup>

<sup>1</sup>Department of Chemistry, Lomonosov Moscow State University, Leninskie gory, 1-3, Moscow, Russia; e-mail: trrisa@bk.ru

<sup>2</sup>N. S. Kurnakov Institute of General and Inorganic Chemistry of Russian Academy of Sciences, Leninsky Avenue, 31, Moscow, Russia

Nitrogen-doped carbon nanotubes (N-CNTs) attract increasing interest owing to their unique physicochemical properties such as high specific surface area, thermal stability and controlled pore structure. The surface chemistry of CNTs, especially the presence of different functional groups, enables their application as catalysts, sorbents and electrode materials for supercapacitors. Controlling morphology and surface properties of CNTs is one of the main challenges in their production and modification. Nitric acid treatment is well known to be the most common way of CNTs structure modification which allows introducing oxygen-containing functional groups on the CNTs surface.

Nitrogen-doped carbon nanotubes were synthesized at 750 °C by chemical vapor deposition technique [1] using acetonitrile as a precursor and Co-Mo/MgO as a mesoporous catalyst. As-grown N-CNTs were refluxed in 68 wt. % HNO<sub>3</sub> for 0–12 hours at 120 °C. According to HRTEM the oxidation resulted in the destruction of surface graphene layers and opening of inner channels of N-CNTs. The increase of structure defectiveness of N-CNTs was confirmed by the increase of I<sub>D</sub>/I<sub>G</sub> ratio in Raman spectra. XPS was used to identify the composition and chemical state of N-CNTs surface. It was found that nitrogen incorporated into CNT structure in quaternary, pyridine, pyrrole, pyridone positions and as N-oxides. The total nitrogen content decreased during oxidation from 2.7 to 0.5 at. %. However the oxygen content on the surface stabilized after 3 hours of acid treatment.

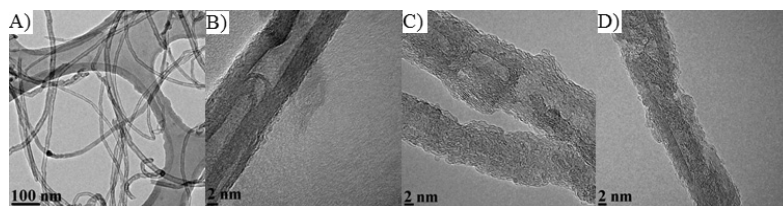


**Fig. 1.** HRTEM microphotographs of N-CNTs: A, B – initial; C, D – acid treated for 7 and 12 hours

The reported study was funded by RFBR according to the research project No. 16-33-00916.

**Reference**

1. S. A. Chernyak, E. V. Suslova, A. V. Egorov, L. Lu, S. V. Savilov and V. V. Lunin: New hybrid CNT–alumina supports for Co-based Fischer–Tropsch catalysts. *Fuel Process. Technol.* **5140**, 267–275 (2015).

**T01\_03****MODIFICATION OF GRAPHENE-OXIDE SURFACE IN ARGON AND NITROGEN PLASMA**

*I. Bertóti, M. Mohai*

Institute for Materials and Environmental Chemistry, Research Centre for Natural Sciences, Hungarian Academy of Sciences, P O Box 286, H-1519 Budapest, Hungary

We performed glow discharge Ar or N<sub>2</sub> plasma treatments of thin layers of commercial graphene oxide (GO) deposited from diluted mixtures with ethanol onto the surface of a stainless steel sample holder. The plasma treatment was performed in the preparation chamber of the X-ray photoelectron spectrometer, providing *in situ* characterization of the treated surface by quantitative XPS. Based on preliminary experiments a 10 min plasma exposure was selected. Intensity of the treatment was intensified by applying negative bias between 0–300 V on the sample.

About 10 atomic % nitrogen was incorporated into the GO samples from N<sub>2</sub> plasma within this short reaction time. When increasing the bias, the N-content increased from 10 to 13 atomic %, together with the decrease of the O content from the starting value of 29 atomic % to about 15 atomic %. The reducing effect of Ar plasma was less pronounced, decreasing the oxygen content to 21 atomic % only. The high resolution C1s, O1s and N1s spectra show several different chemical states. The peak envelopes of the O1s and N1s lines could be decomposed to three, while the C1s spectrum to six different peak components of identical position and widths for all samples. The component peaks were assigned to specific chemical bonding states. Quantitative evaluation of the different C–C, C–O and C–N states were performed and the changes were interpreted in the light of the increasing bias, i.e., of the change of the energy of bombarding Ar<sup>+</sup> and N<sub>2</sub><sup>+</sup> ions.

**T01\_04****SYNTHESIS OF PHOTOACTIVE ANTIMONY OXYIODIDE HIERARCHICAL NANOSTRUCTURES**

*Tamás Boldizsár<sup>1,2</sup>, Balázs Buchholcz<sup>1,3</sup>, Henrik Haspel<sup>1</sup>, Zoltán Kónya<sup>1,3</sup>, Ákos Kukovecz<sup>1,2</sup>*

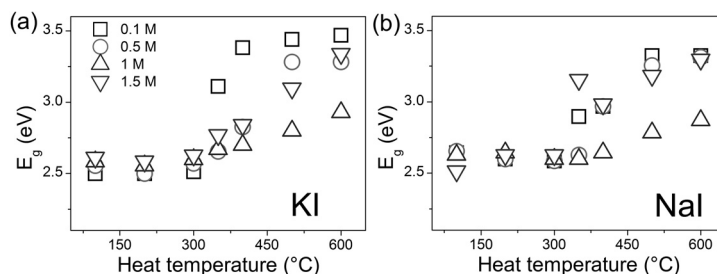
<sup>1</sup>Department of Applied and Environmental Chemistry, University of Szeged, Rerrich Béla tér 1, H-6720 Szeged, Hungary

<sup>2</sup>MTA-SZTE “Lendület” Porous Nanocomposites Research Group, Rerrich Béla tér 1, H-6720 Szeged, Hungary

<sup>3</sup>MTA-SZTE Reaction Kinetics and Surface Chemistry Research Group, Rerrich Béla tér 1, H-6720 Szeged, Hungary

The photocatalytic and photocurrent activity of V-VI-VII semiconductors, mainly bismuth oxyhalides (BiOX), such as BiOCl structures has been well-known in the literature [1]. Despite the vast amount of reports on BiOX structures, information about photoactive antimony oxyhalogenide nanomaterials (SbOX) are almost completely missing. These materials might be very promising alternatives to the bismuth-based photomodifiers. Up to now, antimony nanostructures have been prepared with different sizes and morphologies, such as nanorods and nanowires [2].

In this study we report the preparation of antimony oxyiodide ( $Sb_xO_yI_z$ ) 3D hierarchical nanostructures via a facile precipitation method for the first time ever.  $SbCl_3$  transformed into different antimony oxyiodides applying two iodide salts in various concentrations as iodine source in acidic environment. The systems' morphology was examined by scanning electron microscopy (SEM), while the crystal phase and the electronic properties were studied by powder X-ray diffractometry (XRD) and diffuse reflection spectroscopy (DRS), respectively. The properties and composition of the samples were further varied by a subsequent heat-treatment of the as-prepared materials. The reported oxyhalides ( $Sb_xO_yI_z$ ) were tested in photocurrent measurements to assess their photoactivity.



### Acknowledgements

The financial support of the Hungarian Research, Development and Innovation Office through projects K 112531 and K 120115 is acknowledged.

### References

1. W. W. Lee, C.-S. Lu, C.-W. Chuang, Y.-J. Chen, J.-Y. Fu, C.-W. Siao and C.-C. Chen: *RSC Adv.* **5**, 23450–23463 (2015).
2. X. Y. Chen, H. S. Huh and S. W. Lee: *J. Solid State Chem.* **181**, 2127–2132 (2008).

## T01\_05

### LOW-TEMPERATURE N,F CO-DOPING OF LAYERED TITANATE NANOTUBES AND BULK ANATASE $TiO_2$ : A COMPARATIVE STUDY

*Balázs Buchholcz*<sup>1,3</sup>, *Kamilla Plank*<sup>1,3</sup>, *Henrik Haspel*<sup>1,2</sup>, *Ákos Kukovecz*<sup>1,2</sup>, *Zoltán Kónya*<sup>1,3</sup>

<sup>1</sup>Department of Applied and Environmental Chemistry, University of Szeged, Rerrich Béla tér 1, H-6720 Szeged, Hungary

<sup>2</sup>MTA-SZTE “Lendület” Porous Nanocomposites Research Group, Rerrich Béla tér 1, H-6720 Szeged, Hungary

<sup>3</sup>MTA-SZTE Reaction Kinetics and Surface Chemistry Research Group, Rerrich Béla tér 1, H-6720 Szeged, Hungary

In the past two decades nanotubes have become the symbol of nanotechnology, a new and fast evolving field of science. Inorganic nanotubes with trititanate structure ( $\text{Na}_x\text{H}_{2-x}\text{Ti}_3\text{O}_7$ ) were first synthesized by Kasuga and coworkers. Their intention was to obtain  $\text{TiO}_2$  with high specific surface area and enhanced photocatalytic activity. However, the applied alkaline treatment gave rise to morphological changes and tubular nanostructures with diameter of  $\sim 8$  nm and length of  $\sim 100$  nm appeared in the samples. Many possible applications of titanate nanotubes are known nowadays: high surface area mesoporous catalyst support, adsorbent, insoluble matrix for ion-exchange processes, etc. They are used in the development of lithium-ion batteries, in medical biology and are promising candidates for heterogeneous photocatalysis as well.

In our study titanate nanotubes were synthesized via the alkaline hydrothermal procedure. After a subsequent protonation step the obtained nanotubes were co-doped with nitrogen and fluorine using ammonia and hydrogen-fluoride formed *in situ* by the thermal decomposition of  $\text{NH}_4\text{F}$  [1]. This new method is an economic low temperature alternative to the existing gas phase N, F co-doping procedures. Different doping temperatures were applied to the samples and their effect investigated by transmission electron microscopy (TEM), X-ray diffraction (XRD), nitrogen adsorption measurements, diffuse reflectance infrared Fourier transform (DRIFT) Raman, UV-Vis and X-ray photoelectron (XPS) spectroscopy. Bulk anatase  $\text{TiO}_2$  also underwent the former process, and results were compared to that obtained for layered titanates.

The chemical surround of the nitrogen species and its diversity highly depends on the applied doping temperature and the pristine titanium-oxides modified in the process. Morphology and structure of layered titanate nanotubes change during doping, which further promote the incorporation of N and F.

#### Acknowledgements

The financial support of the Hungarian Research, Development and Innovation Office through projects K 112531 and K 120115 is acknowledged.

#### Reference

1. B. Buchholz, H. Haspel, Á. Kukovecz and Z. Kónya: *CrystEngComm* **16**, 7486–7492 (2014).

## T01\_06

### NOVEL POLYESTER COATINGS FOR PREPARATION OF MAGNETIC CORE SHELL NANOPARTICLES

*Alexander Bunge, Teodora Radu, Xenia Filip, Alexandrina Nan*

National Institute for Research and Development of Isotopic and Molecular Technologies,  
67-103 Str Donat, 400293 Cluj-Napoca, Romania; e-mail: itim@itim-cj.ro

Polyesters – especially polylactides and polyglycolides – have gained considerable interest over the last decade. Polylactic acid is one of the most well-known polymers that can be synthesized from renewable resources, and at the same time is biodegradable and biocompatible [1]. By changing the synthesis conditions and starting material many of its properties like molecular weight, solubility, mechanical strength and melting point can be changed. However, other properties such as hydrophobicity and the ability to be functionalized only at terminal OH-groups

are not easily altered. To circumvent this, several attempts have already been made to synthesize either fully functionalized or mixed polyesters with different structural elements [2]. Generally these attempts start from a suitable lactide undergoing a ring opening polymerization (ROP), but also direct polymerizations of respective  $\alpha$ -hydroxy acids are known.

Magnetic nanoparticles have received much interest in the last years [3]. Their magnetism can be exploited for a variety of applications, from magnetic separation (catalysts or in water purification) to data storage or biomedicine [4] (as targetable drug carrier, for hyper-thermia treatment or as MRI contrast agent). For most applications, however, a suitable coating is imperative to provide chemical and colloidal stability or additional functionality.

Aside from their use as polymers as such in other applications, new polylactides or more general polyesters can be excellent coating materials for magnetic nanoparticles to be used especially in biomedicine due to their biocompatibility.

Thus novel polyesters were prepared based on functionalized mandelic acid. By performing the polymerization in the presence of magnetite nanoparticles or applying the coating after the polymerization was completed, new core-shell magnetite nanoparticles were obtained. Their properties were analyzed using various methods such as FT-IR spectroscopy, ss-NMR, TEM, XPS and magnetic measurements.

These investigations received financial support from the National Authority for Scientific Research and Innovation Romania (ANCS), Project PN-II-RU-TE-2014-4-0654.

#### References

1. S. Slomkowski, S. Penczek and A. Duda: Polylactides – an overview. *Polym. Adv. Technol.* **25**, 436–447 (2014).
2. H. Tian, Z. Tang, X. Zhuang, X. Chen and X. Jing: Biodegradable synthetic polymers: preparation, functionalization and biomedical application. *Prog. Polym. Sci.* **37**, 237–280 (2012).
3. A. H. Lu, E. L. Salabas and F. Schüth: Magnetic nanoparticles: synthesis, protection, functionalization, and application. *Angew. Chem. Int. Ed.* **46**, 1222–1244 (2007).
4. H. Lee, T.-H. Shin, J. Cheon and R. Weissleder: Recent developments in magnetic diagnostic systems. *Chem. Rev.* **115**, 10690–10724 (2015).

## T01\_07

### BIOCOMPATIBLE PHOTOPOLYMER NANOCOMPOSITES FOR ELEMENTS OF PHOTONICS

J. Burunkova<sup>1</sup>, D. Zhuk<sup>1</sup>, I. Denisjuk<sup>1</sup>, A. Stepanov<sup>2</sup>, E. Oresak<sup>2</sup>, I. Csarnovics<sup>3</sup>, K. Bene<sup>4</sup>, E. Rajnavolgyi<sup>4</sup>, A. Bonyár<sup>5</sup>, S. Kokenyesi<sup>3</sup>

<sup>1</sup>University ITMO, St Petersburg, Russian Federation

<sup>2</sup>North West State Medical University named after I. I. Mechnikov, St. Petersburg, Russian Federation

<sup>3</sup>University of Debrecen, Institute of Physics, Debrecen, Hungary

<sup>4</sup>University of Debrecen, Department of Immunology, Debrecen, Hungary

<sup>5</sup>Budapest University of Technology and Economics, Department of Electronics Technology, Budapest, Hungary



Research and development of photonic elements like waveguides, diffractive gratings, photonic crystals and others has become an area of great interest due to fast developing applications in info communication technologies, sensing and optoelectronics. New compositions with enhanced multifunctional characteristics, possibilities of comparatively simple fabrication technologies are desirable for these purposes. Polymer nanocomposites based on acrylates and silica, other oxides as well as gold nanoparticles (AuNPs) were fabricated with special route of direct mixing of preformed nanoparticles (NPs) to the monomer composition. The introduction of AuNPs was important for the development of smart sensing, photonic elements with plasmon effects.

The mechanism of photo-polymerization processes during the direct, one step optical, holographic recording was analyzed. In our case the introduction of AuNPs influences the rate of the refractive index change and the surface relief depth formation in the recorded one- or two dimensional photonic structures. The role of the localized plasmons generated at 530 nm spectral range in AuNPs in the photo-polymerization process and diffusion-mediated mass transport, spatial redistribution of NPs and so the geometrical relief formation was analyzed. The presence of NPs is important for further developments of smart photonic elements, functionalized by different materials.

Biocompatibility of such layers and of the simple surface grating, recorded in the developed nanocomposites was investigated. Dendritic cells (DC) play a role in the first line of defense and polarize the specific immune response against self and non-self structures in the human body. We set up an *in vitro* culture system to test the inflammatory capacity and viability of human DC in the presence of NPs. Further, we also analyzed how NP affects the colony forming ability of commensal bacteria. Also, sorption of microorganism was studied; dependence on composition and surface modification of created nanocomposites was established.

## T01\_08

### CHARACTERIZATION OF LEAD TITANATE THIN FILMS PREPARED BY SOL–GEL PROCESS

*M. El Moussafir, R. Adhiri, M. Moussetad, Y. Guaaybess*

Laboratoire de l'Ingénierie et Matériaux, Faculté des Sciences Ben M'sik, B. P. 20800, Casablanca, Morocco; e-mail: elmoussafir@hotmail.fr

Ferroelectric materials are of high interest for a numerous applications, including non-volatile memories, dynamic random access memories, electrooptic switches, pyroelectric detectors, etc. and considerable attention has recently focused on the development of the technology for their growth in thin films.

Lead titanate ( $\text{PbTiO}_3$ ) PT sol–gel derived thin films have been prepared on glass substrates using lead acetate trihydrate, and titanium isopropoxide as precursors along with 2-methoxyethanol as solvent and acetic acid as catalyst by spin coating method, with Techniques including X-ray diffraction (XRD), scanning electron microscopy (SEM), electrical and ferroelectric hysteresis measurements have been performed for layer characterization.

**T01\_09****MOF-5 ANALOGUE STRUCTURES WITH CUBANE**

*Dávid Földes*<sup>1,2</sup>, *Éva Kováts*<sup>2</sup>, *Gábor Bortel*<sup>2</sup>, *Emma Jakab*<sup>3</sup>, *Sándor Pekker*<sup>1,2</sup>

<sup>1</sup>Institute for Solid State Physics and Optics, Wigner Research Centre for Physics of HAS, Konkoly-Thege Miklós út 29–33, 1121 Budapest, Hungary; e-mail: foldes.david@wigner.mta.hu

<sup>2</sup>Óbuda University, Doberdó út 6, 1034 Budapest, Hungary

<sup>3</sup>Institute of Materials and Environmental Chemistry, Research Centre for Natural Sciences of the HAS, Magyar tudósok körútja 2, 1117 Budapest, Hungary

Metal-organic frameworks are porous coordination polymers. The rigid, metal-containing clusters at the nodes (inorganic Secondary Building Units, inorganic SBUs) are joined by organic linkers [1]. The large inner cavities of metal-organic frameworks are capable for inclusion of gas molecules, inorganic and organic small molecules, that make MOF structures useful for many industrial applications, for example gas storage, heterogenous catalysis, molecular sensing, separation technology or making drug carriers. The most important and best-known MOF is MOF-5 [1]. In its cubic crystalline structure the four-nuclear  $Zn_4O(CO_2)_6$  secondary building units at the vertices are joined by terephthalate linkers at the edges. MOF-5 has a pore volume of 79% of unit cell volume, that results a really high surface area material, capable for safe and effective hydrogen gas storage.

Our goal was to substitute the aromatic terephthalic acid to the aliphatic cubane-1,4-dicarboxylic acid of the literary MOF-5 system [1, 2].

We successfully prepared several new metal-organic framework structures with four-nuclear zinc-containing SBUs at the vertices and cubane dicarboxylic acid linkers at the edges. We determined the crystal structures by single-crystal X-ray diffraction and we also determined the thermal stability of the samples by thermogravimetry/mass spectrometry (TG/MS).

Besides the high symmetry analogue to MOF-5, we prepared two similar high surface area cubic polymorphs with  $Zn_4O(CO_2)_6$  SBUs. These compounds have more disordered structure than the basic MOF-5 material. The void volumes of these compounds are around 72% of unit cell volume, that is comparable to the original MOF-5 structure. The cubic MOF-5 analogue with cubane is stable up to 200 °C and seems to be easy-to-activate, so this material can be also used for gas storage. We also prepared an interesting distorted MOF-5 analogue, in which solvent molecules are coordinated to the metal centers at the nodes, that results the distortion of the original MOF-5 structure and make possible the interpenetration of the independent macromolecules. That is why the resulted structure has much lower, only 14% void volume. The distorted MOF-5 structure is also an easy-to-activate framework with thermal stability up to 200 °C.

**References**

1. H. Li, M. Eddaoudi, M. O’Keeffe and O. M. Yaghi: *Nature* **402**, 276–279 (1999).
2. S. S. Kaye, A. Dailly, O. M. Yaghi and J. R. Long: *Journal of American Chemical Society* **129**, 14176–14177 (2007).

## T01\_10

**ADSORPTION OF SILVER TRIANGULAR NANOPATES ONTO POLYURETHANE FOAM AS A WAY TO PRODUCE A NEW NANOCOMPOSITE MATERIAL WITH SURFACE PLASMON RESONANCE FOR ANALYTICAL APPLICATION**

*Aleksei A. Furletov*<sup>1</sup>, *Vladimir V. Apyari*<sup>1</sup>, *Alexey V. Garshev*<sup>2</sup>, *Pavel A. Volkov*<sup>3</sup>,  
*Stanislava G. Dmitrienko*<sup>1</sup>

<sup>1</sup>Department of Chemistry, Lomonosov Moscow State University, Leninskie gory, 1/3, 119991 Moscow, Russia,

<sup>2</sup>Faculty of Materials Science, Lomonosov Moscow State University, Leninskie gory, 1/3, 119991 Moscow, Russia; e-mail: aleksei\_furletov@mail.ru

<sup>3</sup>Scientific-Research Institute of Chemical Reagents and Special Purity Chemicals, Bogorodsky Val 3, 107076, Moscow, Russia

Recently, silver nanoparticles have been widely used in analytical chemistry. They are used in various types of sensors, among which optical sensors take an important place. The optical properties of silver nanoparticles stem from the surface plasmon resonance (SPR), which causes intense absorption in the visible spectral region. These properties are especially interesting for non-spherical nanoparticles, for example triangular nanoplates (AgTNPs), as they depend on the particle shape and size. This can play a significant role in the development of new type sensors for determination of different compounds.

The aim of this work was to study adsorption of AgTNPs onto polyurethane foam (PUF) as a way to produce a new nanocomposite material with SPR for analytical application.

Synthesis of AgTNPs was carried out by the borohydride approach. The AgTNPs were characterized by transmission electron microscopy and spectrophotometry. There are two maxima in absorption spectra of AgTNPs, at 380–400 nm and 600–800 nm.

It was found that AgTNPs are easily adsorbed onto PUF from aqueous solution. Based on this fact, a sorption approach to the synthesis of a nanocomposite material with AgTNPs and polyurethane foam was developed. It was shown that AgTNPs on the PUF surface retain its ability of surface plasmon resonance. It appears as an absorption band in the diffuse reflection spectra of this material, and its intensity increases with increasing the concentration of AgTNPs. The kinetics of AgTNPs adsorption was described in terms of the pseudo-first-order model. An adsorption isotherm of AgTNPs onto PUF was described. It was shown that, in the tested concentration range, the isotherm was well fitted by the Langmuir's adsorption model. The adsorption capacity was  $19 \pm 2 \mu\text{mol Ag g}^{-1}$ , the adsorption equilibrium constant and the value of Gibbs free energy of adsorption were  $(1.0 \pm 0.1) \cdot 10^5 \text{ L mol Ag}^{-1}$  and  $-28.6 \pm 0.3 \text{ kJ mol Ag}^{-1}$ , respectively.

Interaction of the nanocomposite material with a number of analytes, such as hydrogen peroxide and organic peroxides, some thio-compounds, and mercury(II) ions was studied. In many cases, the new nanocomposite material showed an optical response that opens prospects of its analytical application in optical sensors.

#### Acknowledgments

This work was financially supported by the Russian Foundation for Basic Research (grant N 15-33-70002 mol\_a\_mos). The authors acknowledge instrumental support from M. V. Lomonosov Moscow State University Program of Development.

**T01\_11****SYNTHESIS AND PROPERTIES OF A NEW NANOCOMPOSITE MATERIAL BASED ON GOLD NANORODS AND POLYURETHANE FOAM**

*Maria V. Gorbunova*<sup>1</sup>, *Vladimir V. Apyari*<sup>1</sup>, *Maria A. Baranova*<sup>1</sup>, *Natalia S. Zolotova*<sup>1</sup>,  
*Vadim D. Telitsin*<sup>1</sup>, *Alexey V. Garshev*<sup>2</sup>, *Pavel A. Volkov*<sup>3</sup>, *Stanislava G. Dmitrienko*<sup>1</sup>

<sup>1</sup>Department of Chemistry, Lomonosov Moscow State University, 119991 Leninskie gory. 1/3, Moscow, Russia

<sup>2</sup>Faculty of Materials Science, Lomonosov Moscow State University, 119991 Leninskie gory. 1/3, Moscow, Russia; e-mail: masha13\_1992@mail.ru

<sup>3</sup>Scientific-Research Institute of Chemical Reagents and Special Purity Chemicals, Bogorodsky Val 3, 107076, Moscow, Russia

Gold nanoparticles are widely used in various fields of chemistry. These objects possess unique optical properties conditioned by the surface plasmon resonance (SPR), which causes an intense absorption in the visible spectral region. Spherical gold nanoparticles are usually used in the analysis, and there are much less investigations devoted to non-spherical nanoparticles. Meanwhile, the extra optical properties of non-spherical gold nanoparticles, for example nanorods (AuNRs), caused by the presence of several modes of the surface plasmon oscillations, and several SPR bands could play a significant role in the development of new methods for determination of different compounds. Immobilization of nanoparticles in solid matrices could improve stability of these nanoobjects and provides abilities for synthesis of nanocomposite materials with SPR properties.

The objective of this study was to synthesize a nanocomposite material based on AuNRs and polyurethane foam by sorption modification of the foam, and to investigate the possibility of using this material for spectrophotometric determination of catecholamines.

AuNRs with two SPR bands, at 520 and 700–750 nm, were synthesized. Their adsorption on polyurethane foam was examined. It has been found that quantitative adsorption is achieved after 30 minutes of the phase contact in the presence of 0.4 M NaCl. Kinetics of the adsorption is fitted with the pseudo first-order model, the kinetic rate constant is 0.17 min<sup>-1</sup>. The sorption is described by Langmuir's equation with the constant and the sorption capacity of 77.6·10<sup>3</sup> L mol<sup>-1</sup> and 15 mg g<sup>-1</sup>, respectively.

It has been revealed that modification of the obtained nanocomposite with AgNO<sub>3</sub> yields an optical sensor material for the spectrophotometric determination of catecholamines. The interaction of catecholamines with this new nanocomposite results in reduction of silver ions and formation of a silver layer on the surface of AuNRs. This process leads to a hypochromic shift of the both maxima in the diffuse reflection spectrum of the material which correlates with the concentration of analytes and can be used for their quantitation. The limits of epinephrine and dopamine detection are 0.11 and 0.064 mg L<sup>-1</sup>, respectively.

**Acknowledgments**

This work was financially supported by the Russian Foundation for Basic Research (grant N 15-33-70002 mol\_a\_mos). The authors acknowledge instrumental support from M. V. Lomonosov Moscow State University Program of Development.

**T01\_12****IN SITU STUDY OF SIZE DISTRIBUTION OF  $\text{MoS}_2$  PARTICLES FORMED BY SPRAY PYROLYSIS***Maxim Mishin, Kirill Turikov, Kirill Filatov, Rustam Alekseev, Sergey Alexandrov*

Department of Physical Chemistry and Microsystem Technologies, Peter the Great St. Petersburg Polytechnic University, 29 Polytechnicheskaya str., 195251, Saint-Petersburg, Russia;  
e-mail: max@mail.spbstu.ru

Chemical vapor deposition (CVD) can be considered as an universal nanotechnology because it gives a possibility to synthesize wide spectrum of unique nanomaterials like thin films, nanopowders, nanotubes, nanofibers, etc. [1]. Introduction of precursors as an aerosol of their solutions in an appropriate solvent allows expanding the types of synthesized nanomaterials. It is clear that depending on solution concentration, reaction zone temperature and residual time one can control dimensions and even shape of the particles.

The aim of this work was to study using laser scattering technique correlation between size distributions of aerosol particles and solid particles of synthesized substance.

$\text{MoS}_2$  was used as a model substance to be synthesized by spray pyrolysis technique. Ammonium thiomolybdate was used as a precursor. An aerosol of the ammonium thiomolybdate solution in dimethylformamide, created by a piezoelectric nebulizer operating at a frequency of 2.4 MHz, was delivered to the reactor inlet. Aerosol particles were transported into the reactor by the carrier gas at a rate of  $1.4 \text{ L min}^{-1}$ . Special technique based on registration of laser light scattered in the mist or dust environment was developed to get droplet number and size distribution during deposition. This technique gave us *in-situ* data on thiomolybdate aerosol particle size distribution and their correlation with dimensions of formed  $\text{MoS}_2$  nano-spheres determined with the use of high resolution scanning electron microscopy.

The results from the study of influence of nebulizer power on size distribution of aerosol particles show that an increase of average size of aerosol particles at low power is determined by process of coagulation of smaller particles during their transportation by gas flow. This causes appearance in small amount (0.1–1%) of large particles with diameter about  $3 \text{ }\mu\text{m}$ . Relative amount of large particles was sharply increased (up to 10%) at high values of nebulizer power. The results from the study of  $\text{MoS}_2$  particle size distribution demonstrate that large particles of disulfide can be formed from large aerosol particles and due to coagulation of small solid  $\text{MoS}_2$  particles as well. The second path is typical for low values of nebulizer power and appearance in this case of large disulfide particles in rather small amount ( $\sim 10^{-4}\%$ ) does not cause remarkable decrease of the amount of small particles.

The authors are grateful to the Russian Science Foundation for the financial support of the study under contract no. 15-13-00045.

**Reference**

1. S. E. Alexandrov and M. L. Hichman, in: *Chemical Vapor Deposition: Precursors, Process and Applications*, 2009, C. Jones and M.L. Hichman (Eds.), p. 582, Royal Society of Chemistry (2009).

**T01\_13****BIOACTIVITY OF SYNTHESISED ZIRCONIA/HYDROXYAPATITE NANO BIOCOMPOSITE FROM BOVINE BONE BY HIGH ENERGY BALL MILLING TECHNIQUE**

*F. Mohammaddoost*<sup>1</sup>, *H. M. Yussof*, *K. A. Matori*<sup>2</sup>, *F. Ostovan*<sup>1,2</sup>

<sup>1</sup>Department of Chemical and Environmental, Universiti Putra Malaysia, Kuala Lumpur, Malaysia;  
e-mail: my\_hamdani@upm.edu.my

<sup>2</sup>Department of Physics, Universiti Putra Malaysia, Kuala Lumpur, Malaysia;  
e-mail: khamirul@upm.edu.my

In recent decades Hydroxyapatite (HA) has been widely used as an important material in medical applications. In the present work, the HA was produced from bovine while zirconia powder was supplied by the China (Mainland) Trading Company. In this work, HA/ZrO<sub>2</sub> biocomposite prepared with different wt% (0.0, 0.2, 0.4 and 0.8) of ZrO<sub>2</sub> concentrate sintered at 1250 °C, 1 h milling time. In this project, the bioactivity test was carried out by soaking the sample in simulated body fluid SBF solution, 7 and 15 days in an incubator maintained at 36.5 °C. The materials that are able to form apatite on their surface have been shown in several researches *in vitro* in simulated body fluid. Bioactive ceramics generally bond with natural bone through the apatite layer generated on their surface [1–4]. SBF has ion concentrations nearly equal to those of human blood plasma and has buffered at pH 7.40, at 36.5 °C [5]. SEM images of the biocomposite immersed in the SBF solution for 7 days have shown, some apatite crystals generated on the surface and those crystals gradually grew on the surface of all samples and with the increasing wt% of ZrO<sub>2</sub> content, the area of the precipitated apatite increased [6, 7]. Also, SEM result of samples immersed in SBF for 15 days have shown apatite crystals have rapidly increased with the extension of the immersion time and indicated high bioactivity of the biocomposite. All the samples of biocomposite showed reasonably good bioactivity with high surface coverage. During the immersing period, OH<sup>-</sup> and PO<sub>4</sub><sup>3-</sup> ions on the biocomposite surface attract the Ca<sup>2+</sup> ions from simulated body fluid. This process leads to attaining positive charge on HA surface with respect to surrounding fluid and this positive charge further attracts OH<sup>-</sup> and PO<sub>4</sub><sup>3-</sup> negative ions. As a result of this repetition process, the formation of apatite layer occurs on biocomposite surface [8]. EDX result was revealed that the particles newly formed on the coating surfaces were composed of Ca and P and the presence of very low concentration of C, Mg as well as Na, which helped apatite to grow [9, 10]. The XRD result of immersed biocomposite has shown HA, α-TCP, β-TCP and ZrO<sub>2</sub>, no other phases were detected. The results have elaborated the peaks become sharper after soaking longer in SBF solution, which defends the growth of apatite on the biocomposite [11]. Samples were weighed before and after the SBF immersion to compare weight loss and the biodegradation. ZrO<sub>2</sub> content influences the degradation rate of the biocomposite. However, the results have shown adding the ZrO<sub>2</sub> leads to reduce the weight loss in the biocomposite. As HA dissolves, the undissolved ZrO<sub>2</sub> remaining on the biocomposite may hinder contact between the HA and the SBF, which in turn will reduce the dissolution rate of biocomposite [12]. In general, various causes, such as phase, crystallinity, grain size, porosity, specific area and thickness of materials might affect the dissolution of ions in bioceramic [13].

**References**

1. T. Kokubo, H. M. Kim and M. Kawashita: Novel bioactive materials with different mechanical properties. *Biomaterials*, **24**, 2161–2175 (2003).

2. G. Wang, X. Liu, and C. Ding: Phase composition and in-vitro bioactivity of plasma sprayed calcia stabilized zirconia coatings. *Surface and Coatings Technology* **202**, 5824–5831 (2008).
3. R. Quan, Y. Tang, Z. Huang, J. Xu, X. Wu and D. Yang: Study on the genotoxicity of HA/ZrO<sub>2</sub> biocomposite particles in vitro. *Materials Science and Engineering: C* **33**, 1332–1338 (2013).
4. E. M. Rivera, M. Araiza, W. Brostow, V. M. Castano, J. R. DiazEstrada, R. Hernandez and J. R. Rodriguez: Synthesis of hydroxyapatite from eggshells. *Materials Letters* **41**, 128–134 (1999).
5. W. Kantana, P. Jarupoom, K. Pengpat, S. Eitssayeam, T. Tunkasiri and G. Rujijanagul: Properties of hydroxyapatite/zirconium oxide nanobiocomposite. *Ceramics International* **39**, S379–S382 (2013).
6. Y. Nayak: Hydroxyapatite–TZP biocomposite: processing, mechanical properties, microstructure and in vitro bioactivity. Doctoral dissertation, 2010.
7. K. Khor, Y. Gu, D. Pan and P. Cheang: Microstructure and mechanical properties of plasma sprayed Ha/YSZ/Ti–6Al–4V biocomposite coatings. *Biomaterials* **25**, 4009–4017 (2004).
8. D. Bellucci, V. Cannillo and A. Sola: A new highly bioactive biocomposite for scaffold applications: a feasibility study. *Materials* **4**, 339–354 (2011).
9. P. N. Chavan, M. M. Bahir, R. U. Mene, M. P. Mahabole and R. S. Khairnar: Study of nanobiomaterial hydroxyapatite in simulated body fluid: Formation and growth of apatite. *Materials Science and Engineering: B* **168**, 224–230 (2010).
10. G. Radha, S. Balakumar, B. Venkatesan and E. Vellaichamy: Evaluation of hemocompatibility and in vitro immersion on microwave-assisted hydroxyapatite–alumina nanobiocomposite. *Materials Science and Engineering: C* **50**, 143–150 (2015).
11. J. D. Haman, L. C. Lucas and D. Crawford: Characterization of high velocity oxy-fuel combustion sprayed hydroxyapatite. *Biomaterials* **16**, 229–237 (1995).
12. E. Chang, W. J. Chang, B. C. Wang, and C. Y. Yang: Plasma spraying of zirconia-reinforced hydroxyapatite biocomposite coatings on titanium: Part II. Dissolution behaviour in simulated body fluid and bonding degradation. *Journal of Materials Science: Materials in Medicine* **8**, 201–211 (1997).
13. R. Rojaee, M. Fathi, K. Raeissi and A. Sharifnabi: Biodegradation assessment of nanostructured fluoridated hydroxyapatite coatings on biomedical grade magnesium alloy. *Ceramics International* **40**, 15149–15158 (2014).

## T01\_14

### NOVEL SINGLE AND MULTICORE MAGNETIC NANOPARTICLES DOPED WITH RARE EARTH METALS

*Anca Petran, Monica Circu, Alexander Bunge, Alexandrina Nan, Teodora Radu, Rodica Turcu*

National Institute for Research and Development of Isotopic and Molecular Technologies, 67-103 Donat Str., 400293 Cluj-Napoca, Romania; e-mail: anca.petran@itim-cj.ro

The versatility of magnetic nanoparticles has indeed allowed them to become an important platform for multi-modal imaging applications, such as MRI-optical and MRI-PET/SPECT, fluorescent imaging, computed X-ray tomography, which combines the advantages of each imaging modality to achieve highly accurate images. Rare earth metals chelate single and multicore magnetic nanoparticles are promising materials for such multi-modal imaging [1, 2].

Our target was to synthesize new materials based on magnetic nanoparticles covered with strong chelating agents for good encapsulation of the rare earths metals with applications in molecular imaging [3]. Ethylenediaminetetraacetic acid (EDTA) it is a known ligand and chelating agent which can easily complex metal ions. For the magnetic nanoparticle core we

used standard individual magnetic particles synthesized by coprecipitation method and a new type of magnetic clusters synthesized by solvothermal method using EDTA as surfactant.

Physical-chemical characteristics of the obtained single and multicore magnetic nanoparticles doped with rare earth metals were determined by FT-IR, XRD, XPS, TEM, SEM and magnetization measurements with the focus on the structure-properties relationship.

#### Acknowledgement

Financial support from the National Authority for Scientific Research and Innovation – ANCSI, Core Programme, Project PN16-30 02 02 is gratefully acknowledged.

#### References

1. T-H. Shin, Y. Choi, S. Kim and J. Cheon: Recent advances in magnetic nanoparticle-based multi-modal imaging. *Chem. Soc. Rev.* **44**, 4501–4516 (2015).
2. H. Zhu, J. Tao, W. Wang, Y. Zhou, P. Li, Z. Li, K. Yan, S. Wu, K. W. K. Yeung, Z. Xu, H. Xu and P. K. Chu: Magnetic, fluorescent, and thermo-responsive Fe<sub>3</sub>O<sub>4</sub>/rare earth incorporated poly(St-NIPAM) core-shell colloidal nanoparticles in multimodal optical/magnetic resonance imaging probes. *Bio-materials* **34**, 2296–2306 (2013).
3. D. Dupont, W. Brullot, M. Bloemen, T. Verbiest and K. Binnemans: Selective uptake of rare earths from aqueous solutions by EDTA functionalized magnetic and nonmagnetic nanoparticles. *ACS Appl. Mater. Interfaces* **6**, 4980–4988 (2014).

## T01\_15

### MESOPOROUS SILICAS WITH COVALENTLY IMMOBILIZED $\beta$ -CYCLODEXTRIN MOIETIES FOR METHYL RED REMOVAL

*Nadiia Roik, Iryna Trofymchuk, Lyudmila Belyakova*

Chuiko Institute of Surface Chemistry of National Academy of Sciences of Ukraine,  
17 General Naumov Str., Kyiv, 03164, Ukraine; e-mail:roik\_nadya@ukr.net

Dyes are widely used in different areas of industry and belong to the most important pollutants of water resources. Potential toxicity of dye molecules encourages the creation of effective materials for their concentration and removal. In the present work, a simple strategy was proposed for synthesis of  $\beta$ -cyclodextrin(CD)-containing silica adsorbent with hexagonally ordered mesoporous structure. In the first step, chemical modification of  $\beta$ -CD with (3-aminopropyl) triethoxysilane by use of 1,1'-carbonyldiimidazole as coupling agent was realized. Then synthesized  $\beta$ -CD-containing silane was involved into the co-condensation reaction with tetraethyl orthosilicate in the presence of template – quaternary alkylammonium ionic surfactant. Effect of reaction medium composition used in synthesis of functional silane on chemical and porous structure of  $\beta$ -CD-containing silica materials was elucidated by IR spectral and chemical analysis of surface functional groups as well as low-temperature adsorption-desorption of nitrogen and X-ray diffraction analysis.

Adsorption of methyl red (MR) by parent MCM-41 and synthesized  $\beta$ -CD-silica was studied in dependence of solution acidity and equilibrium concentration of dye in phosphate buffer solutions.



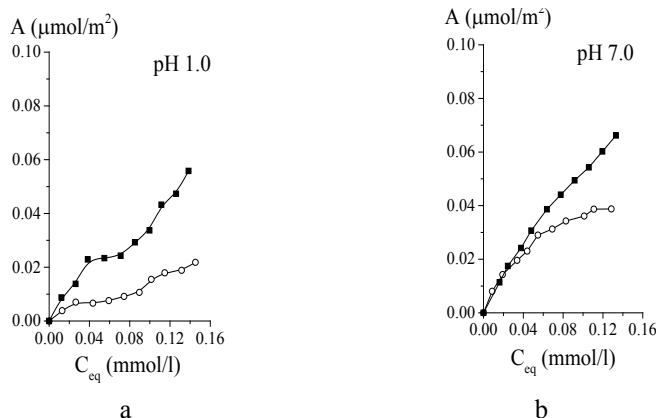


Fig. 1. Isotherms of MR adsorption on MCM-41 (○) and  $\beta$ -CD-MCM-41 (■) silicas

It was found that incorporation of cyclic oligosaccharide moieties into the hexagonally arranged mesoporous framework leads to the enhancement of adsorption efficiency towards MR. To elucidate mechanism of MR distribution between the liquid phase and silica adsorbent and optimize the design of an adsorption system for dye removal the equilibrium adsorption data were analyzed using four widely applied isotherm models: Langmuir, Freundlich, Redlich–Peterson, and BET. Error analysis showed that the Redlich–Peterson is the most appropriate for fitting the experimental data obtained for MR adsorption on  $\beta$ -CD-silica at pH 5.0 and pH 7.0.

## T01\_16

### CRYSTAL SYMMETRY BREAKING IN FEW-QUINTUPLE $\text{Bi}_2\text{Te}_3$ NANOSHEETS

*Punita Srivastava*<sup>1,2</sup>, *Kedar Singh*<sup>1,2</sup>, *S. Patnaik*<sup>2</sup>

<sup>1</sup>Department of Physics, Institute of Science, Banaras Hindu University, Varanasi – 221005 India

<sup>2</sup>School of Physical Sciences, Jawaharlal Nehru University, New Delhi-110067, India;  
e-mail: bhupunita@gmail.com

Bismuth-telluride ( $\text{Bi}_2\text{Te}_3$ ) is one of the best bulk thermoelectric (TE) materials known in present day. In addition, stacked two-dimensional (2D) layers of  $\text{Bi}_2\text{Te}_3$  have attracted strong interest due to topologically protected surface state property. The authors herein report results of micro-Raman spectroscopy study of the “graphene-like” crystalline  $\text{Bi}_2\text{Te}_3$  nanosheets with a thickness of a few atoms (few-quintuples) synthesized by convenient solvothermal route. It is investigated that the optical phonon mode  $A_{1u}$ , which is not-Raman active in bulk  $\text{Bi}_2\text{Te}_3$  crystals, appears in atomically-thin nanosheets due to crystal-symmetry breaking in few quintuples layers (FQLs) and can be used in nanometrology of topological insulators (TIs). It is also suggested that sheets thinning to FQLs and tuning of Fermi level can help in achieving TI surface transport regime. The developed technology for producing 2D layers of  $-\text{Te}^{(1)}-\text{Bi}-\text{Te}^{(2)}-\text{Bi}-\text{Te}^{(1)}$ -creates an thrust for exploration of TIs and their possibility in practical applications.

**T01\_17****SYNTHESIS AND ANALYTICAL APPLICATIONS OF NANOCOMPOSITE MAGNETIC MATERIAL BASED ON HYPERCROSSLINKED POLYESTERENE**

*Veronika V. Tolmacheva*<sup>1</sup>, *Daniil I. Yarykin*<sup>1</sup>, *Vladimir V. Apyari*<sup>1</sup>, *Alexey V. Garshev*<sup>2</sup>, *Pavel A. Volkov*<sup>3</sup>, *Stanislava G. Dmitrienko*<sup>1</sup>, *Yury A. Zolotov*<sup>1</sup>

<sup>1</sup>Department of Chemistry, Lomonosov Moscow State University, Leninskie gory, 1/3, 119991, Moscow, Russia

<sup>2</sup>Faculty of Materials Science, Lomonosov Moscow State University, Leninskie gory, 1/3, 119991, Moscow, Russia; e-mail: nikatolm@mail.ru

<sup>3</sup>Scientific-Research Institute of Chemical Reagents and Special Purity Chemicals, Bogorodsky Val 3, 107076, Moscow, Russia

Nowadays, considerable attention is being paid to magnetic solid-phase extraction (MSPE) as a way to isolate and preconcentrate desired components from sample matrix. MSPE, as a variant of solid-phase extraction (SPE), is an excellent extraction method based on the use of magnetic or magnetically modified sorbents, which can be readily isolated from sample matrix with applying external magnetic field. Compared with traditional SPE procedures, MSPE is more rapid, inexpensive and easy to handle. In many cases, MSPE can be used for the preconcentration, isolation, and purification of analytes directly in samples of complex composition. So the synthesis of new magnetic sorbents is of great interest.

In this work, a novel MSPE sorbent, magnetic hypercrosslinked polystyrene (HCP/Fe<sub>3</sub>O<sub>4</sub>), was prepared. Its structural, magnetic and sorption properties were studied. We propose a simple method to synthesize HCP/Fe<sub>3</sub>O<sub>4</sub> based on the adsorption of pre-synthesized Fe<sub>3</sub>O<sub>4</sub> nanoparticles onto HCP. This nanocomposite combines the outstanding sorption properties of HCP and the separation convenience of magnetic materials.

Conditions of synthesis of the magnetic adsorbents were optimized by varying the weight of HCP, the content of Fe<sub>3</sub>O<sub>4</sub>, time of sorption and different types of surface modification of Fe<sub>3</sub>O<sub>4</sub> nanoparticles. Magnetic nanoparticles and resultant magnetic adsorbents were investigated by the nitrogen adsorption at low temperature, scanning and transmission electron microscopy. The magnetization curves of the materials were also measured. Tetracyclines and sulfonamides were selected as test compounds in the study of sorption behavior of the synthesized adsorbents to achieve the best extraction efficiency, various conditions, such as amount of the adsorbent, pH, extraction time, desorption time and the nature of an eluent, were optimized. It has been shown that the HCP-based magnetic adsorbent retains sorptive properties regarding tetracyclines and sulfonamides ( $R = 95\text{--}99\%$ ) and can be easily separated from solution by applying magnetic field.

The resultant material was used as a MSPE adsorbent for the group preconcentration of sulfamethoxy pyridazine, sulfamethazine, sulfamethoxazole, sulfachloropyridazine, oxytetracycline, chlortetracycline and doxycycline from natural water followed by their determination with high-performance liquid chromatography with amperometric detection.

**Acknowledgments**

This work was financially supported by the Russian Science Foundation (grant N 14-23-00012). The authors acknowledge instrumental support from M.V. Lomonosov Moscow State University Program of Development.

## T01\_18

## SYNTHESIS OF PHOTOACTIVE TUNGSTEN NITRIDE NANOSHEETS BY AMMONIA TREATMENT OF TUNGSTEN OXIDE NANOWIRES

*Tamás Varga*<sup>1,3</sup>, *Henrik Haspel*<sup>1</sup>, *Ákos Kukovecz*<sup>1,2</sup>, *Zoltán Kónya*<sup>1,3</sup>

<sup>1</sup>Department of Applied and Environmental Chemistry, University of Szeged, Rerrich Béla tér 1, H-6720 Szeged, Hungary

<sup>2</sup>MTA-SZTE “Lendület” Porous Nanocomposites Research Group, Rerrich Béla tér 1, H-6720 Szeged, Hungary

<sup>3</sup>MTA-SZTE Reaction Kinetics and Surface Chemistry Research Group, Rerrich Béla tér 1, H-6720 Szeged, Hungary

Tungsten nitrides and oxynitrides are promising materials in a wide variety of potential applications, e.g., methanol oxidation [1], electrochemical [2] and photoelectrochemical hydrogen evolution [3]. These materials can also be used as electrode in electrochemical devices due to their good chemical stability, high strength, hardness, and high melting point accompanied with good electrical conductivity and a relative low band gap energy [4].

In our study, hydrothermally synthesized tungsten oxide nanowires were heat-treated in ammonia/nitrogen atmosphere at different temperatures to produce tungsten oxynitride nanoparticles and tungsten nitride nanosheets. Changes in the morphology, structure and electrochemical properties of the nanowires were investigated with transmission and scanning electron microscopy (TEM, SEM), and electron and X-ray diffraction techniques (ED, XRD). Band gap energies were determined from UV-VIS spectra, while photoelectrochemical properties were also tested in a three-electrode system.

X-ray diffraction results showed that the pristine tungsten oxide nanowires were transformed into tungsten oxynitride particles and tungsten nitride sheets in the high-temperature calcination steps under ammonia atmosphere. Electron microscopy images revealed that along with the above phase transformation, the initial fibrous WO<sub>3</sub> morphology was gradually converted into nanosheets. Band gap energies of the treated samples were significantly decreased in the calcination processes, while two orders of magnitude higher visible-light photocurrent could be measured, compared to that found in as-prepared tungsten oxide nanowires.

#### Acknowledgement

The financial support of the Hungarian Research, Development and Innovation Office through projects K 112531 and K 120115 is acknowledged.

#### References

1. S. Yin, L. Yang, L. Luo, F. Huang, Y. Qiang, H. Zhang and Z. Yan: *New J. Chem.* **37**, 3976 (2013).
2. J. Shi, Z. Pu, Q. Liu, A. M. Asiri, J. Hua and X. Sun: *Electrochim Acta* **154**, 345–351 (2015).
3. V. Chakrapani, J. Thangala and M. K. Sunkara: *Int. J. Hydrogen Energy* **34**, 9050–9059 (2009).
4. L. Villasecaan, B. Morenoa, I. Loritea, J. R. Juradoa and E. Chinarroa: *Ceram. Int.* **41**, 4282–4288 (2015).

**T01\_19****HIGH MAGNETIC MOMENT SUPERPARAMAGNETIC MICROSPHERES IN WATER SUSPENSION: STRUCTURE, MAGNETIC AND MAGNETORHEOLOGICAL PROPERTIES**

Corina Vasilescu<sup>1,4</sup>, Izabell Crăciunescu<sup>2</sup>, Daniela Susan-Resiga<sup>1</sup>, Oana Marinică<sup>3</sup>, Tibor Boros<sup>5</sup>, Tünde Borbáth<sup>5</sup>, Elena Chitanu<sup>6</sup>, Mirela Codescu<sup>6</sup>, Vlad Socoliuc<sup>1</sup>, István Borbáth<sup>5</sup>, Rodica Turcu<sup>2</sup>, Ladislau Vékás<sup>1</sup>

<sup>1</sup>Lab. Magnetic Fluids, Center for Fundamental and Advanced Technical Research, Romanian Academy, Timisoara Branch, 24 Mihai Viteazul Str., 300223 Timisoara, Romania;

e-mails: corina\_m\_vasilescu@yahoo.com; vekas@acad-tim.tm.edu.ro; vekas.ladislau@gmail.com

<sup>2</sup>National Institute for Research and Development of Isotopic and Molecular Technologies,

67-103 Donat Str., 400293 Cluj-Napoca, Romania; e-mails: rodica.turcu@itim-cj.ro;

rodica.turcu14@gmail.com

<sup>3</sup>Research Center for Engineering of Systems with Complex Fluids, University Politehnica of Timisoara, 1 Mihai Viteazul Str., 300222 Timisoara, Romania

<sup>4</sup>Department of Applied Chemistry and Engineering of Organic and Natural Compounds, University Politehnica of Timisoara, 6 Carol Telbisz Str., Timisoara, Romania

<sup>5</sup>SC ROSEAL SA, 5A N. Balcescu Str., 535600 Odorheiu-Secuiesc, Romania

<sup>6</sup>National Institute for R&D in Electrical Engineering ICPE-CA, 313 Splaiul Unirii 030138 Bucharest, Romania

A modified version of the oil-in-water miniemulsion procedure [1] was applied using a light organic carrier magnetite ferrofluid and an iron-cobalt nanopowder to prepare high magnetization magnetic microspheres. The overall size distributions, full magnetization curves and structure of magnetic core of microspheres were studied by Transmission Electron Microscopy (TEM), X-ray diffraction (XRD) and Vibrating Sample magnetometry. Dispersion of microspheres in water and water based ferrofluids resulted in a new type of nano-micro structured magnetorheological suspensions [2], the micron-sized ferromagnetic Fe particles being replaced by nanocomposite particles with superparamagnetic behavior. The magnetic properties and flow behavior were investigated by VSM and rotational magnetorheometry to evidence the influence of composition on the magnetoviscous effect.

**Acknowledgements**

This work was supported by the projects MagNanoMicroSeal nr.157/2012, HiSpeedNanoMag-Seal nr.97/2014 and STAR nr. 99/2013 (PNII-UEFISCDI), as well as by the Research Program LLM-CCTFA 2016-2019 of the Romanian Academy. Financial support from the Romanian National Authority for Scientific Research and Innovation – ANCSI, Core Programme, Project PN16-30 02 02 is gratefully acknowledged.

**References**

1. R. Turcu, I. Craciunescu and A. Nan, in: H. Nirschl and K. Keller (Eds.): *Upscaling of Bio-Nano-Processes, Lecture Notes in Bioengineering*. Springer-Verlag, Berlin Heidelberg, 2014.
2. D. Susan-Resiga and L. Vékás: *Rheologica Acta* 55, 581–595 (2016).

## T01\_20

## GOLD NANOPARTICLE PLASMON RESONANCE IN LAYERED AU NPS / DIELECTRIC SPACER / AL FILM NANOSTRUCTURE: EFFECTS OF SPACER THICKNESS

*O. A. Yeshchenko, V. V. Kozachenko, Yu. F. Liakhov*

Physics Department, Taras Shevchenko National University of Kyiv, 60 Volodymyrs'ka str., 01601 Kyiv, Ukraine; e-mail: yes@univ.kiev.ua

The surface plasmon resonance (SPR) in gold nanoparticles in layered Au NPs/dielectric spacer/Al film nanostructure has been studied in dependence of spacer thickness in the range of 3–200 nm. The SPR frequency and magnitude have been found to be strongly dependent on the spacer thickness. The presence of Al film causes substantial enhancement of the magnitude and red shift of SPR. When the Al film is thinner than about 30 nm the quadrupolar SPR appears in the absorption spectra.

A particularly interesting plasmonic system that recently is under study is that of a metal NPs interacting with a metal film. This system has been predicted to display a lot of interesting optical phenomena caused by the coupling of the NPs with the film through the field of surface plasmons excited in the NPs, e.g. Refs. [1–3]. The study of optical spectra (absorption, scattering) of the metal NPs separated controllably from a metal film using the dielectric spacer gives the possibility to probe the dependence of coupling effects on the distance between the NPs and film.

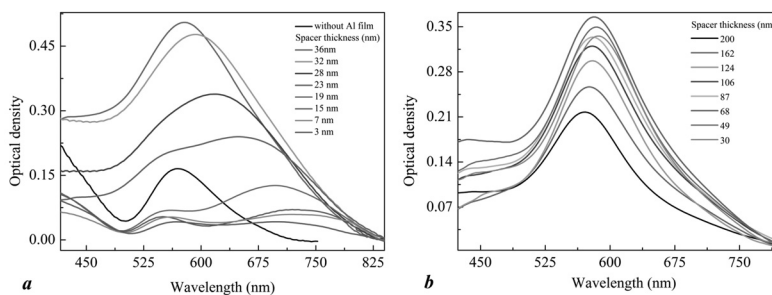


**Fig. 1.** Absorption spectra of three-layer nanostructure Au NPs / shellac film / Al film in dependence on the shellac spacer thickness

The studied samples are the glass substrates with dense 2D monolayer of Au NPs' covered by dielectric film of shellac. The thickness of shellac film was different in different parts of the sample varying in the range of 3–36 nm for sample S1 and 30–200 nm for sample S2. Above the shellac film, the aluminium film of 50 nm thickness was deposited. AFM gave the following Au NPs' layer parameters: NP size  $d = (22 \pm 8)$  nm; mean interparticle distance  $D = (40 \pm 10)$  nm. Thus, the studied Au NPs' layer is quite dense. The absorption spectra of above mentioned three-layer nanostructure were measured at room temperature. The obtained spectra were presented in *Figure 1*. The spectra were fitted by the basic Lorentzian peaks that allowed to obtain the dependences of SPR wavelength and magnitude (area) on the shellac spacer thickness. The respective dependences are shown in *Figure 2*. One can see that coupling of SPR in Au NPs with Al film leads to substantial enhancement (5.3 times) of the SPR magnitude and its appreciable

red shift if comparing to the case of Au NPs without Al film. The increase of SPR magnitude at the decrease of spacer thickness from 200 nm to 70 nm is due to the redirection of the external incoming light as well as the light scattered by NP by Al film back to layer of Au NPs. At thickness values lower than about 70 nm the decrease of dipolar SPR magnitude and the concomitant appearing of the quadrupolar SPR occur at the decrease of spacer thickness. This behaviour is due to the hybridization of the dipolar and quadrupolar plasmons in the Au NP caused by the symmetry-breaking introduced by the presence of the Al film. As a result, the quadrupolar resonance acquires part of the “bright” character of the dipolar mode becoming easily visible on the absorption spectrum. Correspondingly, the dipolar resonance becomes darker, i.e. its magnitude decreases.

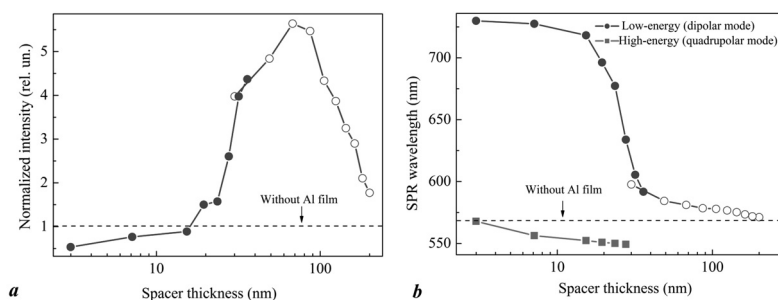


**Fig. 2.** The dependence on the spacer thickness: (a) – the magnitude of SPR absorption band normalized to one taken from the spectra of Au NPs without Al film; (b) – the wavelengths of low-energy (dipolar) and high-energy (quadrupolar) SPR bands. The dashed line corresponds to the values of SPR characteristics for Au NPs without Al film

### Acknowledgement

O. A. Yeshchenko and Yu. F. Liakhov acknowledge the support by the NATO Science for Peace and Security (SPS) Program (grant NUKR.SFPP 984617).

### References

1. J. J. Mock, R. T. Hill, A. Degiron, S. Zauscher, A. Chilkoti and D. R. Smith: Distance-dependent plasmon resonant coupling between a gold nanoparticle and gold film. *Nano Lett.* **8**, 2245–2252 (2008).
2. C. Ciraci, R. T. Hill, J. J. Mock, Y. Urzhumov, A. I., Fernández-Domínguez, S. A. Maier, J. B. Pendry, A. Chilkoti and D. R. Smith: Probing the ultimate limits of plasmonic enhancement. *Science* **337**, 1072–1074 (2012).
3. A. Sobhani, A. Manjavacas, Y. Cao, M. J. McClain, F. J. García de Abajo, P. Nordlander and N. J. Halas: Pronounced linewidth narrowing of an aluminum nanoparticle plasmon resonance by interaction with an aluminum metallic film. *Nano Lett.* **15**, 6946–6951 (2015).

## POSTER PRESENTATIONS

T02 – 2D nanostructures  
and van der Waals solids

### T02\_01

#### FROM BENZENE TO GRAPHENE: OLIGOMERS AND POLYMERS OF TRIGONAL CARBON

Sándor Pekker<sup>1,2</sup>

<sup>1</sup>Wigner Research Centre for Physics, Institute for Solid State Physics and Optics, Konkoly Thege M. út 29–33, H-1121 Budapest, Hungary; e-mail: pekker.sandor@wigner.mta.hu

<sup>2</sup>Faculty of Light Industry and Environmental Engineering, Óbuda University, Doberdó út 6, H-1034 Budapest, Hungary

Polymers and nanostructures of trigonally coordinated C-atoms, like fullerenes, carbon nanotubes, nanoribbons and graphene [1] have been intensively studied for their remarkable physical properties. Polycyclic aromatic compounds (PAHs) [2] are closely related to these materials: they are often the monomers or oligomers of the higher structures. The goal of this work is the simultaneous study of the electronic structures of both families of materials. The total energy of finite and periodic systems are calculated by the same DFT, B3LYP, 6-31G\* method. Heats of formations, HOMO-LUMO gaps and bond length alternations are compared. Various families of nanoribbons and their oligomers are studied. For a better comparison of the oligomers and polymers, a simple method is used to map the molecular orbital (MO) levels of the finite molecules to the band structure of the corresponding polymer. For linear oligomers the mapping is really effective: the band structure of the polymer can be reconstructed from the MO levels of the oligomers and vice versa. The electronic structure of the narrow zigzag ribbons can be described as weakly interacting trans polyacetylene chains. It is shown, that besides the well known zigzag and armchair ribbons a further family of ribbons with 'lacy' edges has remarkable electronic structure. Lacy ribbons can be originated from zigzag ribbons by a regular decoration of the edges with benzoid rings. All lacy structures are full benzoids with high stability and large bandgap, similarly to the armchair-(3k+1) ribbons. The HOMO-LUMO orbitals of these families are originated from two distinct sets of the degenerate orbitals of benzene. On the other hand, armchair-3k and armchair-(3k+2) ribbons consist of different polyene units at the edges and quinoids inside. The quinoid regions of the HOMO and LUMO are formed from two distinct sets of the orbitals of benzene by level crossing. The different properties of these subgroups can be explained by the different bonding interactions of the quinoids and the polyene units.

#### References

1. A. H. Castro Neto et al.: *Rev. Mod. Phys.* **81**, 109 (2009).
2. E. Clar and R. Schoental: *Polycyclic Hydrocarbons*. Springer V., Berlin, 1964.

## POSTER PRESENTATIONS

T03 – Nanomaterials in energy  
conversion and storage

### T03\_01

#### THREE-DIMENSIONAL (3D) LITHIUM MANGANESE/CARBON COMPOSITE CATHODES FOR SOLID-STATE LITHIUM-ION BATTERIES

*Robert Kun*<sup>1,2</sup>, *Ingo Bardenhagen*<sup>2</sup>, *Jens Glenneberg*<sup>1</sup>, *Frederieke Langer*<sup>1</sup>

<sup>1</sup>Department of Production Engineering, Innovative Sensor and Functional Materials Research Group, University of Bremen, Badgasteiner Str. 1, 28359 Bremen, Germany; e-mail: robert.kun@uni-bremen.de

<sup>2</sup>Fraunhofer Institute for Manufacturing Technology and Advanced Materials – IFAM, Wienerstr. 12, 28359 Bremen, Germany

Among various battery chemistries lithium ion technology is considered as one of the most attractive battery system for future applications. This relies basically on the high realizable energy density of this technology. However, safety and toxicity issues still remain in commercial lithium ion batteries with liquid electrolyte. Replacing organic solvent based electrolytes with a lithium-ion conductive polymer or ceramic solid-state electrolyte intrinsic cell safety can be increased. Furthermore due to omission of electrochemically inactive components, such as separator, or the bulk electrolyte solvent itself could result in increased energy density of the cell. However, the main challenge for all-solid-state batteries the lowered ionic conductivity of the solid state electrolyte, compared to their liquid counterparts. Only way to deal with the low ionic conductivity, if the solid-state electrolyte is processed as thin layers. Unfortunately, oxide-type cathode materials are poor electric and ionic conductors in the same time which in turn limit the useable thickness of the cathode. As an effect, the practical specific energy (Wh/kg) of a planar thin-film battery is very low [1]. To solve this problem, three-dimensional (3D) cathodes need to be produced. Here, relatively thin layers of active material are directly in contact with electric and ionic conducting material. Using 3D composite cathode architecture short diffusion path lengths and enhanced lithium ion storage capacity could be realized in the same time [2, 3]. In this contribution we present the fabrication and characterization of a 3D composite cathode containing  $\text{LiMn}_2\text{O}_4$  (LMO) spinel-type oxide as electrochemically active cathode material impregnated on electric conductive carbon matrix. Infiltration of LMO sol into the porous carbon network followed by high temperature treatment results in spinel LMO coated carbon fibers. The cathodes were assembled into a battery cell. Due to consecutive filling cycles of the carbon matrix with LMO resulted in enhanced storage capacity and cells exhibit excellent capacity retention during cycling. Moreover, due to increased electrode loading irreversible capacity was greatly reduced.

#### References

1. F. Andre, F. Langer, J. Schwenzel and R. Kun: Energy storage options for self-powering devices. *Procedia Technol.* **15**, 248–257 (2014).



2. J. W. Long, B. Dunn, D. R. Rolison and H. S. White: Three-dimensional battery architectures. *Chem. Rev.* **104**, 4463–4492 (2004).
3. J. F. M. Oudenhoven, L. Baggetto and P. H. L. Notten: All-solid-state lithium-ion microbatteries: a review of various three-dimensional concepts. *Adv. Energy Mater.* **1**, 10–33 (2011).

## T03\_02

### NANODISPERSED NiO AND CuO<sub>x</sub> SUPPORTED ON CARBON NANOTUBES FOR SUPERCAPACITORS APPLICATIONS

*Alexandra Kuriganova*<sup>1</sup>, *Daria Leontyeva*<sup>1</sup>, *Valentina Shmatko*<sup>2</sup>, *Elena Bogoslavskaya*<sup>2</sup>, *Galina Yalovega*<sup>2</sup>, *Alexander Postnikov*<sup>1</sup>, *Nina Smirnova*<sup>1</sup>

<sup>1</sup>Chemistry Engineering Faculty, Platov South Russian State Polytechnic University (NPI), Prosveschenia st. 132, Russia; e-mail: kuriganova\_@mail.ru

<sup>2</sup>Faculty of Physics, Southern Federal University, Rostov-on-Don, Russia

Electrochemical capacitors (ECs), combining the advantages of the high power of dielectric capacitors and the high energy of rechargeable batteries, have played an increasingly important role in power source applications. Metal oxides dispersed onto carbon support are prominent candidates for supercapacitors applications due to their inexpensive and exhibit pseudocapacitance behavior similar to that of ruthenium and iridium oxide.

Samples of dispersed CuO<sub>x</sub>, NiO and nanocomposites with carbon nanotubes (CuO<sub>x</sub>/CNTs NiO/CNTs) were synthesized by electrochemical dispersion method based on the effect oxidation and metal dispersion when a pulsed alternating current applied [1, 2]. Copper or nickel electrodes were immersed in an aqueous Na<sup>+</sup> containing solution. Alternating current density was 1.0 A cm<sup>-2</sup>. As the carbon content of the nanocomposite were used carbon nanotubes with a diameter in the range of 20–40 nm and a length of 100 μm, obtained by pyrolysis of propane-butane mixture to the copper-nickel.

Analysis of the XRD powder pattern indicates that NiO in the synthesized composite has the face centered cubic cell of β-NiO. The average grain size of synthesized materials estimated using Scherrer equation was 7 nm. Morphological studies by scanning electron microscopy showed that the starting CuO<sub>x</sub> nanoparticles in CuO<sub>x</sub>/CNTs composite are mainly of an octahedral shape with edge lengths ranging from 200 to 1000 nm. According to absorption spectroscopy nanoparticles consist of copper oxide (I), realized in the Cu<sub>2</sub>O phase, with small amounts of CuO.

The capacitive characteristics of the synthesized NiO/CNTs and CuO<sub>x</sub>/CNTs mainly related to pseudocapacity of metal oxides and specific capacitance of the NiO/CNTs and CuO<sub>x</sub>/CNTs was 960 F·g<sup>-1</sup> and 67 F·g<sup>-1</sup>, respectively.

Thus, we have provided a simple electrochemical route toward preparation the NiO/CNT and CuO<sub>x</sub>/CNTs nanocomposites with high specific capacity. We suppose that synthesized NiO/CNT and CuO<sub>x</sub>/CNTs composites could be promising for use in supercapacitors.

#### References

1. D. V. Leontyeva, I. N. Leontyev, M. V. Avramenko, Yu. I. Yuzyuk, Yu. A. Kukushkina and N. V. Smirnova: Electrochemical dispersion as a simple and effective technique toward preparation of NiO based nanocomposite for supercapacitor application. *Electrochimica Acta* **114**, 356–362 (2013).

2. V. Shmatko, G. Yalovega, A. Barbashova, A. Kuriganova, E. Bogoslavskaja and N. Smirnova: Investigation of the morphological, atomic and electronic structural changes  $\text{CuO}_x$  nanoparticles and CNT in a nanocomposite  $\text{CuO}_x/\text{CNT}$ : SEM and X-ray spectroscopic studies. *Key Engineering Materials* **683**, 215–220 (2016).

### T03\_03

#### CHARACTERIZATION OF Ni PLATED CARBON FIBER PREPARED ON Pd LOADED PAN FIBER

*Jae-Young Lee*<sup>1</sup>, *Hyung-Ryul Rim*<sup>1</sup>, *Woo-Kum Lee*<sup>2</sup>, *Hong-Ki Lee*<sup>1</sup>

<sup>1</sup>Hydrogen Fuel Cell RIC, Woosuk University, Jeonbuk 565-902, South Korea;  
e-mail: hongkil@woosuk.ac.kr

<sup>2</sup>Department of Energy Engineering, Woosuk University, Jeonbuk 565-902, South Korea

In our previous works [1, 2], we found that Ni-P alloy were site-selectively deposited on palladium (Pd) loaded polymer thin film, and we also found that palladium(II) bis(acetylacetonate),  $\text{Pd}(\text{acac})_2$  as a precursor was penetrated into a polymer film and spontaneously reduced forming metallic Pd nanoparticles at high temperature. Therefore we could develop a new method to prepare Ni-P coated carbon fiber using electroless plating method on the surface of palladium (Pd) loaded PAN fiber and then PAN fiber stabilized and carbonized. To produce Pd loaded PAN fiber,  $\text{Pd}(\text{acac})_2$  was sublimed at 180 °C in vacuum condition, and then  $\text{Pd}(\text{acac})_2$  vapor penetrated into the PAN fiber and spontaneously reduced forming metallic Pd nanoparticles. And then, Ni-P was coated on the Pd loaded PAN fiber in an electroless Ni plating solution. Finally, Ni-P coated PAN fiber was oxidized at 240 °C for 2 h at air condition and followed by carbonizing the oxidized fiber at 1,400 °C for 15 min at  $\text{N}_2$  atmospheric condition. As was expected, Ni-P was evenly coated on carbon fiber, as shown in *Figure 1*.

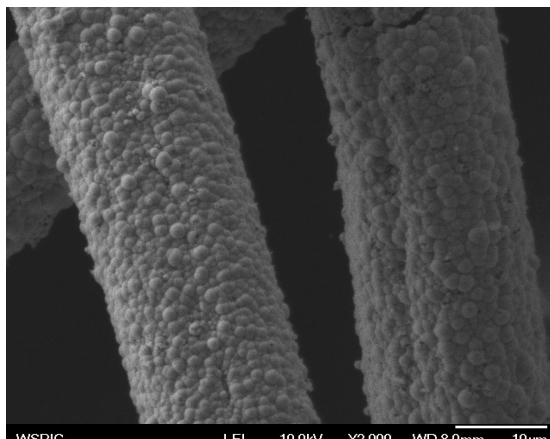


**Fig. 1.** Ni-P coated carbon fiber

#### References

1. J. Y. Lee and S. Horiuchi: Electroless nickel plating on patterned catalytic surfaces by electron beam lithography. *Thin Solid Films* **515**, 7798–7804 (2007).

2. J. Y. Lee, W. K. Lee, S. W. Hong and H. K. Lee: A new incorporation method of metallic precursors into a nafion film via a drying process for the preparation of metallic nanocatalysts/nafion. *J. Nano-science and Nanotechnology* **13**, 7886–7890 (2013).

## T03\_04

### FORMATION OF ZnO NANOROD ON PD LOADED PAN FIBER

*Jae-Young Lee*<sup>1</sup>, *Hyung-Ryul Rim*<sup>1</sup>, *Woo-Kum Lee*<sup>2</sup>, *Sung-Wan Hong*<sup>1</sup>, *Hong-Ki Lee*<sup>1</sup>

<sup>1</sup>Hydrogen Fuel Cell RIC, Woosuk University, Jeonbuk 565-902, South Korea;  
e-mail: hongkil@woosuk.ac.kr

<sup>2</sup>Department of Energy Engineering, Woosuk University, Jeonbuk 565-902, South Korea

As a semiconductor material, zinc oxide (ZnO) spans a wide range of applications from solar cells and chemical sensors to electrical, acoustic, and luminescent devices [1, 2]. In this study, ZnO nanorods were coated on Pd loaded polyacrylonitrile (PAN) fiber and the procedure was as follows: (1) In order to load Pd nanoparticles on the surface of PAN fiber, palladium(II) bis(acetylacetonato) (Pd(acac)<sub>2</sub>) compound was used as a precursor, which was purchased from Johnson Matthey Materials Technology. 0.5 mg of Pd(acac)<sub>2</sub> in a glass reactor was sublimed at 180 °C in vacuo and condensed to the upper side of glass wall. Then PAN fiber was placed into the glass reactor and maintained at 180 °C for 5 min in N<sub>2</sub> atmosphere, and finally the Pd(acac)<sub>2</sub> was spontaneously reduced resulting Pd nanoparticles on the surface of PAN fiber without any reducing agent. (2) To make the ZnO nanorods on Pd catalysts, Pd-loaded PAN fiber was soaked in an aqueous solution of 0.05 M Zn(NO<sub>3</sub>)<sub>2</sub> and 0.05 M dimethylamine borane (DMAB) at 80 °C for 1~3 h. (3) And, finally ZnO nanorod coated PAN fiber was formed, as shown in *Figure 1*.

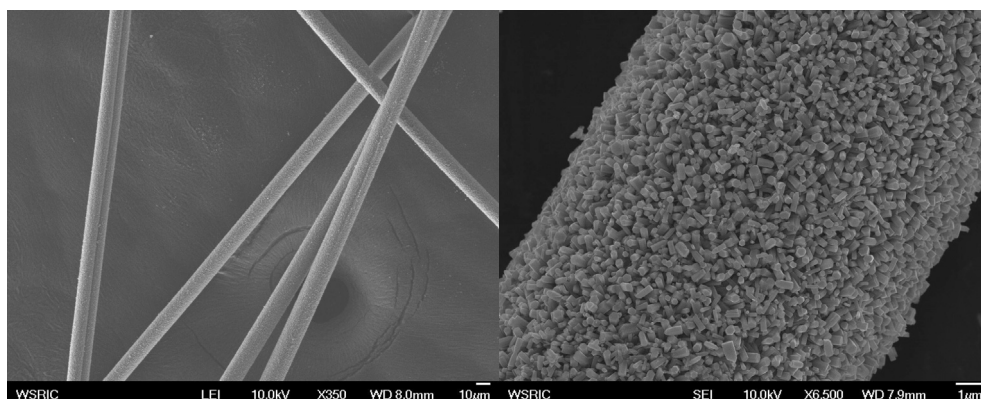


**Fig. 1.** ZnO nanorods on PAN fiber: left scale bar was 10 μm and right one was 1 μm

#### References

1. S. K. Nataraj, B. H. Kim, J. H. Yun, D. H. Lee, T. M. Aminabhavi and K. S. Yang: Formation of ZnO within flexible polymer fibers. *J. Sol-Gel Sci. Technol.* **65**, 283–286 (2013).
2. C. Klingshirn: ZnO: material, physics and applications. *Chem. Phys. Chem.* **8**, 782–803 (2007).

## POSTER PRESENTATIONS

T04 – Pharmaceutical, health  
and biology-related aspects  
of nanomaterials

### T04\_01

#### SILVER NANOPARTICLES IN LIFELIKE ENVIRONMENTS

*Péter Bélteky*<sup>1,3</sup>, *Dávid Kovács*<sup>2</sup>, *Nóra Igaz*<sup>2</sup>, *Mónika Kiricsi*<sup>2</sup>, *Ákos Kukovecz*<sup>1,4</sup>, *Zoltán Kónya*<sup>1,3</sup>

<sup>1</sup>Department of Applied and Environmental Chemistry, University of Szeged, Rerrich Béla tér 1, H-6720 Szeged, Hungary

<sup>2</sup>Department of Biochemistry and Molecular Biology, University of Szeged, Középfasor 52, H-6726 Szeged, Hungary

<sup>3</sup>MTA-SZTE Reaction Kinetics and Surface Chemistry Research Group, Rerrich Béla tér 1, H-6720 Szeged, Hungary

<sup>4</sup>MTA-SZTE “Lendület” Porous Nanocomposites Research Group, Rerrich Béla tér 1, H-6720 Szeged, Hungary

Due to the rapid advancements in nanotechnology, nanoparticles (NPs) are routinely used in most fields of life. One of the most important fields is the therapeutic applications of NPs and although the physiological effects are widely investigated, the stability of these particles in biological media is mostly overlooked.

In this study the colloidal stability of silver nanoparticles (AgNP) in DMEM (Dulbecco's Modified Eagle's Medium) with added FBS (Fetal Bovine Serum) has been observed, since this is a typical environment for *in vitro* experiments on cell cultures. Our measurements were carried out using UV-Vis spectroscopy, DLS and TEM.

The results show that while AgNPs are stable in water, this is not the case in the clean medium. However adding FBS to the system improves the colloidal stability of the particles with the formation of protein corona on the surface of the nanoparticles. The biological effects of the particles have been thoroughly investigated by Kovács et al. [1].

The financial support of the Hungarian Research, Development and Innovation Office through projects K 112531 and K 120115 is acknowledged.

#### Reference

1. D. Kovács, N. Igaz, C. Keskeny et al.: Silver nanoparticles defeat p53-positive and p53-negative osteosarcoma cells by triggering mitochondrial stress and apoptosis. *Sci Rep.* **6**, 27902 (2016). doi: 10.1038/srep27902

**T04\_02****MULTI-WALLED CARBON NANOTUBES MODIFIED GLASSY CARBON ELECTRODE AS A VOLTAMMETRIC NANOSENSOR FOR THE SENSITIVE DETERMINATION OF ANTIPSYCHOTIC DRUG TRIFLUOPERAZINE IN PHARMACEUTICALS***Burcu Dogan-Topal*

Ankara University, Faculty of Pharmacy, Department of Analytical Chemistry, Tandogan, Ankara, Turkey

The trifluoperazine belongs to phenothiazine derivatives, which is the largest group of the main five classes of the antipsychotic, sedative, and antiemetic drugs. Carbon nanotubes (CNTs) are one of the most important nano-materials due to their high chemical stability, high surface area, high mechanical properties, and unique electrical conductivity. The electronic properties suggest that CNTs have the capability to promote electron transfer reactions and improve sensitivity in electrochemistry, and thus, they are widely used as electrode materials for drug analysis. Also, the modification of the electrode substrates with multiwalled carbon nanotubes (MWCNTs) for use in analytical sensing has been documented to result in low detection limits and high sensitivities.

The voltammetric oxidation of trifluoperazine was investigated at multi-walled carbon nanotubes modified glassy carbon electrode using cyclic and differential pulse voltammetry over a wide pH range. The modified electrode exhibits catalytic activity, high sensitivity, and stability. The results revealed that the oxidation of trifluoperazine is an irreversible pH-dependent process in an adsorption-controlled mechanism. The results show that the oxidation signal was remarkably enhanced to provide down to the ultra-trace levels. Operational parameters have been optimized. The calibration curve was linear in the concentration range of  $2.08 \times 10^{-8}$ – $1.67 \times 10^{-6}$  M with the detection limit of  $7.49 \times 10^{-10}$  M. The modified electrode showed good stability and reproducibility, and also it was successfully applied to the sensitive and selective determination of trifluoperazine in its dosage forms.

**T04\_03****DEVELOPMENT OF INTERMETALLIC FILLED CARBON NANOTUBE SENSORS FOR HYPERTHERMIA APPLICATION***Rasha Ghunaim*<sup>1,2</sup><sup>1</sup>IFW Dresden Leibniz Institute for Solid State and Material Research, 01069 Dresden, Germany; e-mail: r.ghunaim@ifw-dresden.de<sup>2</sup>Kirchhoff-Institute for Physics, Heidelberg, Germany

Magnetic nanoparticles (MNPs) are considered as promising tools for an effective therapeutic approach against cancer. These MNPs can be heated up in a (AC) magnetic field, which leads to their use as hyperthermia candidates. A moderate degree of tissue warming results in very effective cancer cell destruction, whereas, the healthy cells remain unaffected [1–3]. However, to consider these MNPs safe and effective for the patient, they are encapsulated inside the hollow

cavity of carbon nanotubes (CNTs). These nano-carriers are chemically stable (protect MNPs from oxidation due to interaction with the biological system), biocompatible (can easily penetrate biological barriers) and have functionalizable surface (for better bonding with matrix elements and compounds) [4]. Such nano-carriers possess fascinating properties, in one hand, the magnetic nanoparticles acquire magnetic functionality such as heating, monitoring and guiding [5], and on the other hand, the carbon shell improve the chemical stability, functionality and biocompatibility.

Here, we presented different nano-magnets encapsulated in CNTs synthesized by different approaches. The structural and magnetic properties for these nanocomposites are presented.

#### References

1. A. Jordan, R. Scholz, P. Wust, H. Fahling and R. Felix: Magnetic fluid hyperthermia (MFH): cancer treatment with AC magnetic field induced excitation of biocompatible superparamagnetic nanoparticles. *J Magn Mat* **201**, 413 (1999).
2. S. Laurent S. Dutz, U. O. Haefeli, M. Mahmoudi: Magnetic fluid hyperthermia: focus on superparamagnetic iron oxide nanoparticles. *Advances in Colloid and Interface Science* **166**, 8 (2011).
3. Q. A. Pankhurst, N. T. K. Thanh, S. K. Jones, J. Dobson: Progress in applications of magnetic nanoparticles in biomedicine. *J. Phys. D Appl. Phys.* **42**, 224001 (2003).
4. S. Hampel, D. Kunze, D. Haase, K. Kraemer, M. Rauschenbach, M. Ritschel, A. Leonhardt, J. Thomas, S. Oswald, V. Hoffmann and B. Buechner: Carbon nanotubes filled with a chemotherapeutic agent: a nanocarrier mediates inhibition of tumor cell growth. *Nanomedicine* **3**, 175 (2008).
5. R. Klingeler, S. Hampel, B. Buechner: Carbon nanotube based biomedical agents for heating, temperature sensing and drug delivery. *Int. J. Hyperthermia* **24**, 496 (2008).

## T04\_04

### THE INFLUENCE OF THE NANOPARTICLES ON hCMEC/D3 CELL LINE

*Katarzyna D. Kania*<sup>1</sup>, *Waldemar Wagner*<sup>2</sup>, *Lukasz Pulaski*<sup>1</sup>, *Michal Gorzkiewicz*<sup>3</sup>

<sup>1</sup>Laboratory of Transcriptional Regulation, Institute of Medical Biology of the Polish Academy of Sciences, 106 Lodowa St, 93-232 Lodz, Poland; e-mail: kkania@cbm.pan.pl

<sup>2</sup>Laboratory of Cellular Immunology, Institute of Medical Biology of the Polish Academy of Sciences, Lodz, Poland

<sup>3</sup>Department of General Biophysics, Faculty of Biology and Environmental Protection, University of Lodz, Lodz, Poland

The blood-brain barrier (BBB) is defined as a dynamic structure, responsible for the maintenance of homeostasis which is necessary for the proper functioning of the cells and tissue of the nervous system. It provides the selective transport of substances between the brain and the rest of the body. Another function of the blood-brain barrier is its natural protection against the effects of fluctuations in nutrient, hormone and metabolite levels. It also protects the brain against the direct influence of many bloodborne factors, endogenous and exogenous, which might impair neuronal transmission [1].

Recently, nanoparticles have become increasingly prevalent both in the environment and in pharmaceutical practice. The main aim of our study is extensive analysis of the effects of

nanoparticles on the maintenance of an integrity and proper function of BBB at cellular and molecular level.

In our experiments we used hCMEC/D3 cell line. This the unique model of blood-brain barrier cell line, derived from human brain microvessel endothelial cells. At the beginning we examined toxicity of nanoparticles: CdTe quantum dots, carbon nanotubes, diamond nanoparticles, gold nanoparticles, aluminum oxide nanoparticles and dendrimers, by resazurine assay. In the next step we investigated the impact of the nanoparticles on immunological aspect of BBB. We analyzed mRNA level of IL-6 gene by Real-time PCR technique with SYBR Green I, we also measured the presence of functional protein, using ELISA method, after treatment hCMEC/D3 cells with nanoparticles. To monitor the integrity of intercellular junctions, we used the method of measurement of transendothelial electrical resistance (TEER), with a dedicated tissue resistance measurement chamber.

In summary, our study shows that some of the compounds used in the experiments can modulate the blood-brain barrier. They can cause the increase of IL-6 at protein and mRNA level and changes of TEER.

The project was funded by National Science Centre (NCN), Poland. No 2012/07/B/NZ4/01770.

#### Reference

1. J. Bernacki, A. Dobrowolska, K. Nierwińska and A. Małecki: Physiology and pharmacological role of the blood-brain barrier. *Pharmacological Reports* **60**, 600–622 (2008).

## T04\_05

### SILICA SPECIES AS A LIMITING FACTOR FOR DRUG RELEASE IN MULTIPARTICULATE SYSTEMS

*Agnieszka Kierys*<sup>1</sup>, *Andrzej Sienkiewicz*<sup>1</sup>, *Marta Grochowicz*<sup>2</sup>, *Regina Kasparek*<sup>3</sup>

<sup>1</sup>Department of Adsorption, Faculty of Chemistry, M. Curie-Skłodowska University, M. Curie-Skłodowska Sq. 3, 20-031 Lublin, Poland; e-mails: agnieszka.kierys@umcs.lublin.pl; andrzej.sienkiewicz@umcs.lublin.pl; jacek.goworek@umcs.lublin.pl

<sup>2</sup>Department of Polymer Chemistry, Faculty of Chemistry, Maria Curie-Skłodowska University, 33 Gliniana Str, 20-614 Lublin, Poland; e-mail: mgrochowicz@umcs.lublin.pl

<sup>3</sup>Department of Applied Pharmacy, Faculty of Pharmacy, Medical University of Lublin, 1 Chodzki Str, Lublin 20-093, Poland; e-mail: reginakasperek@umlub.pl

Formulation is an integral component in the development and manufacturing of a drug product, since it determines whether an active pharmaceutical ingredient (API) reaches an optimal therapeutic effect and minimizes its side effects. Thus, efforts are constantly made to improve the drug delivery technology. One of interesting oral drug formulations is a multiparticulate system, in which the dose of the drug is divided among several discrete units [1]. Therefore, by combining these which exhibit different release characteristics, it is possible to obtain a complex release profiles. For the multiparticulate system, the selection of the appropriate barrier surrounding API and the type of coating technology is a crucial issue, since they affect the rate and location of drug release [2].

This study presents an interesting and highly promising strategy for coating and encapsulation of solid drug dispersion within a polymer carrier by silica derivatives. The polymer selected as a drug carrier was Amberlite XAD7HP, as its developed internal pore structure and the ability to swell make it possible to introduce a large amount of drug by the solvent evaporation method. The diclofenac sodium, a representative of the non-steroidal anti-inflammatory drugs was selected for this study. For such water-soluble drug, the modification of discrete units of the solid dispersion toward reduction of released medium infiltration along with slowing down API desorption are needed. Thus, the silica species were produced *in situ* within the units of the solid dispersion through the hydrolysis and condensation of silica precursors introduced into them by swelling method. The gelation of the precursors was initiated by the use of ammonia as a catalyst, which was supplied in the vapor phase. It is demonstrated that silica gel introduced into the units of solid dispersion not only modifies drug release characteristics but also protects the units against environmental factors (e.g. humidity) and enhances the mechanical strength of the units. The conducted studies involve spectroscopic techniques together with the low temperature N<sub>2</sub> sorption and the drug desorption experiment.

#### References

1. R. Gandhi, C. L. Kaul and R. Panchagnula: Extrusion and spheronization in the development of oral controlled-release dosage forms. *Pharm. Sci. Tech. Today* **2**, 160–170 (1999).
2. L. A. Felton: Characterization of coating systems. *AAPS PharmSci. Tech.* **8**, E1–E9 (2007).

## T04\_06

### BIOACTIVITY AND BIOCOMPATIBILITY OF COPPER CONTAINING SOL-GEL GLASS-CERAMICS

*Klára Magyari*<sup>1</sup>, *Radu A. Popescu*<sup>1,2,3</sup>, *Adriana Vulpoi*<sup>1</sup>, *Emilia Licarete*<sup>1</sup>, *Lucian Baia*<sup>1,2</sup>

<sup>1</sup>Interdisciplinary Research Institute on Bio-Nano-Sciences, Babes-Bolyai University, 400271, Cluj-Napoca, Romania; e-mail: klara.magyari@ubbcluj.ro

<sup>2</sup>Faculty of Physics, Babes-Bolyai University, 400084, Cluj-Napoca, Romania

<sup>3</sup>Faculty of Veterinary Medicine, University of Agricultural Science and Veterinary Medicine, 400372, Cluj-Napoca, Romania

The sol-gel derived glass-ceramics have a great potential for hard and soft tissue regeneration applications. With addition of copper oxide into the glass-ceramic matrix it can be created a multifunctional biomaterial. The copper ions play a very important role in cell differentiation and blood vessel formation [1], and the Cu<sup>2+</sup> ions are vital in human metabolism and they can be found in a significant amount in human endothelial cells during physiological angiogenesis. Nevertheless, the copper oxide content may influence the glass-ceramics bioactivity, a high concentration of copper ions determining the formation of free radicals and creating an important cytotoxic environment.

Considering all these issues, throughout this study we propose to determine the *in vitro* bioactivity and *in vitro* biocompatibility of silicate glass-ceramics with different CuO content. Samples belonging to the following compositions (64 - x)SiO<sub>2</sub>·(36 - x)CaO·8P<sub>2</sub>O<sub>5</sub>·CuO, with x = 0, 0.5, 1.5, 2.5 and 4 mol%; were synthesised by sol-gel method [2]. Material stabilization



was carried out at 600 °C / 3 h. The *in vitro* bioactivity was tested by following the self-assemble process of the calcium apatite layer on the materials' surface after immersion in simulated body fluid (SBF) using FT-IR spectroscopy, X-ray diffraction analysis (XRD) and Scanning Electron Microscopy (SEM). The *in vitro* biocompatibility of materials was assessed using *Human keratinocytes* cells viability.

The obtained results show that on the samples' surface immersed in SBF for a period of 7 days hydroxyapatite crystallites are formed, confirming the *in vitro* bioactivity of all investigated samples. The viability of *Human keratinocytes* cells after 24 h interaction with investigated samples indicates a good *in vitro* tolerance, and furthermore, the samples with 0.5 and 1.5 mol% CuO content reveal a very high proliferation rate.

#### Acknowledgements

This work was supported by a grant of the Romanian National Authority for Scientific Research and Innovation, CNCS – UEFISCDI, project number PN-II-RU-TE-2014-4-1597.

#### References

1. G. L. Semenza: Regulation of oxygen homeostasis by hypoxia-inducible factor 1. *Physiology* 24, 97–106 (2009).
2. K. Magyari, L. Baia, A. Vulpoi, S. Simon, O. Popescu and V. Simon: Bioactivity evolution of the surface functionalized glasses. *J Biomes Mater. Res B* 103, 261–272 (2015).

## T04\_07

### TARGETED NANOPARTICLE DELIVERY ACROSS BRAIN ENDOTHELIAL CELLS USING NUTRIENT TRANSPORTER LIGANDS

*Mária Mészáros*<sup>1</sup>, *Lóránd Kiss*<sup>1</sup>, *Dóra Hantosi*<sup>1</sup>, *Zsolt Bozsó*<sup>2</sup>, *Lívía Fülöp*<sup>2</sup>, *Balázs Szalontai*<sup>1</sup>, *Zoltán Kóta*<sup>1</sup>, *Péter Sipos*<sup>3</sup>, *Piroska Szabó-Révész*<sup>3</sup>, *Mária A. Deli*<sup>1</sup>, *Szilvia Veszelka*<sup>1</sup>

<sup>1</sup>Institute of Biophysics, Biological Research Centre, HAS, Hungary

<sup>2</sup>Department of Medical Chemistry, University of Szeged, Hungary

<sup>3</sup>Department of Pharmaceutical Technology, University of Szeged, Hungary

The blood-brain barrier (BBB) limits efficient drug delivery to the central nervous system and the treatment of neurological diseases. Nanoparticle drug delivery systems targeting physiological transport pathways of the BBB are promising new therapeutical tools. The aim of our study was to test the cellular toxicity, uptake and penetration of vesicular and solid nanoparticles targeted by ligands of nutrient transporters on culture models of the BBB.

Nanosized, biocompatible and biodegradable vesicles containing fluorescent dye were prepared and characterized. Fluorescent solid nanoparticles were purchased and surface modified. The vesicular and solid nanoparticles were labeled with biotin, a glucose analog, alanin and glutathione. As BBB models human hCMEC/D3 and primary rat brain endothelial cells were used. The toxicity of nanoparticles was measured by real-time impedance monitoring (RTCA-SP, ACEA Biosciences) and MTT assay. Brain endothelial uptake was quantified by fluorescent spectroscopy and visualized by confocal microscopy, while the penetration of nanoparticles was measured on hCMEC/D3 cells and a triple co-culture BBB model using Transwell inserts.

The presence of ligands on the surface of nanovesicles increased the uptake and the permeability of the model molecule or the solid nanoparticle in cultured brain endothelial cells. The brain endothelial uptake of both loaded nanovesicles and solid nanoparticles could be followed by confocal microscopy.

Our data indicate that the uptake and transfer of nanoparticles targeted with SLC and other nutrient transporter ligands are increased in brain endothelial cells. The type of the ligands and their coupling to nanoparticles are critical points, however, which need further studies.

Supported by OTKA PD105622 and János Bolyai Research Fellowship.

## T04\_08

### CELL ADHESION OF KERATINOCYTES ON FLUORINATED ETHYLENE PROPYLENE: FOCAL ADHESION PERSPECTIVE

*Lucie Peterková*<sup>1</sup>, *Silvie Rimpelová*<sup>1</sup>, *Nikola Slepícková Kasálková*<sup>2</sup>, *Martin Veselý*<sup>3</sup>, *Václav Švorčík*<sup>2</sup>, *Petr Slepíčka*<sup>2</sup>, *Tomáš Ruml*<sup>1</sup>

<sup>1</sup>Department of Biochemistry and Microbiology, University of Chemistry and Technology Prague, Technická 3, 166 28, Prague 6, Czech Republic

<sup>2</sup>Department of Solid State Engineering, University of Chemistry and Technology Prague, Technická 3, 166 28, Prague 6, Czech Republic

<sup>3</sup>Department of Organic Technology, University of Chemistry and Technology Prague, Technická 5, 166 28, Prague 6, Czech Republic; e-mails: petr.slepicka@vscht.cz; tomas.ruml@vscht.cz

Biocompatibility of polymeric materials is determined mainly by their surface properties such as surface wettability, roughness or availability of functional groups. Strongly hydrophobic polymers, such as that of fluorinated ethylene propylene (FEP), require modification of surface properties in order to allow adhesion and spreading of adherent cells. We exposed FEP foils to argon plasma discharge of two different powers, 3 and 8 W for 0–240 s to improve the suitability of FEP for cell adhesion and proliferation. Using fluorescence and scanning electron microscopy, we found that all tested FEP modifications led to a significant increase in cell adhesion as well as proliferation of HaCaT human keratinocytes. Furthermore, morphology of the cells growing on the modified matrices was similar to that of controls (cells growing on standard tissue culture polystyrene dishes) and differed considerably from cells on pristine FEP. We also characterised cell adhesion using immunoblotting of whole cell lysates and immunostaining of focal adhesions. The amounts of the focal adhesion protein talin 1 varied only slightly among the various tested matrices. The analysis of focal adhesions showed that the amount of focal adhesions per cell increased with prolonged exposition time of FEP to Ar plasma of either power. Altogether, Ar plasma treatment enhanced biocompatibility of FEP observed as improved adhesion, morphology and proliferation of HaCaT keratinocytes on FEP.

**T04\_09****MODIFIED ELECTRODE DESIGN FOR SENSITIVE DETECTION OF VARDENAFIL FROM PHARMACEUTICAL DOSAGE FORMS***Burcin Bozal-Palabiyik<sup>1</sup>, Bengi Uslu<sup>1</sup>, Ersin Demir<sup>2,3</sup>, Recai Inam<sup>3</sup>*<sup>1</sup>Ankara University, Faculty of Pharmacy, Department of Analytical Chemistry, Tandogan, Ankara, Turkey<sup>2</sup>Okan University, Health Services Vocational School, Perfusion Techniques, Istanbul, Turkey<sup>3</sup>Gazi University, Faculty of Science, Department of Chemistry, Ankara, Turkey

Vardenafil is a selective phosphodiesterase type 5 inhibitor used for the treatment of erectile dysfunction. In this study, the electrochemical behavior of vardenafil was examined by using differential pulse adsorptive stripping (DPAdS) and cyclic voltammetry through carbon paste electrode. First, the carbon paste electrode was modified separately by carbon nanotubes and various metal nanoparticles. ZnO was chosen for nano-particular modification because it gave the highest peak current. In order to develop a more sensitive sensor, whether carbon nanotubes have any contribution to this modification was analyzed. For this purpose, multi-walled carbon nanotubes, which include carboxyl groups, amine groups and which do not include any functional group, were used. The highest peak current and the most regular peak form were obtained with carbon nanotubes including amine groups.

In this study, the effect of pH on the oxidation of vardenafil was also examined and for this purpose Britton–Robinson (pH 2.0–10.0) and phosphate (pH 2.0 and 3.0) buffer solutions and H<sub>2</sub>SO<sub>4</sub> (pH 1.0 and 2.0) supporting electrolyte were used. pH 3.0 phosphate buffer was chosen for the detection studies, since it provided the highest peak current. Accumulation potential and accumulation time were optimized for DPAdSV and found 400 mV and 300 s, respectively. The interference effect of dopamine, uric acid and ascorbic acid were examined and it was observed that they did not have a noteworthy change on the peak current of vardenafil. Finally, the developed methods were applied to tablets and all necessary validation studies were performed.

**T04\_10****TARGETED NANOPARTICLE DELIVERY ACROSS BRAIN ENDOTHELIAL CELLS USING NUTRIENT TRANSPORTER LIGANDS***Mária Mészáros<sup>1</sup>, Lóránd Kiss<sup>1</sup>, Dóra Hantosi<sup>1</sup>, Zsolt Bozsó<sup>2</sup>, Livia Fülöp<sup>2</sup>, Balázs Szalontai<sup>1</sup>, Zoltán Kóta<sup>1</sup>, Péter Sipos<sup>3</sup>, Pirooska Szabó-Révész<sup>3</sup>, Mária A. Deli<sup>1</sup>, Szilvia Veszelka<sup>1</sup>*<sup>1</sup>Institute of Biophysics, Biological Research Centre, Hungarian Academy of Sciences, Temesvári krt. 62, Szeged, Hungary; e-mail: meszaros.maria@brc.mta.hu<sup>2</sup>Department of Medical Chemistry, University of Szeged, Szeged, Hungary<sup>3</sup>Department of Pharmaceutical Technology, University of Szeged, Szeged, Hungary

The blood-brain barrier (BBB) limits efficient drug delivery to the central nervous system and the treatment of neurological diseases [1]. Nanoparticle drug delivery systems targeting physiological transport pathways of the BBB are promising new therapeutic tools. The solute car-

rier (SLC) mediated transporters of the BBB, supply the central nervous system with nutrients, vitamins and minerals [2]. The aim of our study was to test the cellular toxicity, uptake and penetration of vesicular and solid nanoparticles targeted by ligands of nutrient transporters on culture models of the BBB.

Nanosized, biocompatible and biodegradable vesicles containing fluorescent dye were prepared and characterized. Fluorescent solid nanoparticles were purchased and surface modified. The vesicular and solid nanoparticles were labeled with biotin, a glucose analog, alanin and glutathione. As BBB models human hCMEC/D3 and primary rat brain endothelial cells were used. The toxicity of nanoparticles was measured by real-time impedance monitoring (RTCA-SP, ACEA Biosciences) and MTT assay. Brain endothelial uptake was quantified by fluorescent spectroscopy and visualized by confocal microscopy, while the penetration of nanoparticles was measured on hCMEC/D3 cells and a triple co-culture BBB model using Transwell inserts.

The presence of ligands on the surface of nanovesicles increased the uptake and the permeability of the model molecule or the solid nanoparticle in cultured brain endothelial cells. The brain endothelial uptake of both loaded nanovesicles and solid nanoparticles could be followed by confocal microscopy.

Our data indicate that the uptake and transfer of nanoparticles targeted with SLC and other nutrient transporter ligands are increased in brain endothelial cells. The type of the ligands and their coupling to nanoparticles are critical points, however, which need further studies.

Supported by OTKA PD105622 and János Bolyai Research Fellowship.

#### References

1. W. A. Banks: From blood-brain barrier to blood-brain interface: new opportunities for CNS drug delivery. *Nat. Rev. Drug Discov.* **15**, 275–292 (2016).
2. P. Campos-Bedolla, F. R. Walter, S. Veszeka and M. A. Deli: Role of the blood-brain barrier in the nutrition of the central nervous system. *Arch. Med. Res.* **45**, 610–638 (2014).

## T04\_11

### DEVELOPMENT OF AMPEROMETRIC BIOSENSOR BASED ON NANOSTRUCTURED TiO<sub>2</sub>

Vasilii S. Mironov, Elena G. Zemtsova, Vladimir M. Smirnov

Institute of Chemistry Saint Petersburg State University, Universitetskaya nab. 7/9, St. Petersburg, 199034, Russian Federation; e-mail: 7vonorim7@gmail.com

Amperometric biosensors consisting of oxidase have attracted great attention because of their wide application. The current work demonstrates a novel approach to construct an enzymatic biosensor based on nanostructured TiO<sub>2</sub> – Si electrodes obtained by atomic layer deposition (ALD) method, as a supporting electrode on which enzyme glucose oxidase (GOx) have been immobilized.

The nanostructured TiO<sub>2</sub> – Si electrodes were explored by the following methods:

1. Scanning electron microscopy
2. Atomic force microscopy

3. X-ray photoelectron spectroscopy
4. Cycle voltamperometry
5. Chronoamperometry

The resulting biosensors exhibits a fast response, wide linear range, and good stability for glucose sensing.

#### References

1. E. G. Zemtsova, P. E. Morozov and V. M. Smirnov: Regulation of surface topography of nanostructured titanium using the method of ML-ALD to create bioactive nanocoatings. *Materials Physics and Mechanics* **24**, 374–381 (2015).
2. M. Viticoli, A. Curulli, A. Cusma, S. Kaciulis, S. Nunziante, L. Pandolfi, F. Valentini and G. Padeletti: Third-generation biosensors based on TiO<sub>2</sub> nanostructured films. *Materials Science and Engineering: C* **26**, 947–951 (2006).

## POSTER PRESENTATIONS

T05 – Multidisciplinary nanoscience:  
new methods and application  
possibilities

### T05\_01

#### GRAPHENE NANOSENSOR FOR ENVIRONMENTAL AND BIOLOGICAL APPLICATION

*Diana Aznakayeva, Emir Aznakayev, Igor Yakovenko*

Department of Electronics, National Aviation University, Kiev, Ukraine; e-mail: fliary@ukr.net

The paper addresses the processes of acoustic waves detection through graphene nanosensor. The scheme of passive acoustic nanosensor device based on graphene has been proposed. Performed numerical simulation reveals the change in the geometry of graphene nanosensor device under the influence of acoustic pressure of different magnitudes for determination spatial position of an object. Functioning organs of living body and the flow of blood in them produce characteristic acoustic image being distorted by their dysfunctions. Determination of spatial position of sources of such disturbances allows nanorobots to be spatially localized and influence them with high precision. In addition, passive acoustic radars with macroscopic sizes can be formed as well from the nanosensors array without any special rotational mechanism. Sound pressure or acoustic pressure is the local pressure deviation from the ambient (equilibrium) atmospheric pressure caused by a sound wave. Light intensity incident on the surface of graphene nanosensor couple to the intensity of acoustic wave source and with the distance to the objects. Hence, by measuring the intensity or pressure exerted by acoustic wave on graphene nanosensor surface and determining the intensity of acoustic wave source it is possible to pinpoint the distance to the detected object. If measure acoustic wave intensity or acoustic pressure exerted on surface of graphene nanosensor by the object located at different distances and from nanosensor, one can define the distance by which observable object has moved. In this paper we propose the scheme of passive acoustic graphene nanosensor construction. The upper electrode plate is constructed from transparent material graphene with the fine electric and optical properties. Under the influence of acoustic wave pressure acting on the graphene layer, graphene bends on the value  $z$  along vertical  $Oz$  axis. To eliminate this deflection of graphene layer it is necessary to apply the electric potential difference  $U$  to graphene plates. The intensity change  $Y$  of laser radiation, incident on graphene layer and detected by light diode, is defined as laser focus displacement at deflection  $z$  of graphene layer:  $Y(z) = Y_0 \exp(-\alpha z)$ . Here  $Y_0$  is laser beam intensity incident on graphene in the absence of acoustic pressure  $p = 0$ ,  $Y(z)$  is laser beam intensity incident on graphene in the presence of acoustic pressure  $p \neq 0$ . Based on the theoretical formula it is achievable to construct calibration curve of nanosensor for dependence of squared difference of electric potential  $U^2$  from the value of acoustic pressure  $p$ . Determined the mag-

nitude of acoustic pressure from calibration plot in three different moments of time  $p(t_1)$ ,  $p(t_2)$ ,  $p(t_3)$  it is possible to define spatial coordinates of detected object  $r(t_1)$ ,  $r(t_2)$ ,  $r(t_3)$  and its velocities  $v(t_1)$ ,  $v(t_2)$ ,  $v(t_3)$  in these moments of time.

#### References

1. A. K. Geim and K. S. Novoselov: The rise of graphene. *Nature Materials*, **6**, 183–191 (2007).
2. D. R. Raichel: *The Science and Applications of Acoustics*. Springer, New York, 2006.

## T05\_02

### CONFORMATIONAL ANALYSIS AND THERMAL EFFECTS ON CALMAGITE IN PROTIC SOLVENTS VARYING PH

*Zuriel Natanael Cisneros García, Francisco José Tenorio Rangel, Jaime Gustavo Rodríguez Zavala*

Departamento de Ciencias Exactas y Tecnología, Centro Universitario de los Lagos, Universidad de Guadalajara, México; e-mail: cisneros.zng@gmail.com

Density functional theory (DFT) has been widely used in molecules and solids, however, its original formulation is applied to systems in vacuum and at absolute zero temperature (0K), there has been some efforts to get improves in calculations as the modeling of a solvent medium or the inclusion of temperature effects. An attempt to include the temperature effects is through the calculation of molar fractions at finite temperature by means of rotor rigid-harmonic oscillator approximation [1], this approach has been mainly applied to endohedral fullerenes [2], nevertheless it is not limited to this kind of systems. Calmagite (3-Hydroxy-4-[(2-hydroxy-5-methylphenyl)azo]-1-naphthalenesulfonic acid) is an azo dye introduced in 1960 as a substitute of erichrome black T in titrations with EDTA for calcium and magnesium determination. Also is a triprotic acid and its protons are detached from the structure as the pH is varying. It is important to mention that at neutral pH its absorption spectrum show a main peak around 525 nm and a shoulder at 560 nm. Here, from a theoretical point of view a conformational analysis of calmagite for each protonation and deprotonation degree was performed [3]. Calculations in gas phase and taking into account implicit protic solvents were performed. The use of a solvent affect in a direct way the relative stabilities of azo and hydrazone tautomers, e.g. when calmagite is once deprotonated, the azo tautomer is the most stable in gas phase, however, when a solvent is utilized, hydrazone tautomer is stabilized. It is worth to mention that small energy differences were found when the first deprotonation was carried out, indicating the need to observe the thermal effects in the isomerization of this molecule. Then, molar fractions were obtained as a function of temperature. Interestingly two isomers presented important molar fractions at room temperature which could support the idea that the main peak in the absorption spectrum belongs to one isomer and the shoulder could be owing to the other isomer. Finally, for the second deprotonation only one peak is observed in experimental spectrum and from the molar fraction calculation the presence of only one isomer at room temperature was found. Therefore, thermal analysis in isomerization had an important role in assignation of the possible conformers contributing in experimental absorption spectrum.

**References**

1. Z. Slanina: Multimolecular cluster: their isomerism and effective characteristics evaluated by quantum chemistry. *Journal of Quantum Chemistry* **16**, 76–86 (1979).
2. F. Uhlík, Z. Slanina, S. Lee, L. Adamowicz and S. Nagase: Stability calculations for Eu@C<sub>74</sub> isomers. *International Journal of Quantum Chemistry* **113**, 729–733 (2013).
3. Z. N. Cisneros-García, P. G. Nieto-Delgado, J. G. Rodríguez Zavala: Conformational analysis on protonation and deprotonation of calmagite in protic solvents and its reactivity through Fukui Function. *Dyes and Pigments* **121**, 188–198 (2015).

**T05\_03****s-SNOM MEASUREMENTS OF BORON NITRIDE NANOTUBES**

*Daniel Datz*<sup>1</sup>, *Gergely Németh*<sup>1</sup>, *Hajnalka Mária Tóháti*<sup>1</sup>, *Tibor Gál*<sup>2</sup>, *Örs Sepsi*<sup>2</sup>, *Pál Koppa*<sup>2</sup>, *Áron Pekker*<sup>1</sup>, *Katalin Kamarás*<sup>1</sup>

<sup>1</sup>Institute for Solid State Physics and Optics, Wigner Research Centre for Physics, HAS, Budapest, Hungary

<sup>2</sup>Department of Atomic Physics, Budapest University of Technology and Economics, Budafoki út 8, 1111 Budapest, Hungary

The Neaspec s-SNOM device is an effective tool to create optical maps of nano-objects. The illuminating laser induces nearfield interaction between the AFM tip and the nano-object or substrate. The scattered electromagnetic radiation can be detected and optical information can be extracted with 20 nm precision, regardless of the illumination laser wavelength.

Despite being an effective tool for the extension of atomic force microscopy to create optical maps, in its original state our s-SNOM device is a microscope, and performing spectroscopy is troublesome and inconvenient. To tackle this problem, the device has been modified by attaching appropriate equipment for the simultaneous control of the laser controller and the s-SNOM device. With a Labview program, spectroscopy with arbitrary wavenumber steps can be performed.

Nanospectroscopy with the modified Neaspec s-SNOM device was performed on a single bundle of boron nitride nanotube with 1.5 cm<sup>-1</sup> resolution. The absorbance of the sample can be calculated from the measured optical amplitude and the phase of the scattered radiation. The acquired optical properties show very good agreement with the known phonon polariton modes in the nanotubes. Finite element simulation also confirms our results.

Funding: OTKA ANN 107580.



**T05\_04****UNDERSTANDING THE PHOTOELECTRICAL RESPONSE OF MESOPOROUS NICKEL OXIDE DECORATED WITH CONTROLLED SIZE PLATINUM NANOPARTICLES IN DIFFERENT ATMOSPHERES**

*Juan Gómez-Pérez*<sup>1,2</sup>, *Dorina G. Dobó*<sup>1</sup>, *Koppány L. Juhász*<sup>1</sup>, *András Sági*<sup>1</sup>, *Henrik Haspel*<sup>1</sup>, *Zoltán Kónya*<sup>1,2</sup>, *Ákos Kukovecz*<sup>1,3</sup>

<sup>1</sup>Department of Applied and Environmental Chemistry, University of Szeged, Rerrich Béla tér 1, H-6720 Szeged, Hungary

<sup>2</sup>MTA-SZTE Reaction Kinetics and Surface Chemistry Research Group, Rerrich Béla tér 1, H-6720 Szeged, Hungary

<sup>3</sup>MTA-SZTE “Lendület” Porous Nanocomposites Research Group, Rerrich Béla tér 1, H-6720 Szeged, Hungary

The electrical photoresponses at 30 °C of nanocomposite samples made of mesoporous nickel oxide and platinum nanoparticles (Pt NP) were analyzed under argon and oxygen atmosphere using a visible light source (emission centered at 407 nm, FWHM = 12.5 nm). In literature, nanoparticles have shown both electrical [1] and chemical sensitization [2] and this work contributes to the understanding on the adsorbates influence and the size effect of the platinum nanoparticles over the photoelectrical response. The addition of controlled size Pt NP (1.6 nm and 6.4 nm) over pristine MNO enhanced up to 3 times the electrical photoresponse (using MNO + 1.6 nm Pt NP), and the argon atmosphere enhanced the response up to 30% in comparison with oxygen atmosphere. These results were explained using heterojunctions theory including a new induced potential depending on the atmosphere around the nanocomposite.

**Acknowledgements**

The financial support of the Hungarian Research, Development and Innovation Office through projects K 112531 and K 120115 is acknowledged.

**References**

1. J. R. Durán Retamal, C. Y. Chen, D. H. Lien, M. R. S. Huang, C. A. Lin, C. P. Liu and J. H. He: *ACS Photonics* **1**, 354–359 (2014).
2. J. Zhang, X. Liu, G. Neri and N. Pinna: Nanostructured materials for room-temperature gas sensors. *Adv. Mater.* 795–831 (2015).

**T05\_05****SIZE-CONTROLLED PLATINUM NANOPARTICLES: FABRICATION, CHARACTERIZATION AND APPLICATION IN HETEROGENOUS CATALYTIC PROCESSES**

*Koppány Levente Juhász*, *M. Szabó*, *Á. Szamosvölgyi*, *D. Dobó*, *A. Sági*, *Á. Kukovecz*, *Z. Kónya*

Department of Applied and Environmental Chemistry, University of Szeged, Rerrich Béla tér 1, H-6720 Szeged, Hungary

Synthesis of monodisperse catalyst nanoparticles is problematic in several industrial applications, therefore, the effect rising from the size in catalytic processes remain unexploited. In this work, 1–12 nm platinum nanoparticles with adjusted size and narrow size distribution were fabricated with a particular wet chemistry method, from various salt precursors, under inert atmosphere, in elevated temperature.

The particles were embedded into 3-dimensional inert mesoporous silica supports with low power sonication for further investigation and testing in heterogenous catalytic model reactions, such as ethanol decomposition and carbon-dioxide hydrogenation reaction. The free-standing and supported catalysts were characterized by Scanning and Transmission Electron Microscopy, the product of the gas-phase reactions were characterized by gas chromatography.

The financial support of the Hungarian Research, Development and Innovation Office through projects K 112531 and K 120115 is acknowledged.

## T05\_06

### OPTIMIZATION OF SP-ICP-MS INSTRUMENTAL PARAMETERS FOR THE MEASUREMENT OF SURFACE MODIFIED NANOPARTICLES

*Ildikó Kálmista<sup>1</sup>, Albert Kéri<sup>1</sup>, Ákos Szamosvölgyi<sup>2</sup>, Dorina Dobó<sup>2</sup>, Koppány Juhász<sup>2</sup>, András Sági<sup>2</sup>, Gábor Galbács<sup>1</sup>, Ákos Kukovecz<sup>2</sup>, Zoltán Kónya<sup>2</sup>*

<sup>1</sup>Dept. of Inorg. and Anal. Chem., University of Szeged, Dóm tér 7, H-6720 Szeged, Hungary; e-mail: galbx@chem.u-szeged.hu

<sup>2</sup>Dept. of Appl. and Environ. Chem., University of Szeged, Rerrich B. tér 1, H-6720 Szeged, Hungary; e-mail: sapia@chem.u-szeged.hu

A promising novel nanoparticle (NP) characterization method is Single Particle Inductively Coupled Plasma Mass Spectroscopy (SP-ICP-MS), which shows distinct advantages over other characterization methods in the case of NPs dispersed in water [1, 2]. The particle size detection limit is around 15–20 nm, and concentrations above 10<sup>3</sup>/mL can be measured in only 5 minutes. The usefulness of SP-ICP-MS has already been demonstrated in a some environmental, biological and food chemistry applications.

Optimization of the main experimental parameters is essential in order to achieve the best possible analytical performance, which here obviously determines the particle size detection limit [3]. The influence of RF power, sampling depth and aerosol dilution gas flow rate have not yet been studied in SP-ICP-MS until now, although they are known to have a great influence on the analytical performance in solution ICP-MS. We found that the optimization of the sampling depth and plasma RF power can provide a several-fold increase in sensitivity, also depending on the mass of the monitored isotope. At the same time, it was revealed that the control of the aerosol dilution gas flow rate, which is a useful tool in solution analysis for the dilution of the matrix, is not efficient and reliable enough for the on-line dilution of NP dispersions.

We also employed the optimized settings for the measurement of such engineered SiO<sub>2</sub> NPs, which are loaded with very small, 1–2 nm in diameter, Pt nanoparticles (Pt:SiO<sub>2</sub>). In this case, the size of the individual Pt NPs is too small for direct detection by SP-ICP-MS, but by using

the optimized parameters, the combined signal from the Pt NPs in the loading can be detected, and after an instrument calibration performed by using Pt particle size standards, the accurate loading could be determined. We also compared the results to data obtained by other measurement method (e.g. XPS, SEM-EDX, solution ICP-MS) and found that the SP-ICP-MS method is accurate and robust.

#### References

1. F. Laborda, J. Jiménez-Lamana, E. Bolea and Juan R. Castillo: Critical considerations for the determination of nanoparticle number concentrations, size and number size distributions by single particle ICP-MS. *J. Anal. At. Spectrom.* **28**, 1220 (2013).
2. S. Lee, X. Bi, R. B. Reed, J. F. Ranville, P. Herckes and Paul Westerhoff: Nanoparticle size detection limits by single particle ICP-MS for 40 elements. *Environ. Sci. Technol.* **48**, 10291–10300 (2014).
3. L. Wan-Waan and C. Wing-Tat: Calibration of single-particle inductively coupled plasma-mass spectrometry (SP-ICP-MS). *J. Anal. At. Spectrom.* **30**, 1245 (2015).

## T05\_07

### OPTICAL EXTINCTION SPECTROSCOPY FOR THE ASSESSMENT OF METHODS OF NANOPARTICLE SYNTHESIS

L. Égerházi<sup>1</sup>, B. Kovács<sup>2</sup>, D. Sebők<sup>3</sup>, Zs. Geretovszky<sup>2</sup>, T. Szörényi<sup>2</sup>

<sup>1</sup>Department of Medical Physics and Informatics, University of Szeged, Korányi fasor 9, H-6720 Szeged, Hungary

<sup>2</sup>Department of Optics and Quantum Electronics, University of Szeged, Dóm tér 9, H-6720 Szeged, Hungary

<sup>3</sup>Department of Physical Chemistry and Materials Science, University of Szeged, Rerrich Béla tér 1, H-6720 Szeged, Hungary

The size distribution of nanoparticles and the efficiency of their production are key variables when comparing the performance of competitive techniques. Wire explosion is a straightforward, yet robust green method of nanoparticle production, however the diversity of particle populations poses a serious challenge for the determination of the multimodal size distribution characteristic to the nanosols formed.

In this contribution we show that fitting the extinction spectra of colloidal solutions produced by explosion of copper wires in aqueous environment by the Mie model allows for obtaining the size distribution of nanoparticles in an exceptionally wide range. Later, we will use this procedure to scrutinize the particle production efficiency of this synthesis route as a function of process parameters. Rising extinction in the UV at the expense of the plasmon absorption band at around 600 nm with increasing energy pumped into the wire evidences significant increase in the abundance of nanoparticles of several nm in diameter to the detriment of those in the 100–300 nm size range.

Exploiting that the extinction cross section is directly proportional to the volume number concentration of particles, variation in the particle number concentration of different populations can also be conveniently determined.

**T05\_08****MULTIFUNCTIONAL THIN FILM PHASE PLATE FOR IN-FOCUS TRANSMISSION ELECTRON MICROSCOPY***Pai Chia Kuo, Jessie Shiue*

Research Program on Nanoscience & Nanotechnology, No. 128, Academia Rd., Nangang, Taipei 11529, Taiwan, paichia@gate.sinica.edu.tw

Organic electron microscopy is limited by the low-contrast images with a poor signal-to-noise ratio since the structure of sample are constituted with light elements. The conventional method to enhance the contrast of transmission electron microscopy (TEM) images is defocused technique, but it also causes some artifacts in images. Multiple kinds of TEM phase plate had been proposed for decades, however, very few of them can be practically used for taking reliable in-focus TEM images. Amorphous carbon film was used to play a phase shifting material in several types of phase plates. Here we present a multifunctional on-chip carbon thin film phase plate which can integrate Zernike Phase Plate (ZPP) and Hole-Free Phase Plate (HFPP) into single device. These two kinds of carbon-based phase plate are the most mature techniques for TEM applications nowadays.

Our on-chip carbon thin film phase plate is fabricated from a gold-wrapped Silicon chip. The chip has numerous apertures and is partially covered by a thin amorphous carbon film. The film is freestanding on the apertures with small drilled holes with different diameter, which serve as ZPP and HFPP, the uncovered aperture serves as an objective aperture. Consequently, multiple phase plates and an objective aperture are well integrated onto one chip device covered with carbon thin film.

In ZPP, the size of the central hole limits the recoverable lower spatial frequencies. Thus different sizes of central hole are proper for observing different size scales of samples. HFPP is also ready in any case if needed. Using this stable system, we were able to identify an unexpected nanophase in a series of polymer solar cell specimens. We were also able to observe some fine structures in unstained *E. coli* with this system. Recently, we surprisingly found some unforeseen structures of lipid nanodisc specimens. The multifunctional film phase plate for TEM provides a convenient and flexible solution for the study of organic materials.

**Reference**

1. P. C. Kuo, J. Shiue et al.: On-chip thin film zernike phase plate for in-focus transmission electron microscopy imaging of organic materials. *ACS Nano* 7, 465–470 (2013).

**T05\_09****INVESTIGATION OF WATER DROPLET EVAPORATION FROM CARBON NANOTUBE AND TITANATE NANOWIRE COMPOSITE FILMS***Krisztina Anita Nagy<sup>1,2</sup>, Erzsébet Sára Bogyá<sup>2</sup>, Zoltán Kónya<sup>1,3</sup>, Ákos Kukovecz<sup>1,2</sup>*

<sup>1</sup>Department of Applied and Environmental Chemistry, University of Szeged, Rerrich Béla tér 1, H-6720 Szeged, Hungary

<sup>2</sup>MTA-SZTE “Lendület” Porous Nanocomposites Research Group, Rerrich Béla tér 1, H-6720 Szeged, Hungary

<sup>3</sup>MTA-SZTE Reaction Kinetics and Surface Chemistry Research Group, Rerrich Béla tér 1, H-6720 Szeged, Hungary

This study is concentrated on sessile water droplet evaporation investigation from nano-porous carbon nanotube composite films. Previous research had revealed that water evaporation behaviour – droplet pinning, surface and pore wetting – can be influenced by the carbon nanotube (CNT) pre-treatment. In this work the effect of titanate nanowire (TiONW) content on the buckypaper droplet evaporation properties is presented.

The composites were synthesized by adding different amounts of TiONW to non-functionalized multiwall carbon nanotubes and filtered to obtain free-standing sheets. The composites and the films were characterized by Scanning – (SEM) and Transmission Electron Microscope (TEM). In addition the specific surface and X-ray powder diffraction were measured.

During solvent droplet evaporation the buckypaper presents a characteristic resistance change, this is the so called evaporation profile (EP). The effect of titanate nanowire content on the shape and size of the EP is thoroughly investigated. Furthermore the evaporation profile results are correlated with infrared camera recordings and droplet weight variation measurements. The optical imaging, electron microscopy and electric resistivity measurements methods gave us full range insight on the composite films properties and surface/pore wetting behaviour.

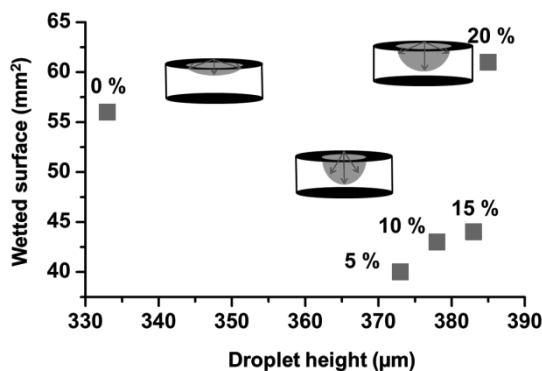


Fig. 1. The effect of TiONW on water droplet evaporation in buckypapers beside different TiONW content

The financial support of the Hungarian Research, Development and Innovation Office through projects K 112531 and K 120115 is acknowledged.

## T05\_10

### SPATIO-TEMPORAL INVESTIGATIONS ON THE INTERFACE PROPAGATION IN A SPIN-CROSSOVER CRYSTAL OBSERVED BY OPTICAL MICROSCOPY

*H. Oubouchou*<sup>1,2,3</sup>, *A. Slimani*<sup>3</sup>, *N. Haine*<sup>2</sup>, *K. Boukheddaden*<sup>3</sup>

<sup>1</sup>Ecole Polytechnique d'Architecture & d'Urbanisme Route de Beaulieu BP 177, 16010 El Harrach, Algérie; e-mail: oh\_hassane@yahoo.fr

<sup>2</sup>Laboratoire de Physique des Matériaux, Faculté de Physique, Université de Sciences et de Technologies Houari Boumediene, Algérie

<sup>3</sup>Groupe d'Etudes de la Matière Condensée UMR8635, CNRS-Université de Versailles/St. Quentin en Yvelines. 45 Avenue des Etats Unis, F78035 Versailles Cedex, France

In this work, We have investigated by optical microscopy, the thermal transition of the spin-crossover dinuclear complexes,  $[\{\text{Fe}(\text{NCSe})(\text{py})_2\}_2(\text{m-bppz})]$ , we have been showing the possibility of controlling the thermal behavior, which is related to the spin transition temperature and cooperativity. The dinuclear unit is robust and can be used as a building block of assembly, and it made possible the investigation of both on-cooling and on-heating processes. We observed well-defined transformation fronts between macroscopic high spin (HS) and low-spin (LS) phases with a sizable hysteresis, at 100 K and 110 K on cooling and heating, respectively, the fronts are almost linear in shape, and propagate through the entire crystals, even in isothermal conditions. The interface orientation was constant and its propagation velocity typically was 1 and 10  $\mu\text{m/s}$  for the on-cooling and on-heating processes, respectively. And we presented the photos of the spin transition processes which show several behaviors. We have also studied in this work the problem of the control of the interface motion by an external command parameter.

## T05\_11

### COHERENT ANTI-STOKES RAMAN SCATTERING AS EFFECTIVE TOOLS FOR VISUALISATION OF SINGLE-WALLED CARBON NANOTUBES

*Alesia Paddubskaya*<sup>1,2</sup>, *Andrej Dementjev*<sup>2</sup>, *Renata Karpicz*<sup>2</sup>, *Polina Kuzhir*<sup>1</sup>, *Sergey Maksimenko*<sup>1</sup>, *Gintaras Valusis*<sup>2</sup>

<sup>1</sup>Research Institute for Nuclear Problems of the Belarusian State University, 11 Bobruiskaya Str., Minsk 220030, Belarus; e-mail: Paddubskaya@gmail.com

<sup>2</sup>Center for Physical Sciences and Technology, Sauletekio al. 3, Vilnius LT-10222, Lithuania

Due to excellent sensitivity, chemical selectivity, spatial resolution and high signal-to-noise ratio coherent anti-Stokes Raman scattering (CARS) has received highest attention in the family of nonlinear optical techniques for investigation and visualisation of different nanoparticles [1, 2]. In this communication, we demonstrate the possibility of applying CARS technique for 3D visualisation of single-walled carbon nanotubes (SWCNTs) in polymer matrix. A picoseconds laser (7 ps, 1064 nm) operating in a cavity dumping regime at the 1 MHz repetition rate was used to pump a travelling wave optical parametric generator, which serves as a two-color (pump and stokes) excitation light source for the CARS microscopy. By varying the excitation power (from 1  $\mu\text{W}$  up to 200  $\mu\text{W}$ ) the optimum regime for non-destructive investigation of nonlinear properties of SWCNTs has been found.

Using SWCNTs with three different average diameters ( $\sim 0.8$  nm,  $\sim 1.1$  nm and  $\sim 1.3$  nm) it was demonstrated that strong, CARS signal (Raman-like spectrum) is observed when the excitation energies close to the electronic excitation energies of SWCNT. The enhanced non-resonance contribution due to two-photon electron resonance was also observed for SWCNTs with larger diameter. Such ability to detect strong coherent nonlinear signal from small SWCNT-

bundles together with main advantages of CARS over Raman scattering such as high imaging rate open new opportunities for fast 3D visualisation SWCNTs in polymer matrix.

#### References

1. H. Kim, C. A. Michaels, G. W. Bryant and S. J. Stranick: *Journal of Biomedical Optics* **16**, 021107 (2011).
2. T. Sheps, J. Brocious, B. L. Corso, O. T. Gul, D. Whitmore, G. Durkaya, E. O. Potma and P. G. Collins: *Phys. Rev. B* **86**, 235412-1-13 (2012).

## T05\_12

### STRUCTURE SENSITIVITY EFFECT OF Pd-Cu/MWCNTs CATALYST FOR NITRATE REDUCTION IN WATER

*Sanja Panic*<sup>1</sup>, *Goran Boskovic*<sup>1</sup>, *Branimir Bajac*<sup>1</sup>, *Srdjan Rakic*<sup>2</sup>, *Zoltán Kónya*<sup>3,4</sup>, *Ákos Kukovecz*<sup>3,5</sup>

<sup>1</sup>Faculty of Technology, University of Novi Sad, Bulevar cara Lazara 1, 21000 Novi Sad, Serbia; e-mail: sanjar@tf.uns.ac.rs

<sup>2</sup>Department of Physics, Faculty of Sciences, University of Novi Sad, Trg Dositeja Obradovica 3, 21000 Novi Sad, Serbia

<sup>3</sup>University of Szeged, Faculty of Science and Informatics, Department of Applied and Environmental Chemistry, Szeged, Hungary

<sup>4</sup>MTA-SZTE Reaction Kinetics and Surface Chemistry Research Group, University of Szeged, Szeged, Hungary

<sup>5</sup>MTA-SZTE "Lendület" Porous Nanocomposites Research Group, University of Szeged, Szeged, Hungary

The pollution of underground water, an important source of potable water, has become a widespread concern in many countries due to excessive use of chemical fertilizers [1]. High level of nitrate in drinking water is known to be a potential risk to human health causing various diseases. Among the current available remediation processes, catalytic denitration has an advantage compared to other methods being an eco-friendly and economically viable process [2]. However, the main drawback of this process is the production of ammonia as a byproduct. In respect to this, the aim of this work was to test the selectivity performance of 2%Pd-1%Cu/MWCNTs catalyst in terms of size of the active metal phase influenced by different properties of two types of multi-walled carbon nanotubes (MWCNTs) used as supports. MWCNTs were previously synthesized by CVD method over bimetallic Fe-Mo-catalyst differing in either Al<sub>2</sub>O<sub>3</sub> or MgO as supports. Before introduction of Pd and Cu by simultaneous wet impregnation, MWCNTs samples were purified by chemical oxidation method and characterized by TEM, XRD, LTNA and Raman spectroscopy. The catalytic reduction of nitrate was carried out in a semi-batch reactor in the presence of H<sub>2</sub> and CO<sub>2</sub>. According to the results, the Al<sub>2</sub>O<sub>3</sub> originated MWCNTs exhibit higher degree of structural defects leading to homogeneously distributed active metal particles on tubes surfaces compared to its MgO originating counterpart. This dispersion effect was confirmed by higher NO<sub>3</sub><sup>-</sup> conversion in the first case. The higher selectivity relative to ammonia obtained in the catalytic activity test indicates predominance of low coordinated metal atoms sitting on the crystal corners, suggesting small Pd particles influenced by enhanced quality of MWCNTs of MgO origin. On another hand, lower quality MWCNTs obtained over Al<sub>2</sub>O<sub>3</sub>

supported catalyst, ensures large Pd particles in the denitration catalyst, preferring nitrogen formation route in the nitrate transformation. Thus, the structure sensitivity of nitrate reduction can be tailored by choosing the MWCNTs support of appropriate quality.

#### References

1. A. O. Costa, L. S. Ferreira, F. B. Passos, M. P. Maia and F. C. Peixoto: *Appl. Catal. A:General* **445–446**, 26–34 (2012).
2. A. Aristizábal, S. Contreras, N. J. Divins, J. Llorca and F. Medina: *Appl. Surf. Sci.* **298**, 75–89 (2014).

### T05\_13

#### INFLUENCE OF ELECTRON INTERFERENCE EFFECTS ON REFLECTION OF ELECTRON WAVES FROM POTENTIAL BARRIER IN 2D SEMICONDUCTOR NANOSTRUCTURES

*V. A. Petrov, A. V. Nikitin*

Institute of Radio Engineering and Electronics, Russian Academy of Science, Moscow, 125009, Russia;  
e-mail: vpetrov@cplire.ru

The influence of the interference of electron waves in the case of their reflection from potential barrier on the spatial distribution of the density of quantum-mechanical current  $ej_x(x,z)$  ( $e$  is the electron charge) in 2D semiconductor nanostructure which is represented by rectangular narrow ( $x < 0$ ,  $QW_1$ ) and wide ( $x > 0$ ,  $QW_2$ ) quantum wells (QWs) sequentially oriented along the direction of the propagation of electron wave has been studied theoretically. It is supposed that the wave falls from the narrow  $QW_1$  on the semi-infinite potential barrier  $V_0$  in height in the wide  $QW_2$ , the energy of the falling wave being less than  $V_0$ . Differing widths of  $QW_1$  and  $QW_2$  provide the non-orthogonality of wave functions of particles in these regions and the corresponding existence of electron interferential effects in this kind of nanostructure. In particular cases these effects lead to the appearance of spatially inhomogeneous distributions  $ej_x^{(1)}(x,z)$  in  $QW_1$  and  $ej_x^{(2)}(x,z)$  in  $QW_2$ . It has been analytically demonstrated that in case of an electron wave falling along the first (lower) quantum-dimensional subband in  $QW_1$  and its kinetic energy  $E_x$  being less than the energy positions of all the other subbands in  $QW_1$  (i.e., the undamped propagation of the wave reflected from the barrier with real quasi-momentum is possible only along this lower subband)  $ej_x^{(1)}(x,z)$  and  $ej_x^{(2)}(x,z)$  are equal to zero. However, if a particle has such an energy that the reflection of the wave with real quasi-momenta is possible along more than one (lower) subband, then the situation completely changes due to the interference of the reflected waves. In this case the interference leads to an existence of a complicatedly oscillating spatially inhomogeneous distribution  $ej_x^{(1)}(x,z)$ , and under the barrier in  $QW_2$  it provides the appearance of exponentially damped at  $x \rightarrow \infty$  and possessing a coordinate dependence of leakage  $ej_x^{(2)}(x,z)$  under the barrier. Besides, three regions of the symmetric along  $z$  axis propagation  $ej_x^{(2)}(x,z)$  are formed under the barrier. They are the central one, in which the current is directed in axis  $x$  positive direction, and two side regions in which the current is directed in negative direction. The presence of the regions of that kind provides the charge flow from under the barrier. The numerical calculations of  $ej_x^{(1)}(x,z)$  and  $ej_x^{(2)}(x,z)$  have also been made taking into account 31 subbands. It should be noted that these kinds of effects have a general nature and exist in 1D and 2D nanostructures with arbitrary profiles of QWs and barriers.



## T05\_14

**LOW PPM-RANGE REFLECTOMETRIC ETHANOL SENSOR AT ROOM TEMPERATURE: IMPROVING THE OPTICAL RESPONSE BY USING MESOPOROUS MATERIALS**

*Dániel Sebők*<sup>1</sup>, *András Sági*<sup>2</sup>, *Dorina G. Dobó*<sup>2</sup>, *Ákos Kukovecz*<sup>2,3</sup>, *Zoltán Kónya*<sup>2,4</sup>,  
*László Janovák*<sup>1</sup>, *Imre Dékány*<sup>1,5</sup>

<sup>1</sup>Department of Physical Chemistry and Materials Science, University of Szeged, Rerrich tér 1, H-6720 Szeged, Hungary; e-mail: sebokd@chem.u-szeged.hu

<sup>2</sup>Department of Applied and Environmental Chemistry, University of Szeged, Szeged, Hungary

<sup>3</sup>MTA-SZTE “Lendület” Porous Nanocomposites Research Group, University of Szeged, Szeged, Hungary

<sup>4</sup>MTA-SZTE Reaction Kinetics and Surface Chemistry Research Group, University of Szeged, Szeged, Hungary

<sup>5</sup>MTA-SZTE Supramolecular and Nanostructured Materials Research Group, University of Szeged, Szeged, Hungary

In this paper a low ppm-range ethanol sensor – operating at room temperature – is presented. The three types of ZnO<sub>2</sub> based hybrid thin films as sensor surfaces consist of semiconductor nanoparticles, polyelectrolyte (polyacrylic acid, PAA) and/or mesoporous silica. The mesostructured silica foam (SF) and 2-D hexagonally ordered SBA-15 samples were characterized by transmission electron microscopy (TEM), small angle X-ray scattering (SAXS) and BET analysis. The TEM and SAXS studies clearly showed the mesocellular structure (SF) and P6mm symmetry (SBA-15) of the samples, as well as, the surface area obtained from SAXS and BET analyses are in good agreement: the  $a^s$  values of the samples are in the range of 6–700 m<sup>2</sup>/g. The thin films were prepared by Layer-by-Layer (LbL) self-assembly method and were subjected to reflectometric interference measurements (RiFS) for testing sensorial application (the principle of LbL method and RiFS are detailed in [1]). The sensor investigation showed that the detection limit of the thin films is in the sub-ppm range. Applying mesoporous silica as surface coating or interlayers in the sandwich-structured thin film (ZnO/SF) improved the optical response, but the sensitivity showed non-linear characteristic. The thin film with mixed structure (ZnO/PAA/ZnO/SF) showed linear response in the 0.5–12 ppm range with 0.6 nm/ppm sensitivity and acceptable selectivity.

**Acknowledgements**

The authors are very thankful for the financial support from The Hungarian Scientific Research Fund (OTKA) PD 116224 and K 116323. The work was also supported by the European Union and the State of Hungary, co-financed by the European Social Fund in the framework of TÁMOP 4.2.4. A/2-11-1-2012-0001 ‘National Excellence Program’, and by the János Bolyai Research Scholarship of the Hungarian Academy of Sciences of SA.

**Reference**

1. D. Sebők and I. Dékány: ZnO<sub>2</sub> nanohybrid thin film sensor for the detection of ethanol vapour at room temperature using reflectometric interference spectroscopy. *Sensor. Actuat. B-Chem.* **206**, 435–442 (2015).

**T05\_15****SYNTHESIS OF MOLYBDENUM AND TUNGSTEN DISULFIDES NANO- AND MICROPARTICLES BY SPRAY PYROLYSIS***S. E. Alexandrov, K. D. Filatov, K. S. Tiurikov*

Department of Physical Chemistry and Microsystem Technologies, Peter the Great Saint-Petersburg Polytechnic University, Polytechnicheskaya, 29, St. Petersburg, Russia;  
e-mail: sevgalexandrov@gmail.com

In recent years, development of technologies for deposition of nanocomposite coatings consisted of superhard matrix material in which molybdenum or tungsten disulfide nano- or microparticles with high antifriction properties uniformly distributed is of particular interest [1]. A two-stage chemical vapor deposition process including synthesis of the nanoparticles in the first zone of the reactor and deposition of nanocomposite coatings in the second zone which nanoparticles are transported to and additional precursors are introduced in can be considered as rather promising. Obviously, the realization of such process requires occurrence of disulfide particles synthesis in the gas stream, thus high reaction rates are necessary. The results of analysis show that it is only possible by using single source precursors containing Mo or W and sulfur. Among the molybdenum or tungsten and sulfur-containing chemical compounds ammonium thiotungstate and thiomolybdate are of particular interest because they decompose at relatively low temperatures with formation of sulfides of tungsten and molybdenum, respectively [2]. However these compounds decompose at temperatures lower than the sublimation temperature at atmospheric pressure. The simplest approach to their use as precursors for the chemical vapor deposition processes is introduction aerosol of their solutions in an appropriate solvent in the reactor. The synthesis of molybdenum and tungsten nano- and microparticles by spray pyrolysis of  $(\text{NH}_4)_2\text{MoS}_4$  or  $(\text{NH}_4)_2\text{WS}_4$  was experimentally studied. Aerosol of precursors solutions in dimethylformamide of various concentrations (0.00125–0.0075 M) was formed using a piezoelectric nebulizer operating at a frequency of 2.4 MHz and then was introduced into a tubular reactor equipped with two heaters. The first heater was used for preliminary solvent evaporation (100–350 °C), and the second – for the pyrolysis zone heating (500–900 °C). The influence of the precursor concentration in the solution, nebulizer power, evaporation and pyrolysis temperatures on size distribution, composition and structure of the synthesized particles was studied. A decrease in the concentration of the precursor in the range of (0.00125–0.0075 M) is accompanied by a decrease in the average molybdenum and tungsten disulfides particle size from 40 to 25 nm and from 40 to 30 nm, respectively, an increase of the solvent evaporation and pyrolysis temperatures from 300 to 800 °C and from 600 to 900 °C led to a decrease in the average particle size from 125 to 80 nm and from 135 to 100 nm respectively while solution concentration was 0.01 M, and an increase of the nebulizer power led to a decrease in the average particle size. It was found that both separate particles and large amounts of powder had a stoichiometric composition –  $\text{MoS}_2$  and  $\text{WS}_2$ . The powders obtained in the temperature range of 750–850 °C comprised mainly of hexagonal (about 70%) and a rhombohedral  $\text{MoS}_2$  structures (30%).

The authors are grateful to the Russian Science Foundation for the financial support of the study under contract no. 15-13-00045.

**References**

1. V. N. Bakunin, A. Yu. Suslov, G. N. Kuzmina and O. P. Parenago: *Lubrication Science* **17**, 127–145 (2005).
2. T. P. Prasad, E. Diemann and A. Muller: *J. Inorg. Nucl. Chem.* **15**, 1895–1904 (1973).

## AUTHOR INDEX

- A**
- Adhiri, R. 73
- Ahmadova, Kh. M. 63
- Ajayan, P. M. 10, 15
- Aldoshin, S. 59
- Alekseev, R. 77
- Alexandrov, S. E. 77, 114
- Almásy, L. 36
- Apyari, V. V. 67, 75, 76, 82
- Arkipova, E. 68
- Ayala, P. 8, 19, 49, 58
- Aznakayev, E. 102
- Aznakayeva, D. 102
- B**
- Baia, L. 96
- Bajac, B. 111
- Bálint, Zs. 17
- Bandur, G. 45
- Banys, J. 41
- Baranova, M. A. 76
- Bardenhagen, I. 56, 88
- Batratkov, K. 40
- Beke, D. 47
- Belinova, T. 33
- Bellucci, S. 28
- Bélteky, P. 92
- Belyakova, L. 80
- Bene, K. 72
- Berkó, A. 61
- Bertóti, I. 69
- Bíró, I. 42
- Bíró, L. P. 6, 7, 17, 28, 29, 30, 42
- Bogoslavskaya, E. 89
- Bogya, E. S. 108
- Boldizsár, T. 69
- Bonyár, A. 72
- Borbáth, I. 84
- Borbáth, T. 84
- Boros, T. 84
- Bortel, G. 65, 74
- Boskovic, G. 111
- Boukheddaden, K. 109
- Bozal-Palabiyik, B. 99
- Bozsó, Zs. 97, 99
- Brunetti, G. 8, 51
- Buchholcz, B. 69, 70
- Bunge, A. 71, 79
- Burunkova, J. 72
- Bůžek, D. 33
- C**
- Cahangirov, S. 49
- Castro, A. 21
- Chernozatonskii, L. 6, 7, 28, 37, 39
- Chernyak, S. 9, 57
- Chitanu, E. 84
- Cigler, P. 53
- Circu, M. 79
- Cisneros García, Z. N. 103
- Codescu, M. 84
- Crăciunescu, I. 84
- Csarnovics, I. 72
- D**
- Datz, D. 60, 104
- Deák, A. 29
- Deák, L. 62
- Dékány, I. 113
- Deli, M. A. 97, 99
- Demel, J. 7, 33, 36
- Dementjev, A. 110
- Demin, V. 7, 28, 37
- Demir, E. 99
- Denisjuk, I. 72
- Dimiev, A. M. 8, 49
- Dmitrienko, S. G. 67, 75, 76, 82
- Dobó, D. 105, 106, 113
- Dogan-Topal, B. 93
- Dudás, Z. 7, 36
- E**
- Égerházi, L. 107
- Egorov, A. 57
- El Moussafir, M. 73
- Endródi, B. 55
- Erostyák, J. 47
- F**
- Farkas, A. 61
- Ferrari, A. C. 6, 12
- Ferreira, P. 21
- Filatov, K. 77, 114
- Filip, X. 71
- Földes, D. 65, 74
- Fucikova, A. 33
- Fujii, M. 33
- Fülöp, L. 97, 99
- Furletov, A. A. 75
- G**
- Gál, T. 104
- Galbács, G. 106

- |                       |                    |                       |                   |                       |
|-----------------------|--------------------|-----------------------|-------------------|-----------------------|
| Gali, Á.              | 8, 47              | <b>K</b>              | Kuriganova, A.    | 89                    |
| Garamus, V. M.        | 45                 | Kakemam, J.           | Kuzhir, P.        | 7, 40, 41,<br>42, 110 |
| Garshev, A. V.        | 75, 76, 82         | Kálomista, I.         | Kvashnin, A. G.   | 7, 38, 39             |
| Geretovszky, Zs.      | 107                | Kamarás, K.           | Kvashnin, D. G.   | 28                    |
| Gharib, A.            | 10, 24             |                       | <b>L</b>          |                       |
| Ghunaim, R.           | 93                 | Kania, K. D.          | Lambin, P.        | 28, 42                |
| Glenneberg, J.        | 56, 88             | Kanno, T.             | Lang, K.          | 33, 36                |
| Gómez-Pérez, J.       | 105                | Kaplas, T.            | Langer, F.        | 56, 88                |
| Gorbunova, M. V.      | 76                 | Karpicz, R.           | Lapin, Z.         | 49                    |
| Gorzkievicz, M.       | 94                 | Kasperek, R.          | Lapko, K.         | 41                    |
| Grätzel, M.           | 53                 | Kavan, L.             | Laurila, R.       | 58                    |
| Grochowicz, M.        | 95                 | Kecsenovity, E.       | Lee, H-K.         | 90, 91                |
| Guaaybess, Y.         | 73                 | Kéri, A.              | Lee, J-Y.         | 90, 91                |
| Gubó, R.              | 61                 | Kertész, K.           | Lee, W-K.         | 90, 91                |
| <b>H</b>              |                    | Khannanov, A. A.      | Len, A.           | 36                    |
| Haine, N.             | 109                | Khlobystov, A. N.     | Leontyeva, D.     | 89                    |
| Halasz, I.            | 6, 16              | Kierys, A.            | Liakhov, Yu. F.   | 85                    |
| Haluska, M.           | 10, 23             | Kirakci, K.           | Licarete, E.      | 96                    |
| Hantosi, D.           | 97, 99             | Kiricsi, M.           | Liska, P.         | 53                    |
| Haspel, H.            | 69, 70, 83,<br>105 | Kiss, J.              | Liu, W.           | 23                    |
| Hierold, C.           | 23                 | Kiss, L.              | Lunin, V.         | 57, 59, 68            |
| Hong, S-W.            | 91                 | Kokenyesi, S.         |                   |                       |
| Horváth, Z. E.        | 17                 | Konakov, V. G.        | <b>M</b>          |                       |
| Hubalek Kalbacova, M. | 7,<br>33           | Kónya, Z.             | Macutkevič, J.    | 41                    |
| Hursán, D.            | 55                 |                       | Magda, G. Zs.     | 28                    |
| Hwang, C.             | 28, 29, 30         | Koppa, P.             | Magyari, K.       | 96                    |
| Hynek, J.             | 7, 36              | Kordas, K.            | Maksimenko, S.    | 40, 110               |
| <b>I</b>              |                    | Kormányos, A.         | Mamedov, H. M.    | 9, 63                 |
| Igaz, N.              | 92                 | Kóta, Z.              | Mamedova, V. J.   | 63                    |
| Inam, R.              | 99                 | Kotakoski, J.         | Marinică, O.      | 45, 84                |
| Ivanov, A.            | 42, 57, 68         | Kovács, B.            | Márk, G. I.       | 7, 17, 42             |
| <b>J</b>              |                    | Kovács, D.            | Maroni, P.        | 27                    |
| Jakab, E.             | 65, 74             | Kováts, É.            | Maslakov, K.      | 57, 68                |
| Janáky, Cs.           | 9, 55              | Kozachenko, V. V.     | Matori, K. A.     | 78                    |
| Jánosi, T. Z.         | 47                 | Kozuka, H.            | Mészáros, M.      | 97, 99                |
| Janovák, L.           | 113                | Krasheninnikov, A. V. | Meyer, J. C.      | 49                    |
| Javadian, S.          | 8, 50              | Krysova, H.           | Mironov, V. S.    | 100                   |
| Juhász, K.            | 105, 106           | Kukovecz, Á.          | Mishin, M.        | 77                    |
|                       |                    |                       | Mishra, A. K.     | 46                    |
|                       |                    |                       | Mishra, S. B.     | 8, 46                 |
|                       |                    | Kumar, V.             | Mitoseriu, L.     | 21                    |
|                       |                    | Kun, R.               | Mohai, M.         | 69                    |
|                       |                    | Kuo, P. C.            | Mohammadooost, F. | 78                    |
|                       |                    | Kurapova, O. Yu.      | Molnár, Gy.       | 29, 30                |

- |                   |              |                         |               |                          |             |
|-------------------|--------------|-------------------------|---------------|--------------------------|-------------|
| Moussetad, M.     | 73           | Plank, K.               | 70            | Singh, K.                | 81          |
| Muradov, M. B.    | 63           | Plyushch, A.            | 7, 41         | Sipos, P.                | 97, 99      |
| Mustafina, A.     | 44           | Popescu, R. A.          | 96            | Slepička, P.             | 98          |
| <b>N</b>          |              | Popov, Z.               | 28            | Slepičková Kasálková, N. | 98          |
| Nagy, K. A.       | 108          | Postnikov, A.           | 89            | Slimani, A.              | 109         |
| Nagy, N.          | 29           | Pulaski, L.             | 94            | Smirnov, V. M.           | 100         |
| Nakanishi, S.     | 34           | <b>R</b>                |               | Smirnova, N.             | 89          |
| Nan, A.           | 71, 79       | Radu, T.                | 71, 79        | Socoliuc, V.             | 45, 84      |
| Németh, G.        | 9, 60, 104   | Rajeshwar, K.           | 9, 14         | Sokal, A.                | 41          |
| Niimi, Y.         | 49           | Rajnavolgyi, E.         | 72            | Sorokin, P. B.           | 7, 28, 38   |
| Nikitin, A. V.    | 112          | Rakic, S.               | 111           | Srivastava, P.           | 81          |
| Novotny, L.       | 49           | Rance, G. A.            | 16            | Stepanov, A.             | 72          |
| <b>O</b>          |              | Raooof, H. A.           | 47            | Strokova, N.             | 9, 59       |
| Oresak, E.        | 72           | Rathouský, J.           | 36            | Suenaga, K.              | 49          |
| Ostovan, F.       | 78           | Rawal, A.               | 8, 19, 48     | Sugimoto, H.             | 33          |
| Ostrovská, L.     | 33           | Rim, H-R.               | 90, 91        | Süle, P.                 | 30          |
| Osváth, Z.        | 6, 29, 30    | Rimpelova, S.           | 98            | Susan-Resiga, D.         | 45, 84      |
| Oubouchou, H.     | 109          | Rodríguez Zavala, J. G. | 103           | Suslova, E.              | 57          |
| Óvári, L.         | 61           | Rodríguez, B.           | 21            | Svirko, Y.               | 40          |
| <b>P</b>          |              | Rohringer, P.           | 49, 58        | Švorčík, V.              | 98          |
| Paddubskaya, A.   | 40, 110      | Roik, N.                | 80            | Szabó, M.                | 105         |
| Padurariu, L.     | 21           | Roman, C.               | 23            | Szabó, T.                | 6, 27       |
| Pálinkás, A.      | 6, 30        | Rouster, P.             | 32            | Szabó-Révész, P.         | 97, 99      |
| Panic, S.         | 111          | Rubio, A.               | 49            | Szalontai, B.            | 97, 99      |
| Pashkin, E. Y.    | 38           | Ruml, T.                | 33, 98        | Szám, A.                 | 16          |
| Patnaik, S.       | 81           | <b>S</b>                |               | Szamosvölgyi, Á.         | 105, 106    |
| Pavlovic, M.      | 32           | Sadeghi, A.             | 50            | Szenti, I.               | 9, 62       |
| Pécz, B.          | 9, 10, 22    | Saeed, M.               | 8, 47         | Szilágyi, I.             | 7, 27, 32   |
| Pekker, Á.        | 16, 60, 104  | Sakamoto, R.            | 6, 7, 26      | Szörényi, T.             | 107         |
| Pekker, S.        | 65, 74, 87   | Sami, S.                | 58            | <b>T</b>                 |             |
| Peter, F.         | 45           | Sápi, A.                | 105, 106, 113 | Takanabe, K.             | 9, 20       |
| Peterková, L.     | 98           | Savilov, S.             | 57, 59, 68    | Tapasztó, L.             | 28          |
| Peterlik, H.      | 49           | Sebők, D.               | 107, 113      | Telitsin, V. D.          | 76          |
| Pető, J.          | 28           | Sepsi, Ö.               | 104           | Tenorio Rangel, F. J.    | 103         |
| Petran, A.        | 79           | Shamsutdinova, N.       | 44            | Terenteva, E. A.         | 67          |
| Petrov, V. A.     | 112          | Shi, L.                 | 8, 49, 58     | Tiurikov, K. S.          | 114         |
| Pichler, T.       | 6, 9, 49, 58 | Shin, H.                | 9, 54         | Tóháti, H. M.            | 16, 60, 104 |
| Piszter, G.       | 17, 42       | Shiozawa, H.            | 58            | Tolmacheva, V. V.        | 82          |
| Pitkänen, O.      | 58           | Shiue, J.               | 108           | Tománek, D.              | 38          |
| Pitna Laskova, B. | 64           | Shmatko, V.             | 89            | Tombácz, E.              | 45          |
|                   |              | Sibal, A.               | 8, 48         | Tour, J. M.              | 49          |
|                   |              | Sienkiewicz, A.         | 43, 95        | Trofymchuk, I.           | 80          |
|                   |              |                         |               | Turcu, R.                | 45, 79, 84  |
|                   |              |                         |               | Turikov, K.              | 77          |

<b>U</b>		Veszeka, Sz.	97, 99	Yalovega, G.	89
Uchiyama, H.	7, 34	Vilarinho, P. M.	8, 9, 21	Yarykin, D. I.	82
Uslu, B.	99	Vlckova-Zivcova, Z.	53	Yeshchenko, O. A.	85
<b>V</b>		Volkov, P. A.	75, 76, 82	Yussov, H. M.	78
		Vulpoi, A.	96	<b>Z</b>	
Vajtai, R.	6, 12	<b>W</b>		Zairov, R.	8, 44
Valenta, J.	33	Wagner, W.	94	Zakeeruddin, S. M.	53
Valusis, G.	110	Walker, K.	16	Zaleski, R.	43
Valynets, N.	40	Wanko, M.	49	Zelenka, J.	33
Vancsó, P.	6, 28	Willner, I.	7, 13	Zemtsova, E. G.	100
Varga, T.	83	<b>Y</b>		Zhuk, D.	72
Vári, G.	9, 61	Yakovenko, I.	102	Zolotov, Y. A.	67, 82
Vasilescu, C.	8, 45, 84			Zolotova, N. S.	76
Vékás, L.	45, 84			Zukalova, M.	10, 64
Vesely, M.	98				

